Summer 2021

Physiological and Molecular Responses of Eurythermal and Stenothermal Populations of *Zostera Marina* L (Eelgrass) to Climate Change

Carmen C. Zayas-Santiago
Old Dominion University, ccastula@gmail.com

PHYSIOLOGICAL AND MOLECULAR RESPONSES OF EURYTHERMAL AND STENOTHERMAL POPULATIONS OF *ZOSTERA MARINA* L (EELGRASS) TO CLIMATE CHANGE

by

Carmen C. Zayas-Santiago
B.S., 2004, University of Puerto Rico at Humacao
M.Sc., 2011, University of Puerto Rico at Mayagüez

A Dissertation Submitted to the Faculty of
Old Dominion University in Partial Fulfillment of the
Requirements for the Degree of

DOCTOR OF PHILOSPHY

OCEANOGRAPHY

OLD DOMINION UNIVERSITY
August 2021

Approved by:

Richard C. Zimmerman (Director)

Victoria J. Hill (Member)

Dreux P. Chapell (Member)

Dan Barshis (Member)

ABSTRACT

PHYSIOLOGICAL AND MOLECULAR RESPONSES OF EURYTHERMAL AND STENOTHERMAL POPULATIONS OF *ZOSTERA MARINA* L (EELGRASS) TO CLIMATE CHANGE

Carmen C. Zayas-Santiago
Old Dominion University, 2021
Director: Dr. Richard C. Zimmerman

As CO_2 levels in Earth's atmosphere and oceans steadily rise, varying organismal responses may produce ecological losers and winners. Increased ocean CO_2 can enhance seagrass productivity and thermal tolerance, providing some compensation for climate warming. However, the consistency of this CO_2 effect across populations of cosmopolitan species such as *Zostera marina* L. (eelgrass) remains largely unknown. This study analyzed whole-plant performance metabolic profiles and gene expression patterns of distinct eelgrass populations in response to CO_2 enrichment. Populations were transplanted from Nisqually Landing and Dumas Bay, two cold water environments in Puget Sound, WA (USA) that rarely experience summer water temperatures above 15° C, and one population from South Bay, VA (USA) that frequently experiences summer heat waves exceeding 25° C. All three populations were grown in outdoor aquaria and exposed to five different CO_2 concentrations, under natural light and ambient water temperature of southeast Virginia, for 18 months. The three eelgrass populations showed similar instantaneous metabolic responses to CO_2 treatments. However, only eelgrass from South Bay, VA and Dumas Bay, WA exhibited physiological stimulation to seasonally increasing temperature under elevated CO_2 treatments, increasing shoot numbers, plant size, and leaf growth. The plants from Nisqually Landing, WA were unable to survive the warm summer

water temperature even in the presence of high CO_2 concentrations. Metabolomic profiling revealed differences among CO_2 treatments and eelgrass populations. CO_2 enrichment increased the abundance of Calvin Cycle and nitrogen assimilation metabolites while suppressing the abundance of stress-related metabolites. However, target genes involved in carbohydrate fixation, photosynthesis and proteins that function as molecular chaperones did not respond to CO_2 enrichment even though they changed through in response to light and temperature. Transcriptome profiles by themselves did not predict how gene expression translates into physiological and metabolic consequences under high CO_2 conditions. The differential response among eelgrass populations suggest that seagrass populations will respond variably to increasing CO_2 concentrations in which some eelgrass phenotypes may be better suited to cope with an increasingly hot and sour sea than others.

This dissertation is dedicated to Jorge, ILán, Teresa, Nala, Knelo and Visi.

ACKNOWLEDGMENTS

Throughout this PhD journey, life has presented me with personal and professional challenges. However, it has allowed me to meet the right people when I most needed it and least expected it.

First, thanks to Dr. Ben Cucker your encouragement and commitment are one of the main reasons I started this journey. To Dr. Richard Zimmerman for guiding me through the PhD; providing ideas, substantive comments and suggestions that greatly improved my scientific tool pack. To my fellow PhD students Billur Celebi, Malee Jinuntuya and Ariel Degree for friendly and supportive conversations along the way, for your assistance with sampling, protocols, data analysis and instrumentation. To all members of Bio-Optical Research Group, especially David Ruble and Dr. Victoria J. Hill for their insight and help throughout. Thanks to my ODU friends and colleagues that made the PhD life enjoyable by helping me, sharing a story and a beer (Molly, Brittany, Matt, Rob, Chris, Bonnie, Will, Andrea, Diego, Kevin, Stephanie, Harmony and Courtney).

Thank you Jeff Gaeckle, for taking the time to sample and send the eelgrass from Washington. Albert Rivas-Ubach, thanks for your statistical input. Your help was key in finishing this project. And thank you Kim Powell for always willing to help me and for giving me the tools and access I needed during the final stretch.

Words cannot express my immense gratitude to Alexandra, José, Luna, Wrinkles, Red, Lale and Moomoo: thank you for taking me and my family in since the moment we met until the moment we left. I'm so lucky to be part of your life and your family. Jeanette Ocasio thanks for your positive thoughts and for being a strong woman who I admire. Thanks for having a

beautiful relationship with many mothers and their children, including us. To my supportive husband, Jorge, your encouragement and love have allowed me to navigate this PhD while becoming a new mother. To Nala, Knelo and Visi for making me smile every day. To ILán, you have brought a new perspective to my life and taught me new things through your immense curiosity. To my parents, especially my mom, Teresa: I'll be forever grateful for your help, love and compassion. To Dr. Jyoti Upadhyay and the CHKD nurses and staff for taking care of my son during his multiple procedures and answering all of our questions.

Financial support for this research was provided by the National Science Foundation (Award OCE-1061823 and OCE-1635403). The Laboratory Directed Research and Development (LDRD) Program at the Pacific Northwest National Laboratory (PNNL) provided assistance with metabolomic analyses and interpretation under U.S. Department of Energy (DOE) Contract DE-AC05–76RL01830. Assistance with transcriptomic analysis was provided by the Facilities Integrating Collaborations for User Science (FICUS) initiative (#50358) and used resources at the Environmental Molecular Sciences Laboratory (EMSL), which is sponsored by the DOE Office of Biological and Environmental Research and operated under contract DE-AC05-76RL01830. The Kirk Wetlands Student Research Award that supported the gene expression research performed at ODU.

¡Gracias, gracias, gracias!

TABLE OF CONTENTS

Page

LIST OF TABLES

LIST OF FIGURES

Figure Page

CHAPTER 1

INTRODUCTION

Background

Increased atmospheric levels of carbon dioxide (CO_2) resulting from human activities have been absorbed by the ocean. This climatic scenario is likely to change the biogeochemistry in the oceans and affect the response of organisms, generating ecological losers and winners. Among the losers, benthic calcifiers are expected to respond negatively to elevated CO_2 as calcification rates become energetically more expensive (Kleypas et al. 2005). In today's ocean, CO_2 is a potentially limiting substrate for photosynthesis in aquatic ecosystems (Zimmerman et al. 1997) as photosynthesis in many marine autotrophs such as cyanobacteria (Hutchins et al. 2007), coccolithophores (Rivero-Calle et al. 2015) and seagrasses (Invers et al. 2001, Jiang et al. 2010, Zimmerman et al. 2017) respond positively to increase CO_2.

Seagrass meadows help mitigate the impacts of climate change by removing CO_2 from the water column through photosynthesis, by promoting organic carbon deposition from the water column to the sediments and from root and rhizome growth in the sediment, known as "blue carbon" (Greiner et al. 2013). However, seagrass populations are declining worldwide from anthropogenic impacts due to increasing temperature, eutrophication, sediment loading, and physical destruction. A number of studies consistently indicate that CO_2 enrichment enhanced photosynthesis and leaf sugar content for eelgrass (*Zostera marina* L.)(Beer 1989, Durako 1993, Zimmerman et al. 1995, Koch & Beer 1996, Zimmerman et al. 2017) decreasing their light requirements, increasing their productivity and helping them survive high temperatures (Björk et al. 1997, Zimmerman et al. 1997, Zimmerman & Mobley 1997, Touchette & Burkholder 2000,

Palacios & Zimmerman 2007, Zimmerman et al. 2015, Zimmerman et al. 2017). Exposure to increased CO_2 availability also increases production of vegetative and flowering shoots, the allocation of biomass to below ground tissues and stimulates changes in leaf chemical composition (Palacios & Zimmerman 2007, Campbell & Fourqurean 2013, Zimmerman et al. 2017).

Z. marina, the most widely distributed seagrass species in the temperate northern hemisphere, experiences a varied range in light availability, salinity, and temperature across different habitats (Zimmerman et al. 1989). These habitat differences provide numerous opportunities for adaptation of geographically isolated populations, making eelgrass useful for exploring the impacts of climate change on marine ecosystems. Many geographically isolated eelgrass populations appear to be genetically distinct (Alberte et al. 1994, Williams & Orth 1998, Reusch et al. 1999) and display consistent differences in leaf morphology, suggesting that populations may be adapted to different conditions (Reusch et al. 1999, Staehr & Borum 2011). However, the true degree of functional plasticity among these populations remains unknown.

Z. marina best photosynthetic performance is between 5° C and 25° C (Evans et al. 1986, Bulthuis 1987) but sustained temperatures above 25° C can affect their carbon metabolism, producing meadow-wide die-offs (Dillon 1971, Thayer et al. 1975, Evans et al. 1986, Zimmerman et al. 1989, Moore & Jarvis 2008, Orth et al. 2010). Temperature stress appears to be mediated primarily by its effect on sucrose metabolism (Zimmerman et al. 1989, Gu et al. 2012), it has also been shown to induce genes involved in protein degradation, presenting photosynthetic damage and failed metabolic compensation (Bergmann et al. 2010, Franssen et al. 2011, Winters et al. 2011). Consequently, photosynthetic stimulation resulting from CO_2 enrichment, which increases sucrose formation, should reduce the effects of thermal stress.

Prolonged exposure to elevated CO_2 quantitatively enhances leaf photosynthesis, shoot survival, growth and flowering of eelgrass populations from climates characterized by a narrow annual thermal range (predominantly cool) (Zimmerman et al. 1997, Palacios & Zimmerman 2007) and of eelgrass that experienced a wide annually a thermal range that include stressfully warm summers (Zimmerman et al. 2017). Computer simulations based on these studies demonstrated that eelgrass productivity and thermal tolerance in the modern-day and the future ocean can be mediated by CO_2 availability (Zimmerman et al. 2015). Accordingly, this study compared eelgrass physiological processes, such as survival and growth, in response to the environment and characterized the gene expression and metabolome of the plants. Understanding gene expression patterns and the metabolome helps to assess the response of an organism to a change in its environment (Macreadie et al. 2014, Ceccherelli et al. 2018, Gargallo-Garriga et al. 2018) and/or to evaluate the differential response of populations to the same change (Hoffmann & Willi 2008, Franssen et al. 2011).

The objective of this dissertation was to evaluate the responses of two distinct eelgrass populations from Puget Sound, Washington and one from Chesapeake Bay, Virginia, USA that come from contrasting (cool summer vs. warm summer) thermal environments to increase CO_2 and thermal summer stress. These populations were subjected to an experimental gradient of five CO_2 conditions in an outdoor facility under natural varying temperature and insolation for one year. Increased CO_2 availability should stimulate carbon fixation of the Puget Sound populations, improving their tolerance to temperature stress, as has been previously shown for Chesapeake Bay eelgrass (Zimmerman et al. 2017). I expected that comparing growth and development, metabolome and patterns of gene expression among eelgrass populations in

response to high CO_2 and temperature would provide unique insights into their potential ability to adapt to future changes in their respective environments.

Specific Objectives

The research presented here addresses several important questions regarding the response of distinct *Z. marina* L. populations to increasing CO_2 and temperature in the context of a changing climate. The work addressed the following specific questions:

a. What are the effects of increase in CO_2 concentrations and temperature on isolated eelgrass populations?
    i. How do CO_2 and high temperatures affect growth, size and survival of these populations?
    ii. Are oxygenic photosynthesis and respiration rates of the populations different when exposed to the same temperature and CO_2 conditions?
    iii. Do eelgrass leaf optical properties differ among populations under the same CO_2 conditions?
b. What are the effects on stenothermal and eurythermal eelgrass population's metabolome due to climate change?
    i. Which are the main affected metabolic pathways?
    ii. Are the metabolic fingerprints different among *Z. marina* populations?
    iii. Are the metabolic fingerprints different between CO_2 treatments?
c. What are the effects of CO_2 and temperature exposures on the gene expression in C metabolism, photosynthesis and stress associated genes?
    i. Is the gene expression of *Z. marina* different among populations?

ii. Do the gene expression patterns on *Z. marina* differ among CO_2 treatments?

iii. How does the gene expression affect regulation of the carbon budget among eelgrass populations?

Significance

Seagrass meadows will benefit from the CO_2 increase in the oceans helping them to survive high temperatures. This study extended our quantitative understanding of eelgrass response to climate change by focusing on the response of populations from South Bay, VA near the southern limit of eelgrass distribution on the Atlantic coast experiencing warm summer temperatures and populations from Puget Sound, WA subjected to less temperature stress. The research performed here coupled molecular responses with eco-physiological approaches to explore the performance of different eelgrass populations to potential future climate scenarios providing insight into to the key pathways that control the photosynthetic acclimation, carbon fixation, growth and respiration.

CHAPTER 2

DIFFERENTIAL IMPACTS OF CO_2 AND TEMPERATURE ON METABOLIC PERFORMANCE AND SURVIVAL OF GEOGRAPHICALLY DISTINCT POPULATIONS OF *ZOSTERA MARINA* L (EELGRASS)

Introduction

The mean atmospheric concentration of CO_2 measured by the Mauna Loa Global Monitoring Laboratory, surpassed 415 ppm in 2020, a level not experienced on earth in nearly 20 million years (Thomas 2008, Zhang et al. 2013, NOAA-ESRL 2018). This concentration, and the global warming it causes, would be even higher if the oceans did not absorb at least 25% of the anthropogenically released CO_2 each year. However, the oceans are not a benign sink for this greenhouse gas, as the absorbed CO_2 results in ocean acidification that alters the carbonate chemistry of the ocean, decreasing seawater pH (IPCC 2014) and negatively affecting marine calcifiers, from pelagic pteropods to hermatypic corals and oysters (Kleypas et al. 2005, Byrne et al. 2011). However, rising CO_2 concentrations also create ecological winners, including some terrestrial plants (Leakey et al. 2009) and the marine angiosperms commonly known as seagrasses (Invers et al. 2001, Palacios & Zimmerman 2007, Zimmerman 2021). The positive photosynthetic response of seagrasses to CO_2 concentration has helped maintain a positive balance between photosynthesis and respiration in the face of increasing temperature, thereby increasing the accumulation of labile carbon reserves, rates of plant growth and reproduction, and plant size (Björk et al. 1997, Zimmerman et al. 1997, Touchette & Burkholder 2000, Palacios & Zimmerman 2007, Zimmerman et al. 2015, Zimmerman et al. 2017). Growth under elevated CO_2 also inhibits the synthesis of photosynthetic pigments in a manner reminiscent of photoacclimation to high light environments (Celebi et al. 2021).

Seagrasses are well recognized as important ecosystem engineers (Jones et al. 1994), but their populations are increasingly threatened by anthropogenic degradation of water quality and climate warming (Orth et al. 2006). Negative effects of rising seawater temperatures on seagrasses result in negative carbon balance (Bulthuis 1983, Ralph 1998) and photosynthetic protein denaturation (Bruggemann et al. 1992, Ralph 1998). Sustained temperatures above 25° C frequently results in stress and die-offs of eelgrass (Dillon 1971, Thayer et al. 1975, Evans et al. 1986, Zimmerman et al. 1989, Moore & Jarvis 2008, Orth et al. 2010). However these effects can be offset by CO_2 enrichment in many seagrasses, including eelgrass (Beer 1989, Durako 1993, Koch & Beer 1996). In addition, seagrass meadows have been identified as being among the most productive aquatic habitats in terms of Blue Carbon burial (Mcleod et al. 2011), suggesting that enhanced seagrass productivity under increasing CO_2 conditions may exert a negative feedback on climate change.

Z. marina is the most widely distributed seagrass species in the temperate northern hemisphere (Green & Short 2003), exposing populations to a varied range in light availability, salinity, and temperature. These circumstances provide numerous opportunities for genetic adaptation to different environments making eelgrass useful for exploring the impacts of climate change on different populations. *Z. marina* populations had demonstrated localized adaptation where populations increased their biomass in their home environment under reciprocal transplant experiments (Hämmerli & Reusch 2002). Therefore, geographically isolated eelgrass populations appear to be genetically distinct (Alberte et al. 1994, Williams & Orth 1998, Reusch et al. 1999), and display a large range in leaf morphology (Fig.1), suggesting that populations may be adapted to different local conditions (Reusch et al. 1999, Staehr & Borum 2011). For example, eelgrass leaves from cold regions exhibit greater mechanical elasticity and flexibility,

they tend to be narrower, and showed higher fiber content than plants growing in warmer regions (Engle & Miller 2005, Paul & de los Santos 2019).

Understanding the combined impacts of multiple factors on the response of species to future climate change is crucial to understanding the performance and distribution of organisms (Zimmerman, 2020). The aim of this study was to compare the physiological responses to the combined effects of CO_2 availability and summer heat stress of two eelgrass populations from cool thermal environments (Puget Sound, WA) to that of a locally adapted population from coastal Virginia. The hypothesis is that increased CO_2 availability should stimulate carbon fixation of the Puget Sound populations, improving their tolerance to temperature stress, as has been previously shown for Virginia eelgrass (Zimmerman et al. 2017). Comparing survival, growth, plant size, leaf sugar, and photosynthetic pigment among eelgrass populations in response to high CO_2 and temperature will provide unique insights into the potential ability of these populations to acclimate to future changes in their respective environments, and help identify ecologically important performance features that can be exploited to facilitate restoration and conservation of these important ecosystem engineers.

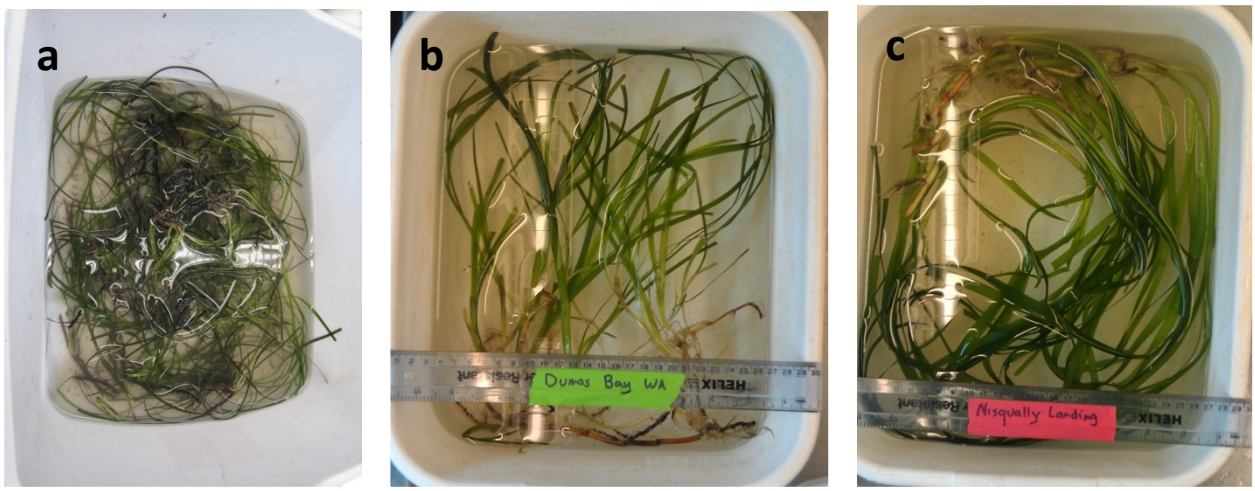

Figure 1. Photographs of eelgrass from (a) South Bay, VA, (b) Dumas Bay, WA and (c) Nisqually Bay, WA showing morphological differences such as leaf length and width at the time of original collection.

Materials and Methods

Eelgrass Source Populations and Experimental Facility

Eelgrass shoots were collected from Dumas Bay (47.327°N, 122.382°W) and Nisqually National Wildlife Refuge (47.109°N, 122.740°W) in southern Puget Sound, WA (DBW and NBW respectively) by representatives of the Washington State Department of Natural Resources in May 2013. Shoots were carefully uprooted by hand to avoid breaking roots and rhizome internodes, washed free of all sediment, packed in paper towels moistened with seawater and shipped overnight to VA. The leaves were cleaned of epiphytes by gently scraping with a razor blade and the entire shoots were surface sterilized by a 30 sec soak in filtered seawater containing 10% sodium hypochlorite (v/v). The sterilized shoots were then transplanted into rectangular fiberglass-reinforced plastic containers (0.04 m^3 volume, 0.075 m^2 surface area) filled with intertidal beach sand and placed into the 20 outdoor aquaria at the experimental climate change facility constructed at the Virginia Aquarium & Marine Science Center, Virginia Beach, VA (Zimmerman et al. 2017). Eelgrass from South Bay VA (SBV) (37.265° N, 75.808° N), a coastal lagoon on the Delmarva Peninsula that regularly experiences summer temperatures >25° C that has been identified as a threshold for eelgrass stress (Evans et al. 1986, Zimmerman et al. 1989), were also collected carefully by hand then cleaned similar to the WA eelgrass and transplanted into the experimental facility. Parallel experiments were running in the aquaria limiting the space, therefore five seagrass containers were into each aquaria (three plastic containers for SBV, one for DBW, and one for NBW). From the 20 aquaria only in 10 aquaria DBW and NBW were placed into each aquarium, having up to two replicates per CO_2 treatment for these populations and up to 4 replicates for SBV. Each aquarium was plumbed with running water (10 turnovers/day) pumped from the adjacent Owls Creek estuary just south of Chesapeake

Bay that exchanges water with the Atlantic Ocean through Rudee Inlet. Water depth in the aquaria was 0.85 m, placing the top of the SBV canopy at about 0.5 m beneath the surface of the water at the beginning of the experiment.

The outdoor facility was exposed to natural daily and seasonal variations in water temperature and sunlight (Fig. 2-3). Light, temperature, and salinity were measured continuously throughout the experiment. Temperature was monitored continuously in each aquarium using an Omega 44005 precision thermistor and custom voltage divider circuits calibrated to a precision of 0.1° C. Sunlight was measured as photosynthetically active radiation (PAR) using a LI-COR LI190SBV plane irradiance sensor (μmol photons m^{-2} s^{-1}) placed 3 m above the tanks. Salinity was monitored using a SeaBird SBE-37 MicroCAT CTD placed in one of the aquaria. From the salinity data, along with temperature and pH, values of total CO_2 in the aquaria and CO_2 in dry at 1 atm (ppm) were determine using CO2SYS Ver. 2.3 (Lewis & Wallace 1998). The CO_2 concentration in each experimental aquarium was individually manipulated using CO_2 bubblers with solenoid valves controlled by Eutech Alpha pH 190 controller/transmitters equipped with submersible glass electrodes. CO_2 concentrations in dry ranged from a median of 30.5 ppm (pH 8) to 50,136 ppm (pH 6). This represented CO_2 concentrations for the present day in Virginia (2013), mid-century (2050), and the end-of-century (2100) based on IPCC (2013) and also past projections. This set up enabled the twenty aquaria to be maintained at five CO_2 concentrations ranging from ambient (~55μmol CO_2 Kg^{-1} SW, pH ~8.0) to 2121 μmol CO_2 Kg^{-1} SW (pH 6) that encompasses >200-years of projected CO_2 increase and yielded a 3-fold gradient in light-saturated photosynthesis for the duration of the experiment (Invers et al. 2001, Cottingham et al. 2005). This CO_2 gradient is useful to determine functional

responses (slopes and intercepts) required to build predictions for eelgrass survival in a variety of CO_2 concentrations.

Plant Size, Growth and Shoot counts

Plant size, growth rate, shoot counts and sucrose content of leaf tissues of all three populations were measured each month to track performance responses to the CO_2 treatments across time. Shoots from each container were selected at random, tagged with plastic cable ties and marked with a 20 gauge hypodermic needle (Zieman 1974, Zimmerman et al. 1996). One week later, lengths of all leaves was measured with a flexible meter tape. New growth was measured as the sum of the distance from the original punch on the leaf sheath to the mark on each leaf plus the entire length of unmarked young leaves that emerged from the leaf sheath after marking. Leaf widths were measured with a digital caliper. Absolute linear growth rates (cm^2 day^{-1}) were calculated by normalizing the total new leaf area by the time interval between marking and measuring. Percent growth rates (% d^{-1}) was calculated by normalizing absolute growth rates by the total leaf area measured at the end of the marking period.

Plant size (one sided leaf area, cm^2 $shoot^{-1}$) was calculated as Σ *Length x Width* of all the leaves on each plant. Relative change in plant size between months was calculated by normalizing the difference in size between successive measurements by plant size at the beginning of the period and multiplied by 100 to express it as percent of the original plant. Relative growth rates (% d^{-1}) were calculated as the ratio of new leaf area to total leaf area, normalized by the time interval between marking and measuring, and multiplied by 100. Relative shoot survival (% of original) was calculated as the difference between shoot counts each month and the initial shoot count, multiplied by 100.

Sucrose determination

Sucrose was extracted from the 2nd youngest leaf collected from two shoots growing under each CO_2 treatment each month. Epiphytes were removed from each leaf segment by gently scraping the leaves with a razor blade, followed by a quick rinse in clean water and wiped dry with a paper towel prior to drying. Leaves were then dried at 60° C, ground in liquid nitrogen using a mortar and pestle and the powder re-dried at 60° C for at least one day. An aliquot of the dry powder was weighed using an analytical balance and extracted in hot (80° C) ethanol. The ethanol extracts from each leaf were evaporated to dryness at room temperature and the residue redissolved in ultrapure (18 MΩ) deionized water. Sucrose concentration was determined spectrophotometrically at 486 nm using a resorcinol assay standardized to sucrose (Huber & Israel 1982).

In vivo leaf absorption spectra and chlorophyll concentrations were measured using clean segments of the 2nd youngest leaf of a shoot from each population tray during summer, as described above. Spectral absorbance [$D(\lambda)$] and reflectance [$\rho(\lambda)$] of intact leaf segments between 350 and 750 nm were measured using a Shimadzu UV 2101PC scanning spectrophotometer fitted with an integrating sphere. Photosynthetic leaf absorptances [$A_L(\lambda)$] were calculated by subtracting the non-photosynthetic absorptance at 750 nm [$A(750)$] from each spectrum (Kirk, 1994).

$$A(750) = [\ 1 - 10^{D(750)}\ ] - \rho(750)$$

$$A_L(\lambda) = [\ 1 - 10^{D(\lambda)}\ ] - \rho(\lambda) - A(750)$$

Chlorophyll was extracted by grinding each leaf in 90% acetone with a glass tissue homogenizer, followed by centrifugation to pellet the debris. Spectral absorbance of the supernatant was measured using the Shimadzu UV 2101 PC scanning spectrophotometer and pigment concentrations were calculated using the equations of Jeffery and Humphrey (1975).

Metabolic Rates

During summer 2013 and 2014, using 2nd leaves, photosynthesis and respiration were measured using polarographic O_2 electrodes and water-jacketed glass incubation chambers (5mL volume, Rank Bros., Cambridge, UK). Incubation water pH was measured using a pH meter calibrated with the same NBS buffers used to calibrate the aquarium pH sensors. A magnetic stirrer provided turbulent flow inside the chambers to prevent boundary layer limitation of gas exchange across the leaf and electrode membrane surfaces. Continuous analog signals from the sensors were measured using a Pico Technology ADC-20 digitizer and recorded using custom software written with LabView (2009 edition, National Instruments). Voltage data were post processed into metabolic rates using MATLAB R2014 (The MathWorks Inc.). Leaves were illuminated with a photosynthesis-saturating irradiance of 300 μmol photons $m^{-2}sec^{-1}$ provided by a Kodak slide projector (ELH bulb). The water used during all incubations was from Owls Creek that provided source water for the experimental aquaria. This stock, with salinity of 24 (PSS-78), was filtered through 0.2 μm Nucleopore membrane filters and stored under refrigeration in glass bottles until use.

Water temperature was controlled by a circulating water bath to six different temperatures ranging from 5° to 30° C. Leaves were cleaned of epiphytes by gentle scraping with a clean razor blade and kept in dark before the incubation measurements. A three cm long piece of leaf

tissue was used during a 10 min dark (i.e. dark respiration) and a 10 min light (i.e. net photosynthesis) measurement. One leaf per temperature per chamber was used and two simultaneous chambers were measured for replication. Short-term responses to temperature were analyzed by linear regression of log-transformed metabolic rates against measurement temperature (T), according to the following relationship (Berry & Raison, 1981):

$$\log \text{rate} = T\,(\log Q_{10}/10) + C$$

where C was the log rate at 0° C and ($\log Q_{10}$/10) was the slope. To further evaluate differences in temperature sensitivity of the metabolic parameters across CO_2 treatments, Q_{10} of P_g and R was calculated as $Q_{10}=10^{(\text{slope}*10)}$.

Statistical Analysis

Temperature sensitivity of the metabolic rates was quantified by calculating the slope of log-transformed rates for gross photosynthesis ($P_g = P_{net} - R$) and dark leaf respiration (R) plotted against the temperature for each population. Statistical significance of treatment and population effects was determined using the mixed model analysis of the linear mixed model component of IBM SPSS Statistics 22 with population as the fixed factor (within subjects) and temperature as the covariate (between subjects).

CO_2 effects on each eelgrass population were quantified by linear regression of each performance metric described above against log [CO_2]. Linear regressions and slopes statistics of each performance metric are shown in Appendix Figs. 22-27 and Tables 29-34. Within-aquarium replicate measures of each performance property were combined each month to generate statistically independent means for each aquarium (without error), resulting in statistically independent replicate measurements for each CO_2 treatment each month. Consequently, statistical significance of treatment effects was determined using a repeated-measures ANCOVA implemented in the mixed model analysis of the linear mixed model component of IBM SPSS Statistics 22 using population and month as the fixed factors (within subjects) and log [CO_2] as the covariate (between subjects). The time series observations were treated as repeated subjects for each measured parameter. When ANCOVA revealed statistically significant effects of time, multiple comparison tests were performed to identify significant differences among monthly values. All error terms were expressed as standard errors unless otherwise noted.

Results

Environmental Parameters & Experimental CO_2 Manipulation

The time series of environmental conditions and manipulated CO_2 concentrations for each aquarium during this 20-month experiment were detailed by Zimmerman et al. (2017). To summarize briefly, irradiance varied seasonally changing with solar elevation and day length, resulting in higher total daily irradiances during summer than winter. These plants received approximately 8h of photosynthesis-saturating irradiance each day, during summer and 4 h each day during winter (Fig. 2)(Celebi 2016). Due to heavy snowfall in February and March 2014 the window screening was removed to ensure light infiltration therefore during that time an increase in light was observed in the tanks (Fig. 2).

In their native habitat, the two eelgrass populations from Puget Sound, WA, experience a typical seasonal temperature cycle ranging between 5° and 15° C (Fig. 3). However, this experiment exposed them to temperatures that varied seasonally from a low of 2° C in winter to an extreme high temperature of 30° C in summer. The summer warm period included 97 days during summer 2013 were seawater temperature exceeded 25° C for at least 1 h each day. Water temperature was consistently below 25° C from October 2013 through May 2014 and 5° C in average from January through March 2014 approaching 0° C on a few days in February 2014 (Fig. 3). The seasonal cycle in water temperature lagged daily irradiance by 6 to 8 wk. On the other hand, salinity did not vary seasonally resulting in a mean salinity of 24 ± 3 (PSS), with low salinity events (11 PSS) resulting from periodic rainfall events that sent freshwater runoff into Owls Creek as described in Zimmerman et al., 2017.

Prior to the onset of CO_2 manipulation on 1 June 2013, all aquaria experienced nearly identical variations in CO_2 concentration, temperature, salinity, alkalinity and pH, and no

systematic variations among aquaria were detected that might have biased the experimental results. Natural fluctuations in the source-water pH (7.4 to 8.1) and [CO_2] (55 ± 19 μmol Kg^{-1} SW) were more variable during summer than winter. On top of these natural variations, the experimental CO_2 manipulation produced a consistent gradient in CO_2 concentrations and pH values across the treatments throughout the duration of the experiment as describe in (Zimmerman et al. 2017).

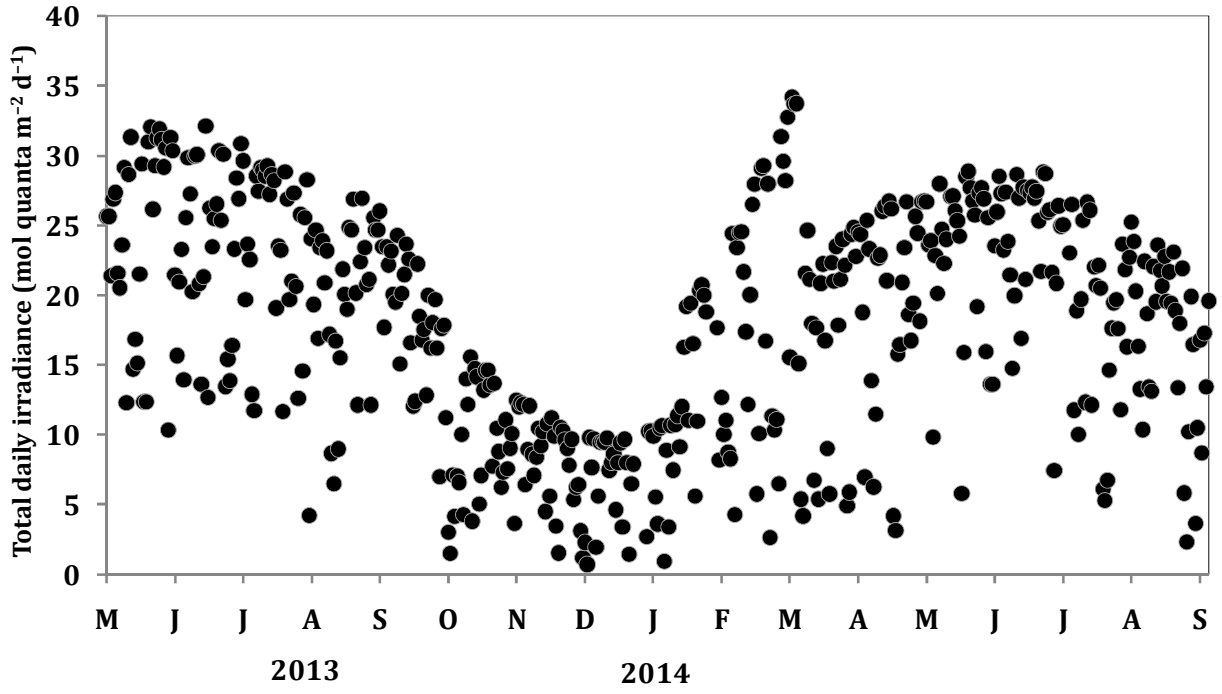

Figure 2. Incident daily irradiance on the plants after correcting to 40% reduction using window screening.

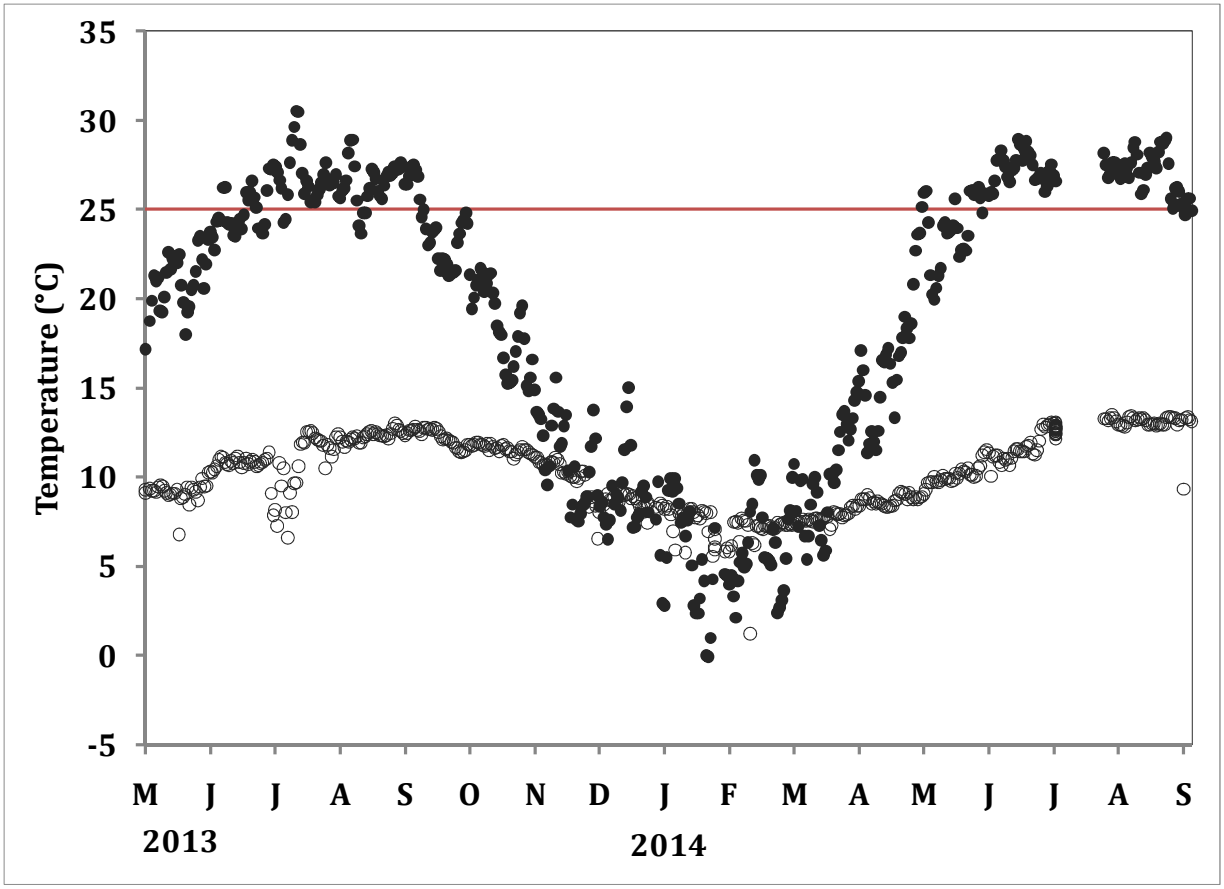

Figure 3. Daily average water temperatures during 2013-2014 measured in the experimental tanks at Owl's Creek (filled circles), VA and the NOAA buoy closest to Dumas Bay WA (Station 9446484)(open circles). NOAA data were obtained from http://tidesandcurrents.noaa.gov/physocean.html.

Survival and Growth

Survival of SBV and DBW shoots remained constant across CO_2 treatments throughout June and July 2013 (white symbols, Figs.4a-c, Tables 1 -3). By August 2013, shoot numbers of SBV and DBW populations increased becoming positively related to CO_2 availability, a trend that continued for the duration of the experiment. During this time, SBV and DBW shoot numbers doubled in the high CO_2 treatment (823 μM CO_2) through vegetative propagation. However, shoot numbers of both populations decreased under ambient CO_2 (55 μM CO_2/ pH 8) during the summer period of warm (>25° C) water temperature. SBV and DBW shoot losses continued under ambient CO_2 as water temperature dropped throughout the fall 2013 and into the winter of 2014. Unlike SBV and DBW, shoot numbers of NBW eelgrass declined throughout May to August 2013 as temperature rose above 25° C. The vast majority of NBW shoots were dead by October 2013 and only one shoot growing under 370 μM CO_2 (pH 7) survived the experiment.

The effect of CO_2 on shoot survival was strongest from December to May 2014 for SBV and from February 2014 to late May 2014 for DBW plants, as indicated by the significant slopes during this time (white symbols, Fig4a, b, Appendix Table 29). Slopes of percent survival vs. log [CO_2] for NBW were not significantly different from zero or each other, indicating no effect of CO_2 on shoot survival from May 2013 to October 2013 and no change over time (white symbols, Fig 4c, Table 3, Appendix Table 29). Monthly slopes of percent survival vs log [CO_2] did not differ among populations (Table 4). However, the October slopes of percent survival vs log [CO_2] was significantly higher for SBV (53.62 % Survival log $[CO_2]^{-1}$) than DBW (13.42% Survival log $[CO_2]^{-1}$) and NBW (-3.11 % Survival log $[CO_2]^{-1}$).

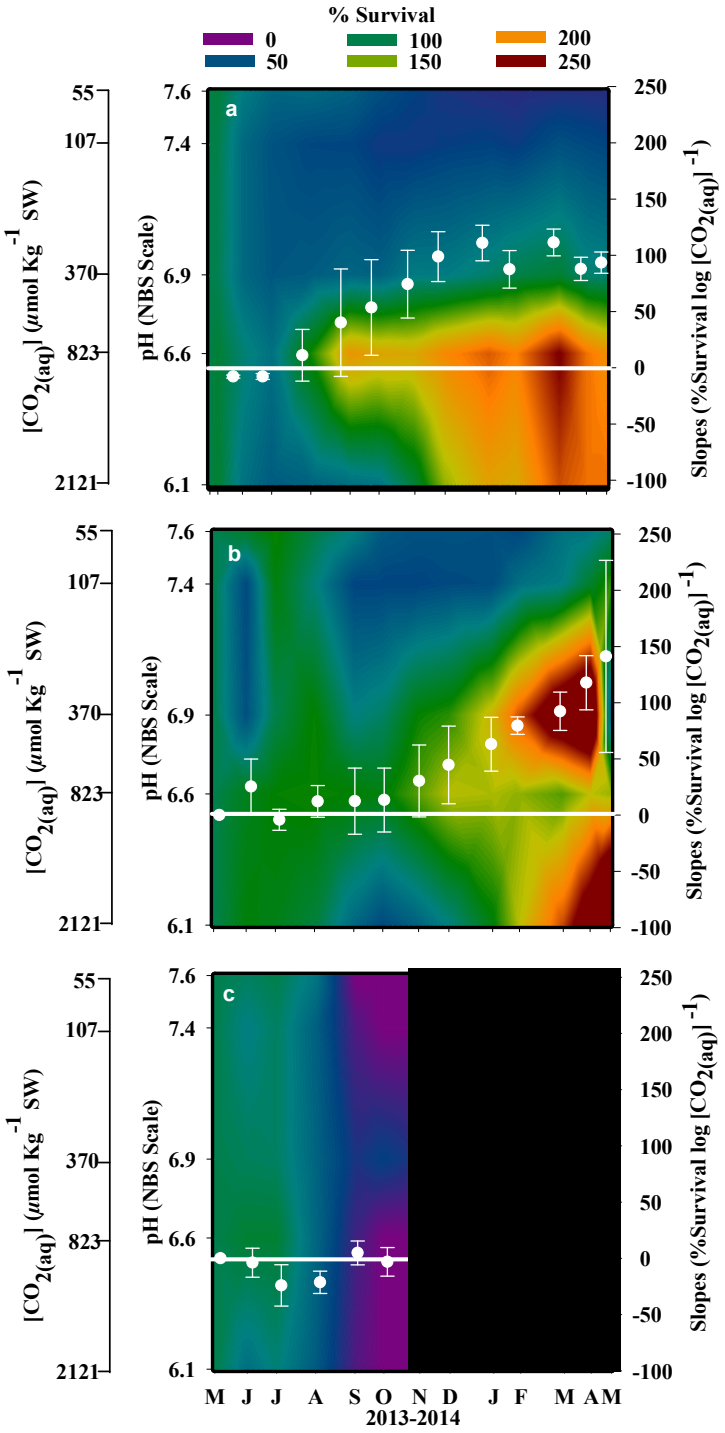

Figure 4. Heat maps of percent survival as a function of pH/CO_2 treatment and time. (a) South Bay, VA. (b) Dumas Bay, WA. (c) Nisqually Bay, WA. Tick marks on the left vertical axis of each plot indicate the mean pH/CO_2 value for each treatment. Tick marks on the right vertical axis of each plot indicate the values of the slopes. White horizontal line represents the zero slope. White symbols represent the monthly slopes of the percent original population vs. log [CO_2] derived from linear regression analysis for each CO_2 treatment. Black panel represents no data. Error bars represent ± 1 SE of the regression slope.

Table 1. Results of linear mixed model ANCOVA with repeated measures comparing physiological properties of South Bay VA plants over time. Summary ANCOVA tables for Type III tests of fixed effects (Month) using the mixed linear model routine implemented in SPSS. DW: dry weight.

Dependent variable	**Source**	**Numerator *df***	**Denominator *df***	***F***	***p***
% Survival	Month	12	4.32	95.97	<0.001*
	log [CO_2]	1	4.32	824.55	<0.001*
	Month X log [CO_2]	12	4.32	53.00	<0.001*
% Rel growth rate	Month	12	234	6.83	<0.001*
	log [CO_2]	1	234	2.52	0.114
	Month X log [CO_2]	12	234	1.08	0.377
% Original Plant Size	Month	12	157	1.80	0.053
	log [CO_2]	1	157	60.94	<0.001*
	Month X log [CO_2]	12	157	1.78	0.056
Sucrose (μmol g^{-1} DW)	Month	11	235	4.78	<0.001*
	log [CO_2]	1	235	223.39	<0.001*
	Month X log [CO_2]	11	235	3.82	<0.001*
Total Chl (μg Chl cm^{-2})	Month	2	56	1.20	0.310
	log [CO_2]	1	56	18.27	<0.001*
	Month X log [CO_2]	2	56	0.26	0.698
Chl *a:b*	Month	2	56	0.93	0.399
	log [CO_2]	1	56	7.30	0.009*
	Month X log [CO_2]	2	56	1.53	0.225

Table 2. Linear mixed model with repeated measurements results for comparison of physiological properties of Dumas Bay between treatments. Summary ANCOVA tables for Type III tests of fixed effects (Month) using the mixed linear model routine implemented in SPSS. DW: dry weight.

Dependent variable	**Source**	**Numerator *df***	**Denominator *df***	***F***	***p***
% Survival	Month	12	91	0.26	0.994
	log [CO_2]	1	91	8.01	0.006*
	Month X log [CO_2]	12	91	0.53	0.893
% Rel growth rate	Month	11	81	2.40	0.012*
	log [CO_2]	1	81	1.31	0.255
	Month X log[CO_2]	11	81	1.78	0.070
% Original Plant Size	Month	12	97	1.65	0.091
	log [CO_2]	1	97	1.26	0.264
	Month X log [CO_2]	12	97	1.33	0.216
Sucrose (μmol g^{-1} DW)	Month	11	80	1.10	0.372
	log [CO_2]	1	80	14.28	<0.001*
	Month X log [CO_2]	11	80	1.03	0.425
Total Chl (μg Chl cm^{-2})	Month	2	20	0.14	0.708
	log [CO_2]	1	20	1.95	0.178
	Month X log [CO_2]	2	20	0.15	0.702
Chl *a:b*	Month	2	20	0.45	0.509
	log [CO_2]	1	20	0.09	0.766
	Month X log [CO_2]	2	20	0.14	0.715

Table 3. Linear mixed model with repeated measurements results for comparison of physiological properties of Nisqually Bay between treatments. Summary ANCOVA tables for Type III tests of fixed effects (Month) using the mixed linear model routine implemented in SPSS. DW: dry weight.

Dependent variable	**Source**	**Numerator *df***	**Denominator *df***	***F***	***p***
% Survival	Month	5	15.31	0.80	0.569
	log [CO_2]	1	25.41	0.82	0.373
	Month X log [CO_2]	5	19.36	0.73	0.610
% Rel growth rate	Month	4	31	2.02	0.116
	log [CO_2]	1	31	12.26	<0.001*
	Month X log [CO_2]	4	31	2.27	0.840
% Original Plant Size	Month	4	36	0.52	0.719
	log [CO_2]	1	36	1.82	0.186
	Month X log [CO_2]	4	36	0.63	0.644
Sucrose (μmol g^{-1} DW)	Month	3	21	0.17	0.918
	log [CO_2]	1	21	4.00	0.059
	Month X log [CO_2]	3	21	0.49	0.694
Total Chl (μg Chl cm^{-2})	Month	2	5	1.21	0.321
	log [CO_2]	1	5	8.18	0.035*
	Month X log [CO_2]	2	5	1.27	0.312
Chl *a:b*	Month	2	5	0.42	0.546
	log [CO_2]	1	5	0.20	0.674
	Month X log [CO_2]	2	5	0.45	0.531

Table 4. Linear mixed model with repeated measurements results for comparison of physiological properties among populations. Summary ANCOVA tables for Type III tests of fixed effects (Population and Month) using the mixed linear model routine implemented in SPSS. DW: dry weight.

Measure	%Survival	% Original Plant Size	GR (% d^{-1})	Leaf Sucrose (μmol g^{-1} DW)	TChl (µg Chl cm^{-2})	Chl *a*:*b*
Intercept	0.942	<0.001*	<0.001*	0.974	0.999	<0.001*
Population	0.292	0.014*	0.016*	0.532	0.607	0.886
Month	<0.001*	0.029*	0.010*	0.112	0.909	0.913
log [CO_2]	<0.001*	0.002*	0.015*	0.911	1.000	1.000
Population X Month	<0.001*	0.398	0.366	0.333	0.935	0.882
Population X log [CO_2]	0.086	0.002*	0.017*	0.045*	0.597	0.968
Month X log [CO_2]	<0.001*	0.299	0.072	0.054	0.909	0.978
Population X Month X log [CO_2]	<0.001*	0.608	0.237	0.455	0.959	0.956

SBV exhibited higher growth rates under CO_2 enrichment during late summer and early fall of 2013, even when water temperature exceeded the 25° C threshold for eelgrass heat stress (Figs. 5a-b). In contrast, DBW relative growth rate decreased by August 2013 and became negatively related to CO_2 availability and high temperatures but then in September 2013, followed the same response as SBV. The growth-stimulating effect of increasing [CO_2] observed in late summer and fall declined in winter for SBV and DBW in response to low light and cold temperatures, then recovered as temperature and light availability increased during spring 2014 (Figs. 5a-b, Tables 1, 2). In contrast, growth rates of NBW eelgrass declined across all CO_2 treatments throughout the summer of 2013 and did not recover (Fig. 5c, Table 3). Consequently, rates of relative shoot growth (but not absolute growth) became significantly lower for NBW than for DBW and SBV by July 2013 and continued to decline through September 2013. During this period (September 2013), DBW growth rates increased across treatments and SBV showed its seasonal growing pattern confirmed by the significantly higher slopes of DBW and SBV than NBW, -0.08 and 0.06 respectively (Figs. 5a-c, white symbols and lines, Table 4). Monthly slopes statistics of the relative growth rates vs. log [CO_2] derived from linear regression analysis showed that the slopes of the three populations were not different from zero throughout the experiment (Appendix Table 30).

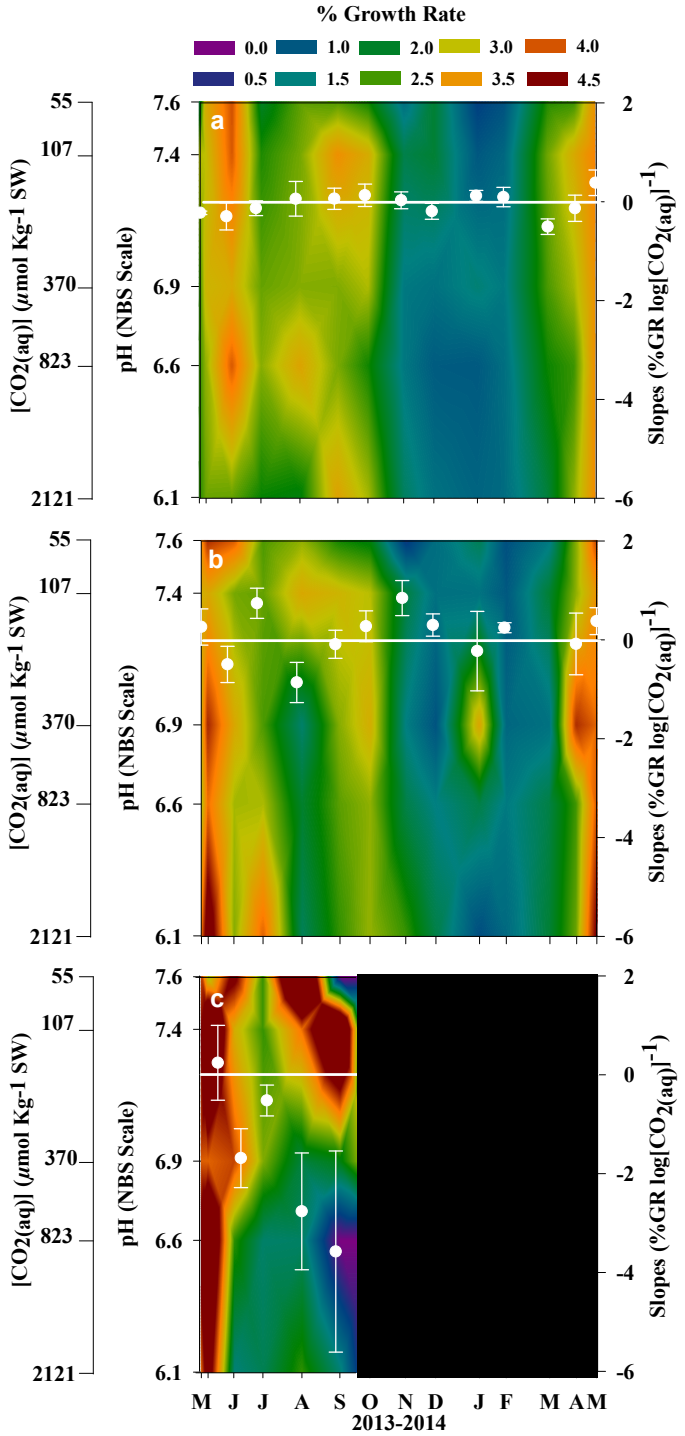

Figure 5. Heat maps of percent growth rates as a function of pH/CO_2 treatment and time. (a) South Bay, VA. (b) Dumas Bay, WA. (c) Nisqually Bay, WA. Tick marks on the left vertical axis of each plot indicate the mean pH/CO_2 value for each treatment. Tick marks on the right vertical axis of each plot indicate the values of the slopes. White horizontal line represents the zero slope. White symbols represent the monthly slope of the absolute growth rates vs. log [CO_2] derived from linear regression analysis for each CO_2 treatment. Black panel represents no data. Error bars represent ± 1 SE of the regression slope.

Plant Size

Initially, Puget Sound WA plants were much larger than VA plants. Some WA plants exceeded 1m in length and 0.3-0.5 cm in width while Chesapeake region eelgrass leaves reached about 30 cm in length and 0.1-0.5 cm in width. As with growth rates, plant sizes of the SBV and DBW shoots sizes started to increase with CO_2 availability throughout the summer and early fall 2013 when water temperature were above 25° C and decreasing during the winter of 2014 when light levels were low, temperatures were cold and CO_2 had no effect (Fig 6a-b,Tables 1, 2). However, only SBV showed slopes different from zero from October 2013 to February 2014 (Appendix Table 31). The significant CO_2 effect returned in spring for SBV as growth rates and plant sizes increased with warmer temperatures, longer days and higher irradiances (Figs.6a-b, 2, 3). At over 70 cm^2 $shoot^{-1}$, NBW plants were initially much larger than DBW or SBV, and decreased in size right after being transplanted into the experimental aquaria in May and June 2013 (Fig. 6c). However, in July 2013 CO_2 availability had a positive effect on the size of NBW shoots, but afterwards size started to decrease again when temperatures exceed the 25° C stress threshold for four consecutive weeks between August and September 2013 (Figs. 2, 6c, Table 3).

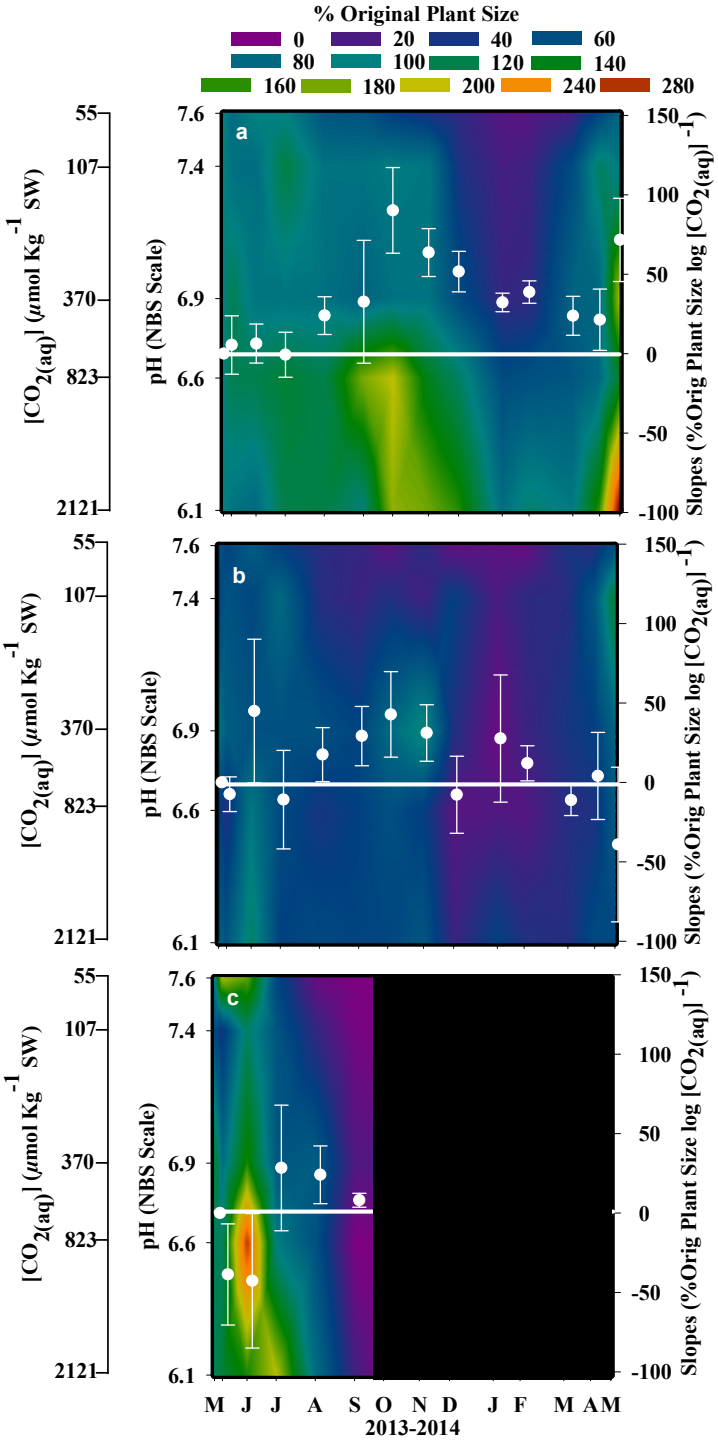

Figure 6. Heat maps of percent of original plant size as a function of pH/CO_2 treatment and time. (a) South Bay, VA. (b) Dumas Bay, WA. (c) Nisqually Bay, WA. Tick marks on the left vertical axis of each plot indicate the mean pH/CO_2 value for each treatment. Tick marks on the right vertical axis of each plot indicate the values of the slopes. White horizontal line represents the zero slope. White symbols represent the monthly slope of the percent of original plant size vs. log [CO_2] derived from linear regression analysis for each CO_2 treatment. Black panel represents no data Error bars represent ± 1 SE of the regression slope.

Leaf Sugar

Sugar content of SBV and DBW leaves increased 2 to 3 fold under high CO_2 availability (Fig 7a-b). However, SBV leaves maintained higher sugar concentrations (a measure of labile carbon reserves) than eelgrass from both WA populations during summer and winter. During summer SBV leaf sugar concentration in the highest CO_2 treatment was 1.7 and 2.5-fold higher than DBW and NBW, respectively. During winter, SBV leaf sugar was 2 times higher than DBW (Fig. 7, Table 4). However the monthly trends of leaf sucrose did not differ among populations where plants under high CO_2 accumulated more sugar (Table 4). In general, the monthly trends demonstrated a sinusoidal pattern, showing a CO_2 effect during summer, but not in the winter, which is consistent with the observed patterns in growth. The effect of CO_2 on sugar content was most pronounced during August 2013 for SBV and July 2013 for DBW (white symbols, Figs.7a-b, Tables 1 and 2).

Sugar concentrations increased in all CO_2 treatments during March for SBV and January 2014 for DBW (Figs.7a-b, Tables 1 and 2), when temperature, shoot proliferation and growth were the lowest (Figs 2, 4a-b, 5a-b). The relationship between leaf sugar and CO_2 for SBV was different from zero most part of the experiment (Appendix Table 32) and remained positive throughout the duration of the experiment (white symbols, Fig 7a). Monthly slopes statistics of the sucrose concentration vs. log [CO_2] for DBW was different from zero during July and September 2013 (Appendix Table 32). However, the sugar content of DBW leaves decreased during December 2013 becoming negatively related to CO_2 availability in conjunction with decreasing temperature and growth decreased (Figs. 1, 5b, white symbols 7b). Then in January of 2014, DBW sugar concentrations started to increase across all CO_2 treatments and become significantly different from zero in April 2014 (white symbols, Figs.7b, Appendix Table 32).

Although survival and growth of NBW shoots did not respond positively to CO_2 availability, leaf sugar content did (Fig.7c). Differences across CO_2 treatments were most pronounced during September 2013 when sucrose concentration in the highest CO_2 reached 500 μmol g^{-1} DW. The relationships (slopes) between CO_2 treatment and NBW leaf sugar were positive but not different from zero throughout the experiment, indicating accumulation of sugar under high CO_2 in September 2013 (white symbols, Fig.7c, Appendix Table 32). Despite the accumulation of carbon reserves in response to [CO_2], NBW plants did not survive beyond September 2013.

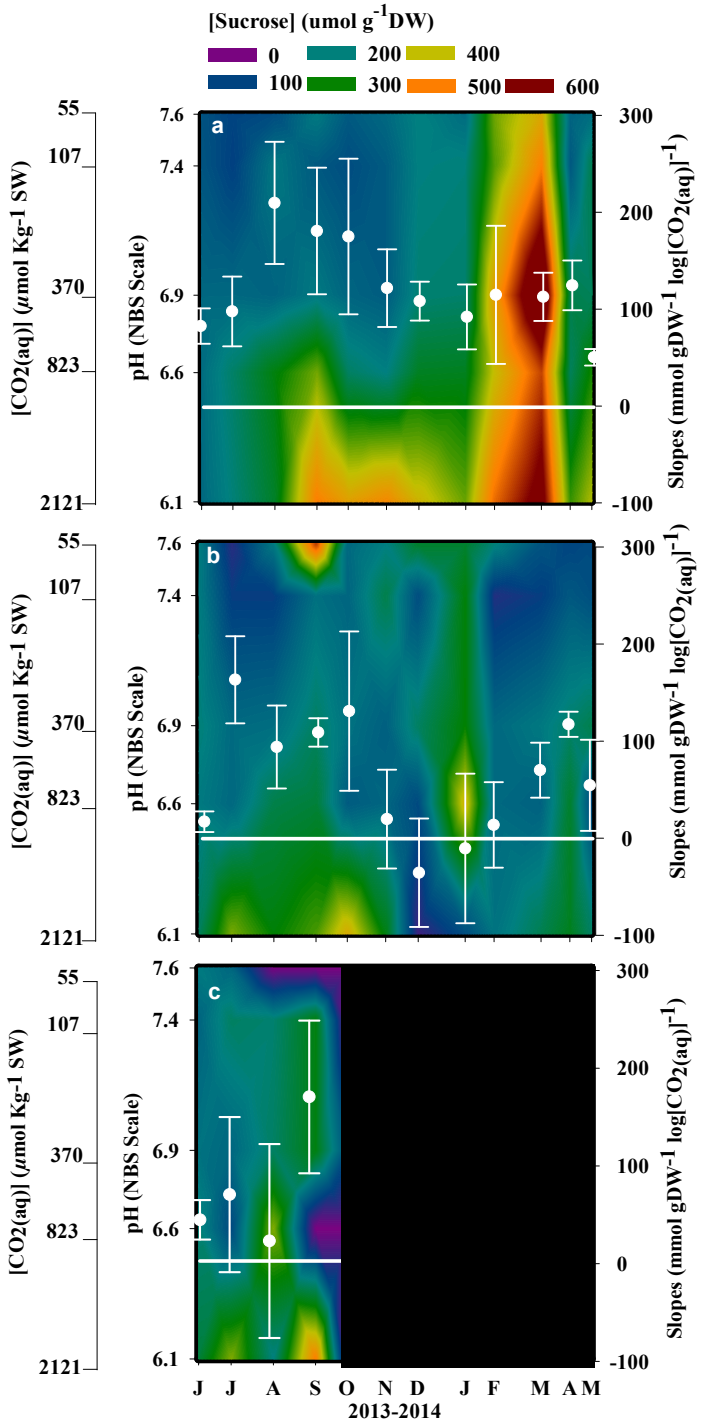

Figure 7. Heat maps of leaf sucrose concentration as a function of pH/CO_2 treatment and time. (a) South Bay, VA. (b) Dumas Bay, WA. (c) Nisqually Bay, WA. Tick marks on the left vertical axis of each plot indicate the mean pH/CO_2 value for each treatment. Tick marks on the right vertical axis of each plot indicate the values of the slopes. White horizontal line represents the zero slope. White symbols represent the monthly slope of the leaf sucrose concentration vs. log [CO_2] derived from linear regression analysis for each CO_2 treatment. Black panel represents no data. Error bars represent ± 1 SE of the regression slope.

Metabolic Rates

Instantaneous rates of gross photosynthesis (P_g) measured in air-saturated seawater ([CO_2] = 15 μM) increased with temperature up to 30° C across all CO_2 treatments for all populations (Figs.8a, Table 5). Similarly, the slopes of the log-transformed rate of P_g response to temperature were not different across all CO_2 treatments and populations (Table 5, Fig.8b). Leaf respiration (R) also increased with temperature up to 30° C and showed no significant differences among populations or CO_2 treatment (Fig. 9a). The slopes of the log-transformed rate of R to temperature showed no significant difference across populations from different CO_2 conditions even when measured at ambient CO_2 in the oxygen chamber showing no significant evidence of thermal stress for the populations (Table 6, Fig.9b).

As a result of the similarity among the slopes of temperature-dependent leaf respiration and gross photosynthesis among populations and despite the high variability of the SBV population, the ratio of P_g:R showed almost no change with temperature. Moreover, plants grown across the CO_2 treatments also showed no particular effect of temperature on P_g:R (Figs. 10a-b, Table 7).

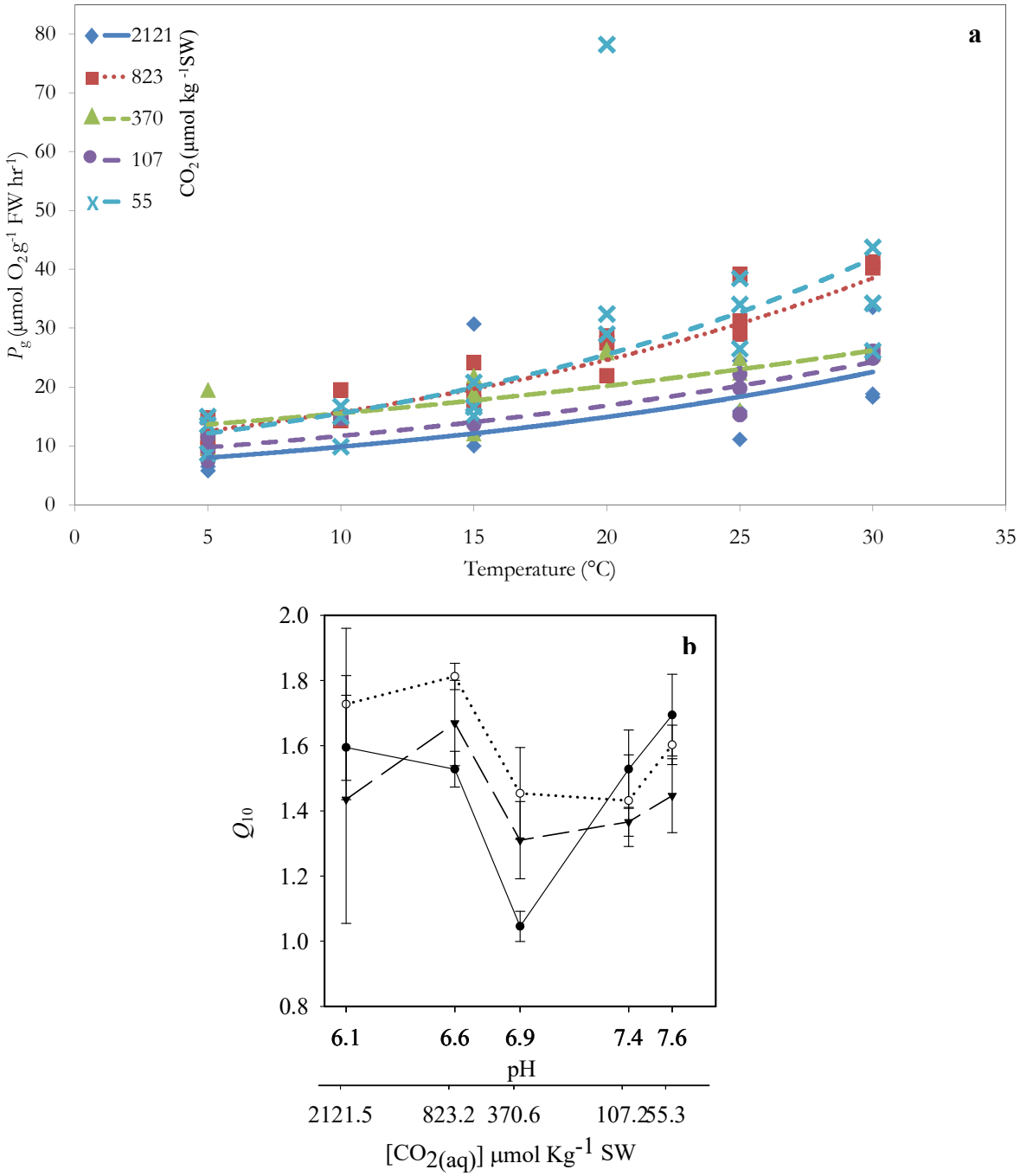

Figure 8. (a) Effect of short-term temperature exposure on gross photosynthesis, P_g, of *Z. marina* leaves grown at (˙˙×˙˙) 55, (- -●- -) 107, (---▲---) 370, (˙˙˙■˙˙˙) 823, and (–♦–) 2121 µmol CO_2 Kg^{-1} SW and measured at ambient CO_2 conditions. (b) Q_{10} of gross photosynthesis resulting from the slope of the log P_g vs. temperature for each growth pH/CO_2 treatment (–●–) South Bay VA, (˙˙˙○˙˙˙) Dumas Bay WA, (–▲–) Nisqually Bay WA. Error bars represent ± 1 SE of the Q_{10} calculated from the slope.

Table 5. Linear mixed model with repeated measures results for comparison of log P_g among populations. Log P_g ANCOVA table for Type III tests of fixed effects using the mixed linear model routine implemented in SPSS. [CO_2] and population were treated as fixed factors with temperature as the covariate.

Source	**Numerator *df***	**Denominator *df***	***F***	***p***
Intercept	1	147	770.201	<0.001*
Population	2	147	1.270	0.284
Temperature	1	147	110.703	<0.001*
Population X Temperature	2	147	1.511	0.224
[CO_2] X Temperature	4	147	1.495	0.207
Population X [CO_2]	12	147	0.961	0.488
Population X [CO_2] X Temperature	8	147	0.464	0.879

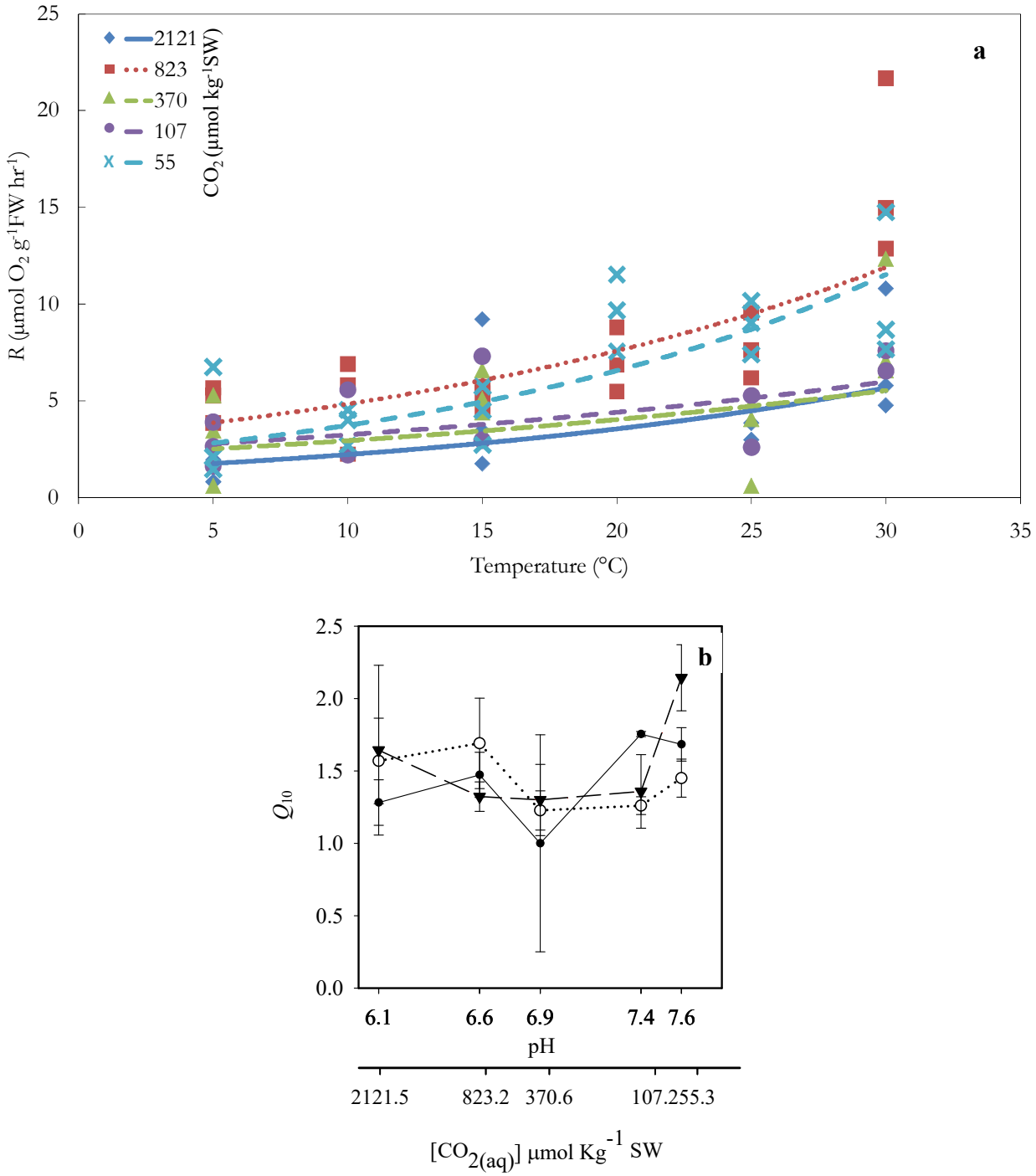

Figure 9. (a) Effect of short-term temperature exposure on respiration, *R*, of *Z. marina* leaves grown at (···×···) 55, (- -●- -) 107, (---▲---) 370, (···■···) 823, and (–♦–) 2121 μmol CO_2 Kg^{-1} SW and measured at ambient CO_2 conditions. (b) Q_{10} of the respiration rates resulting from the slope of the log *R* vs. temperature for each growth pH/CO_2 treatment (–●–) South Bay, VA (···○···) Dumas Bay, WA (–▲–) Nisqually Bay, WA. Error bars represent ± 1 SE of the Q_{10} calculated from the slope.

Table 6. Linear mixed model with repeated measurements results for comparison of log *R* among populations. Log *R* ANCOVA table for Type III tests of fixed effects using the mixed linear model routine implemented in SPSS. [CO_2] and population were treated as fixed factors with temperature as the covariate.

Source	Numerator *df*	Denominator *df*	*F*	*p*
Intercept	1	145	28.172	<0.001*
Population	2	145	0.087	0.917
Temperature	1	145	31.884	<0.001*
Population X Temperature	2	145	0.397	0.673
[CO_2] X Temperature	4	145	2.263	0.065
Population X [CO_2]	12	145	0.874	0.575
Population X [CO_2] X Temperature	8	145	0.817	0.588

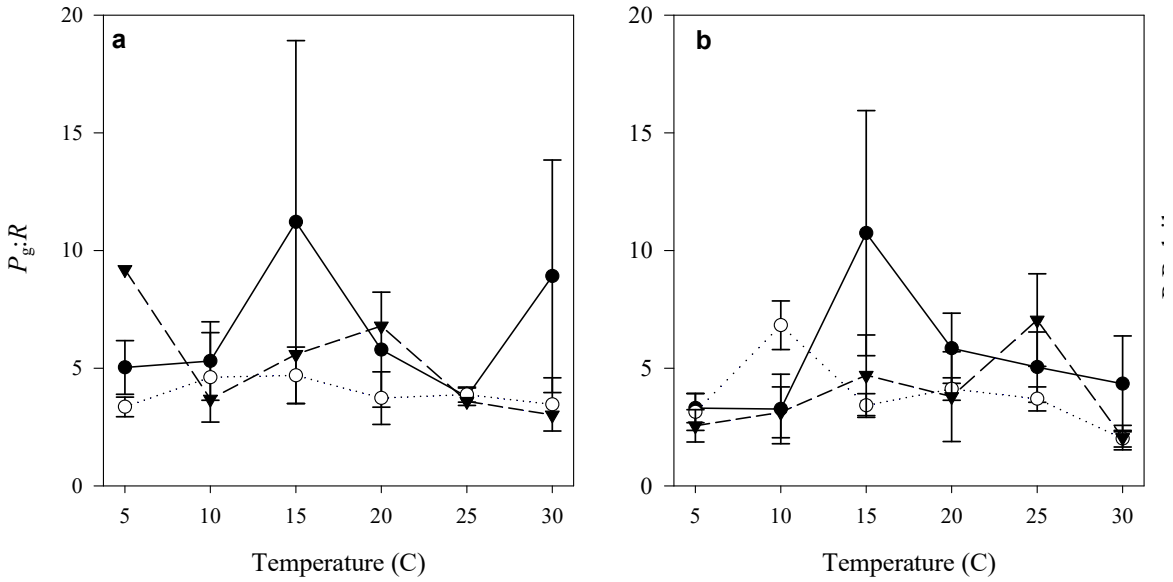

Figure 10. Calculated ratio of gross photosynthesis to dark respiration as a function of temperature from eelgrass grown at (a) low CO_2 and (b) high CO_2, measured at ambient CO_2 conditions in the oxygen electrode. Error bars represent ±1 SE. (–●–) South Bay VA, (···○···) Dumas Bay WA, (–▲–) Nisqually Bay, WA.

Table 7. Linear mixed model with repeated measurements results for comparison of $\underline{P_g:R}$ among populations. $P_g:R$ ANCOVA table for Type III tests of fixed effects using the mixed linear model routine implemented in SPSS. [CO_2] and population were treated as fixed factors with temperature as the covariate.

Source	Numerator *df*	Denominator *df*	*F*	*p*
Intercept	1	93	12.523	<0.001*
Population	2	93	0.708	0.495
[CO_2]	4	93	0.129	0.971
Temperature	1	93	0.115	0.735
Population X [CO_2]	8	93	0.084	1.000
Population X Temperature	2	93	0.238	0.789
[CO_2] X Temperature	4	93	0.828	0.511
Population X [CO_2] X Temperature	8	93	0.281	0.971

Photosynthetic Pigments

At the beginning of the experiment in May 2013 leaf total chlorophyll concentrations were equal across treatment but different among populations where SBV started with a higher chlorophyll concentration (28.72 μg Chl cm^{-2}) than DBW (20.08 μg Chl cm^{-2}) and NBW (23.64 μg Chl cm^{-2}) eelgrass. However, the total chlorophyll (Chl *a* + *b*) decreased with increasing CO_2 availability in all populations even though they were exposed to the same light environment (Figs. 11a-c, Tables 4-6). The three populations showed chlorophyll concentrations increasing with temperature (Fig.3) and irradiance (Fig.2) during August and September 2013 when sucrose differences across CO_2 treatments were most pronounced (Fig.7). Monthly slopes between total chlorophyll vs log [CO_2] were not different among populations (Table 7). Ratios of Chl *a:b* did not respond to CO_2 enrichment in any of the populations during summer (Figs. 12a-c, Tables 1-4).

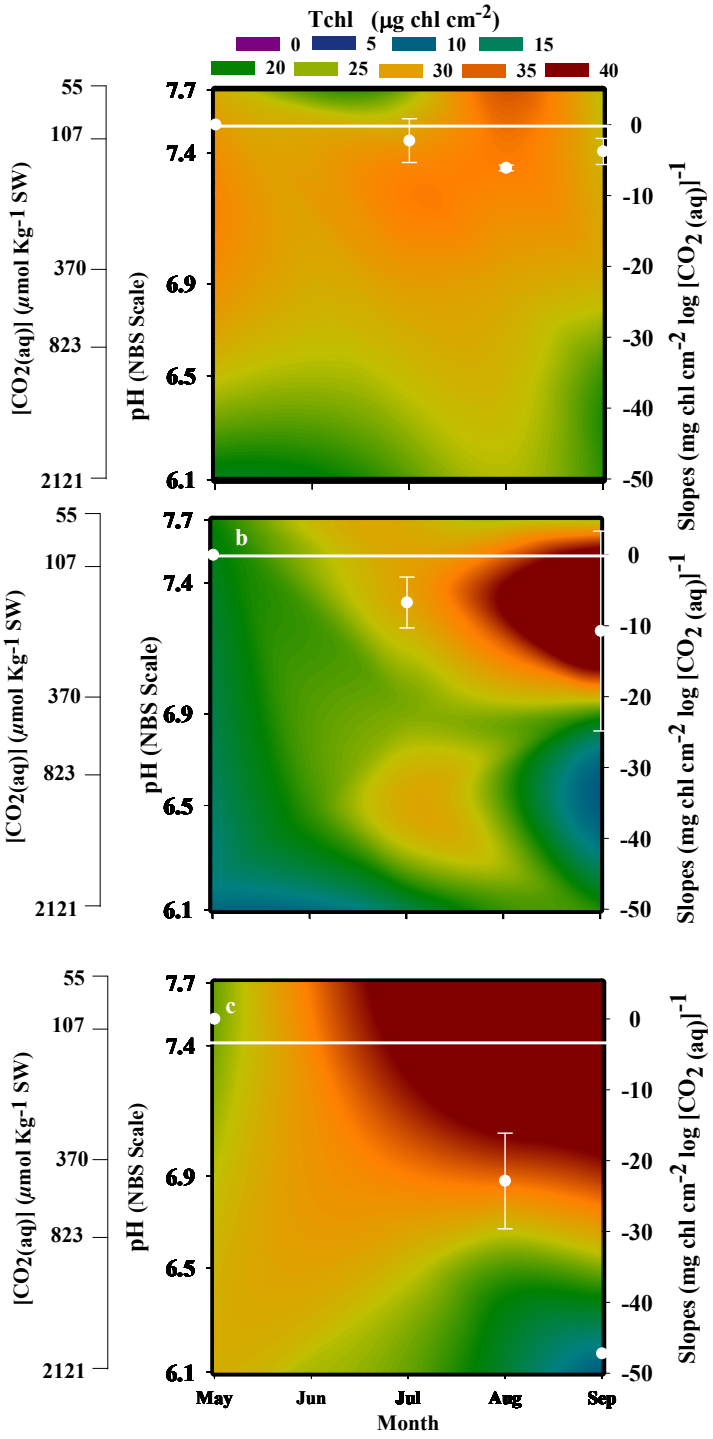

Figure 11. Heat maps of photosynthetic pigments per leaf area as a function of pH/CO_2 treatment and time. (a) South Bay, VA. (b) Dumas Bay, WA. (c) Nisqually Bay, WA. Tick marks on the left vertical axis of each plot indicate the mean pH/CO_2 value for each treatment. Tick marks on the right vertical axis of each plot indicate the values of the slopes. White horizontal line represents the zero slope. White symbols represent the slope effects of CO_2 enrichment on chlorophyll content as a function of the leaf area from linear regression analysis for each CO_2 treatment. Error bars represent ± 1 SE of the regression slope.

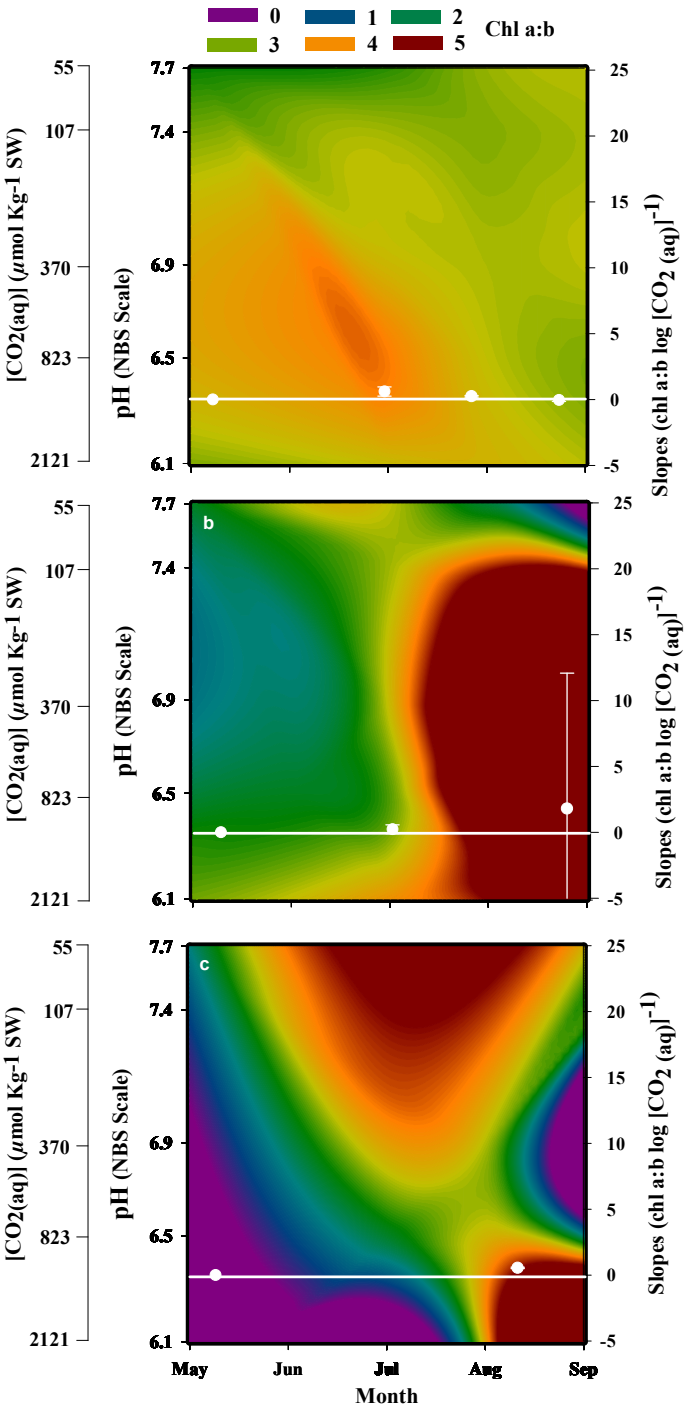

Figure 12. Heat maps of photosynthetic pigments chl a:b as a function of pH/CO_2 treatment and time. (a) South Bay, VA. (b) Dumas Bay, WA. (c) Nisqually Bay, WA. Tick marks on the left vertical axis of each plot indicate the mean pH/CO_2 value for each treatment. Tick marks on the right vertical axis of each plot indicate the values of the slopes. White horizontal line represents the zero slope. White symbols represent the monthly slopes of the Chl a:b vs. log [CO_2] derived from linear regression analysis for each CO_2 treatment. Error bars represent ± 1 SE of the regression slope.

Discussion

The experimental results revealed important differences in the combined responses of the three eelgrass populations to CO_2 availability and temperature. All populations revealed significant positive effects of CO_2 on leaf sucrose, but the local population, SBV, was most responsive to CO_2 availability in terms of whole plant survival, shoot size and growth. CO_2 also helped eelgrass from the cool waters of DBW to survive summer temperatures exceeding the 25° C threshold, as evidenced by increased shoot numbers, growth, plant size and sucrose concentration, even if they did not respond as well as SBV. On the other hand, the survival and growth of NBW eelgrass did not respond positively to the CO_2 treatment even though plants did not show significant evidence of metabolic stress (>1 P_g:R) relative to the other eelgrass populations. These differences suggest some degree of ecotypic differentiation/adaptation to local conditions, some of which may be related to carbon balance but some of which appear to be related to other processes not yet determined.

It has been demonstrated both theoretically and experimentally that CO_2 could counteract the impacts of high temperature on eelgrass (Zimmerman et al. 2015, Zimmerman et al. 2017), but there appear to be signficant differences on the CO_2 effect on eelgrass distributed throughout the Northern Hemisphere affecting resilience to temperature stress (Backman 1991, van Lent & Verschuure 1994, Olsen et al. 2004). Throughout summer water temperature in the experiment aquaria was 15° C higher than the temperature in Washington eelgrass natural habitat, and was above the 25º C temperature threshold for 97 days. Prolonged thermal stress above 25° C has been shown to trigger die-backs when P_g:R is <1 (Evans et al. 1986, Zimmerman et al. 1989, Ehlers et al. 2008). In terms of carbon balance, the three populations were consistent showing no differences in P_g:R, all above 1, and sugar accumulation during summer under high CO_2,

however the relative speed of NBW demise suggests an acute direct response to temperature. The specific cause of the NBW mortality is unknown and may also relate to differences in photosynthetic performance after the heat stress which was not measured in this experiment. In essence, after the heat stress when temperatures were falling, NBW plants could be diverting energy towards respiration or storage and experiencing low optimum temperatures for growth (Marsh et al. 1986, Campbell et al. 2006, Winters et al. 2011). On the other hand, the increased plant size, growth, sucrose, and shoot proliferation in SBV and DBW suggest that the CO_2 enhancement was able to compensate for temperature stress by increasing the availability of labile carbon reserves required for growth and repair. Eelgrass studies had shown an increase in carbon balance in plants grown in elevated CO_2 conditions in comparison to plants grown in low CO_2 when measured at their respective growth conditions (Zimmerman et al. 1997, Invers et al. 2001, Palacios & Zimmerman 2007, Zimmerman et al. 2017).

Studies with Atlantic and Pacific Ocean eelgrass populations indicate that the degree of population genetic variability is location dependent (Ort et al. 2012). Along with displaying higher survival and bigger changes in growth among populations, Virginia eelgrass from the Chesapeake Bay and the Atlantic have low genetic diversity (Williams & Orth 1998, Olsen et al. 2004, Rhode & Duffy 2004) than populations from the east Pacific (Olsen et al. 2004) and Puget Sound (Ruckelshaus 1998). High genetic diversity in the Pacific eelgrass suggest that these plants may be adapted to localized conditions that could not transfer to other sites, although those with lower diversity tend to be more vulnerable to extinction (Beardmore 1983), may be more generalists, and therefore able to tolerate a broader range of environmental conditions. Species with a wide distribution like eelgrass suggests that populations adapted to locally warm climates should have a higher thermal tolerance than populations from colder climates, having the

potential for genetic rescue against high temperatures and increasing the fitness of endangered populations (Davis & Shaw 2001, Whiteley et al. 2015). Thus, high temperature water conditions in the Mid Atlantic appear to increase Virginia eelgrass population thermal tolerance due to local adaptation suggesting greater capacity for thermal acclimation under high CO_2. On the other hand, NBW plants survival response suggests dissimilarity in the recovery regardless of the CO_2 treatment, where this population coming from a cooler environment declined even after water temperatures started to drop, while Dumas Bay and South Bay eelgrass did not show signs of thermal stress.

European eelgrass also showed survival differences among populations and differential expression of genes that regulate the stress response and subsequent recovery from thermal stress (Bergmann et al. 2010, Winters et al. 2011, Gu et al. 2012, Franssen et al. 2014, Jueterbock et al. 2016). However, gene expression comparison among these eelgrass populations showed the same patterns where stress genes were affected by temperature and sucrose but did not respond to CO_2 enrichment (Chapter 4). Moreover we also know that CO_2 provides stress relief for these populations by increasing Calvin Cycle and nitrogen assimilation metabolites although the degree of relief differs among eelgrass populations (Zayas-Santiago et al. 2020).

In general, eelgrass biomass allocation in response to CO_2 availability depends upon the population. The eelgrass population from Elkhorn Slough, CA showed no difference in above ground biomass, but large differences in below ground biomass (Palacios & Zimmerman 2007) while SBV population used here showed a nearly allometric increase in both above and below ground biomass (Zimmerman et al. 2017). The response to temperature stress under high CO_2 of NBW revealed a biomass loss expressed in decreased size and growth and increased leaf sucrose similar to *Cymodocea nodosa* under 6-wk thermal stress (Marín-Guirao et al. 2018). However,

under heat stress eelgrass mobilize soluble sugars, amino acids and organic acids stored in below-ground tissues (Staehr & Borum 2011, Gao et al. 2019, George 2019) important for growth and coping with stress (Gu et al., 2012; Rolland et al., 2006). This important carbon and nitrogen mobilization could indicate that during and after the heat stress regardless of CO_2 availability, NBW rhizomes may have transferred compounds towards the few standing shoots and might not be enough to support growth under thermal stress. Furthermore, NBW may have increased photorespiratory and stress-related compounds resembling its counterpart DBW under high CO_2 (Zayas-Santiago et al. 2020).

Although shoot survival differed significantly among the three populations, they all showed the same decrease in leaf chlorophyll content under high CO_2 conditions. These long-term results conflict with a short-term experiments (days) in which genes coding for carbon fixation and light reactions increased in response to CO_2 availability (Ruocco et al. 2017) suggesting an increase in sucrose production and chlorophyll. However, while sucrose increase was evident in this experiment, leaf pigment content decreased under high CO_2 when exposed to long-term (months) CO_2 availability suggesting that it may be triggering photoacclimation mechanisms (Celebi et al. 2021) caused by the higher redox state of thylakoid membranes of the plants exposed to high CO_2 (Eberhard et al. 2008, Pfannschmidt & Yang 2012).

Differences in initial plant size and the positive response to CO_2 availability under thermal stress of one of the populations from the cooler environment, DBW, suggest differentiation along the Puget Sound coast likely due to other environmental factors (e.g. water temperature fluxes, differences in exchange water flow with oceanic waters, nutrient inputs, etc.). Although the WA populations experience similar water temperature patterns throughout the year (Roberts 2014), other environmental conditions, such as prevailing winds and local water movement can

contribute to fine-scale population genetic structure in seagrasses (Backman 1991, Oliva et al. 2014, Sinclair et al. 2014).

The survival dissimilarity among population is not linked to loss of basic metabolic functions during summer, therefore suggesting differences in the acclimation ability of *Z. marina* populations. Perhaps seagrasses populations with large plants sizes and thick rhizomes, require stable environments to support their growth while smaller plants grow in frequently disturbed habitats because they have the potential to develop during short time intervals between disturbances as previously found in studies between seagrass species (Duarte 1991). Therefore, *Z. marina* with large plants sizes might improve their performance reducing sensitivity to heat stress (Staehr & Borum 2011, Jueterbock et al. 2016) under slow environmental changes (short-term high-temperature) if other factors are not limited (i.e. light, nutrients, DIC) (Alexandre et al. 2012, Beca-Carretero et al. 2018).

Differences in population survival responses to CO_2 availability observed here point to differences in the acclimation ability of the populations. However, a full understanding of whole-plant responses to climate-driven environmental change requires us to link environment influences on whole plant performance to changes in the transcriptome and the metabolome that ultimately drive plant performance. Such knowledge will help predict earth system interactions in the context of global cycles and help inform best practices for seagrass restoration.

CHAPTER 3

METABOLOMICS REVEAL BIOCHEMICAL PATHWAYS RESPONSIBLE FOR EELGRASS RESPONSE TO CLIMATE CHANGE

Introduction

Metabolomics is a field of the biological sciences studies based on the simultaneous measurement of multiple metabolites, using analytical chemistry techniques such as mass spectrometry and/or NMR spectroscopy, followed by statistical analysis like multivariate or repeated univariate tests (Bundy et al. 2008). The metabolome consists of thousands of low molecular weight metabolites (typically <800 Da) such as amino acids, organic acids, sugars and phenolic compounds derived from primary and secondary cellular metabolism. There are two types of metabolomic analysis: targeted and untargeted. Targeted metabolomics refers to the detection and precise quantification of known compounds and requires the availability of the purified form (Cambiaghi et al. 2016). Currently, only few purified standards are identified and available for a calibration process limiting a comprehensive analysis of the metabolome (Cambiaghi et al. 2016). On the other hand, the untargeted approach, also called 'metabolite fingerprinting', is used for comprehensive metabolome comparison examining the metabolite variations as changes of chromatographic patterns without previous knowledge of the compounds (Cambiaghi et al. 2016). Therefore, metabolite profiling provides a snapshot of the chemical composition of a sample at a given moment in time. Interpreting metabolomic data is essential to relate the metabolite to both biochemical causes and physiological consequences (Mehrotra & Mendes 2006).

Plant response to environmental changes involve an array of biochemical, molecular and metabolic processes. The metabolome of an organism is considered its chemical phenotype

(Fiehn 2002) as it is the first component responding to external stressors (Gargallo-Garriga et al. 2018). Therefore the accumulation and/or deficiency of metabolites are believed to play adaptive roles in plant stress tolerance. Previous studies have demonstrated that increasing concentrations of CO_2 in Earth's atmosphere and oceans produce significant impacts on seagrasses physiology. For example, enhanced photosynthesis stimulated by rising CO_2 availability can offset the effects of thermal stress for seagrasses such as eelgrass (*Zostera marina* L.) (Palacios & Zimmerman 2007, Zimmerman et al. 2017). However, ssignificant variation exists in the physiological level of responsiveness of eelgrass populations to CO_2 availability (Chapter 2). However, the extent to which *Z. marina* physiological plasticity is grounded in molecular regulation remains largely unknown.

This study evaluated the metabolic profiling of two distinct eelgrass populations from contrasting thermal environments (Puget Sound, Washington and Chesapeake Bay, Virginia, USA) subjected to an experimental gradient of increased CO_2 conditions in the context of a seasonal temperature cycle. The hypothesis of this study is that increased CO_2 availability should stimulate carbon fixation pathways and reduce the biosynthesis of stress-related compounds. Consequently, differential responses among populations may help examine how the environment influences critical downstream performance features linked to plant survival of these important ecosystem engineers.

Materials and Methods

Tissue Collection, Storage and Processing

As previously stated (Chapter 2), one leaf sample (2nd youngest leaf) was collected monthly at random from each plastic container (three plastic containers for SBV and one for DBW in every aquarium) across the gradient in CO_2 treatments. Epiphytes were removed by gently scraping each leaf with a clean razor blade, followed by a brief rinse in 0.2 μm-filtered seawater. The clean leaves were patted dry with a tissue, flash frozen in liquid nitrogen and stored at -80° C.

Due to limited access to the instrumentation, only one set of samples was analyzed. Leaves collected on May 2014 from SBV and DBW, after a year acclimated to CO_2 exposure, were shipped overnight on dry ice to the Environmental and Molecular Sciences Division of the Pacific Northwest National Laboratory (EMSL, U.S. Dept. of Energy) in Richland WA, where the metabolite analyses were performed. This set of samples did not include NBW due to high mortality of these plants after experiencing 97 days of temperatures above their threshold in September 2013. The set of samples included SBV eelgrass populations under five CO_2 concentrations (55, 107,370,823, 2121 μmol CO_2 Kg^{-1} SW) and DBW leaves under low CO_2 (107μmol CO_2 Kg^{-1} SW, pH ~7.5) and high CO_2 (823μmol CO_2 Kg^{-1} SW, pH ~6.5). The frozen leaf samples were lyophilized for at least 48 h and powdered using a ball mill. The powdered samples were then incubated in methanol/deionized water (4/1 v/v) at 10° C on an orbital shaker (1 h) and followed by gentle sonication for 2 min using a Branson ultrasonic cleaner (40 kHz). The extracts were centrifuged and the supernatants transferred to pre-combusted (450° C for 8 h) amber glass vials for metabolite analysis. Three solvent-only vials were prepared using only methanol/deionized water (no plant material) processed as above.

GC-MS Analysis

50 μL of eelgrass extract from each sample was dried and subsequently derivatized in two different steps (Kim et al. 2015). First, compounds were derivatized to a trimethylsilyl ester form using methoxyamine in pyridine solution (30 mg/mL). Briefly, 20 μL of methoxyamine solution was added to each dried extract and samples were incubated at 37° C during 90 min in a Thermomixer operating at 1,200 rpm. Later, amine, carboxyl and hydroxyl groups were derivatized using 80 μL of MSTFA (N-Methyl-N-(trimethylsilyl) trifluoroacetamide), subsequently incubated at 37° C for 30 min at 1,200 rpm. All extracts were subsequently vortexed for 10 s and centrifuged at 2,750 × g for 5 minutes and supernatants were used for GC-MS analyses.

GC-MS analyses were performed using an Agilent GC 7890A equipped with an HP-5MS column (30 m × 0.25 mm × 0.25 μm; Agilent Technologies) coupled to a MSD 5975C mass spectrometer (Agilent Technologies, Santa Clara, CA). The injection port temperature was 250° C. Injection volume was set at 10 μL and split-less (most sensitive GC-MS mode where the entire sample vaporized in the injector goes onto the column). The column was maintained at 60° C for 1 min and then increased at a rate of 10° C min^{-1} to 325° C during the following 26.5 min and held for 10 min. Experimental blanks from the solvent-only vials were injected every 15 samples and a mixture of fatty acid methyl esters (FAMEs; C8-C28) was analyzed at the beginning of the sequence.

Chromatograms were deconvoluted and calibrated according to the retention indices (RI) from the FAME (Fatty Acid Methyl Ester) mixture. Metabolite identification was conducted by matching mass spectra and RIs to an updated version of FiehnLib database (Kind et al. 2009).

Assigned metabolites were subsequently validated using fragmentation spectra from the National Institute of Standards and Technology library (NIST14 GC-MS library). Parameters used in the metabolite detector are shown in Appendix Table 35. Metabolite matching information in GC-MS is shown in Appendix Table 36 and more details as previously described (Kim et al. 2015).

LC-MS Analysis

LC-MS analyses were performed using a Vanquish ultra-high pressure liquid chromatography system (UHPLC) coupled to an LTQ Orbitrap Velos mass spectrometer equipped with heated electrospray ionization (HESI) source (Thermo Fisher Scientific, Waltham, Massachusetts, USA). Chromatography was performed with a Hypersil gold C18 reversed-phase column (150 × 2.1 mm, 3μ particle size; Thermo Scientific, Waltham, Massachusetts, USA) operating at 30° C. Mobile phases consisted of 0.1% formic acid in water (A) and 0.1% formic acid in acetonitrile/water (90:10) (B). The injection volume was 5 μL and flow rate was constant at 0.3 mL min^{-1}. The elution gradient started at 90% A (10% B) constant for 5 min and then linearly changed to 10% A (90% B) during the following 15 min. Those conditions were held for 2 min before returning to initial conditions during the consecutive 2 min. The column was washed and stabilized for 11 min. All samples were injected in both negative (-) and positive (+) ionization modes. The MS operated at a resolution of 60,000 in Fourier Transform Mass Spectrometry (FTMS) full-scan mode measuring a mass range of 50 to1000 m/z (Rivas-Ubach et al. 2016). Experimental blanks from the solvent-only vials were injected every 15 samples.

LC-MS negative and positive chromatograms were separately processed with MZmine 2.26 (Pluskal et al. 2010). Chromatograms were baseline corrected, deconvoluted, aligned and metabolic features were assigned to metabolites according to retention time (RT) and exact mass

of standard compounds included in the EMSL in-house library (second level identification according to Sumner et al. 2007). The parameters used for the extraction of the metabolic fingerprints are given in Appendix Table 37. Metabolite matching information in LC-MS is shown in Appendix Table 38.

Statistical Analysis

The final metabolomic dataset was composed of two categorical factors (Population and CO_2 treatment) and 5757 continuous variables (metabolomic features), including 133 metabolites identified by the LC-MS and GC-MS libraries. Full factorial permutational multivariate analyses of variance (PERMANOVA Population + CO_2 + Population × CO_2) were performed to test for overall metabolomic differences between populations and CO_2 levels. Since DBW population had a low number of replicates in some CO_2 treatments, only two levels of CO_2 (823 and 107 μmol $CO_2 \cdot Kg^{-1}$ SW) were examined here to maintain analytical consistency for both populations with respect to the full PERMANOVA model. Additional PERMANOVAs were performed to test for overall differences for CO_2 treatments within each eelgrass population. All PERMANOVAs were computed using the Euclidean distance and 10,000 permutations. Each dataset (SBV +DBW, SBV alone, and DBW alone) were subsequently subjected to principal component analysis (PCA) to explore the overall metabolomic variability of the study cases.

Results and Discussion

Morphology and whole plant performance

CO_2 enrichment yielded strong positive effects on individual shoot size, vegetative shoot numbers (shown as % survival) and sucrose content of both populations during the 12-month CO_2 exposure (Figs 4, 6, 7). However, plants from SBV showed larger changes in size and leaf sucrose concentration compared to those from DBW (Figs. 6, 7 a, b, and Table 4). High [CO_2] also stimulated vegetative shoot survival in both eelgrass populations throughout the entire experiment, in May 2014 the highest CO_2 treatment shoot numbers doubled through vegetative proliferation. However, shoot numbers decreased under ambient [CO_2] during summer for both eelgrass populations as water temperature increased and into the winter of 2014 having less than half of the originally transplanted shoots in May 2014. During May 2014 SBV increased in size and growth and decreased leaf sugar concentrations. DBW showed no changes in size but a decreased in leaf sucrose across CO_2 treatments (Fig. 5 a, b, Fig.6 a, b white symbols and lines).

Metabolomic Response of Eelgrass: Comparison between populations at high and low CO_2

Both eelgrass populations showed significantly different metabolomic patterns after 1-year growth in the experimental aquaria (Table 8). However, the interaction term between CO_2 treatment and population (p=0.077), suggested that both populations showed similar responses to elevated CO_2 even though there were significant differences in the abundance of some primary metabolites (Glycolysis – Krebs – Calvin) between SBV and DBW plants across CO_2 treatments (Table 8) and overall plant performance (Chapter 2). Principal Component Analysis (PCA) of the eelgrass metabolomic fingerprints separated the two populations along the first Principal Component Axis (PC1), with CO_2 treatments separated along PC2 (Fig. 13a), showing differences between plants growing at high [CO_2] (823 μmol CO_2 $Kg^{-1}SW$).

Table 8. Summary Factorial PERMANOVA for metabolomics fingerprints.

	Source	*df*	Sum of Squares	Mean Square	*F*	*p*
All populations, All log [CO_2]	log [CO_2]	1	1.7×10^{17}	1.7×10^{17}	6.46	<0.001
	Population	1	1.5×10^{17}	1.5×10^{17}	5.41	<0.001
	log [CO_2] x Population	1	6.5×10^{16}	6.5×10^{16}	2.41	0.077

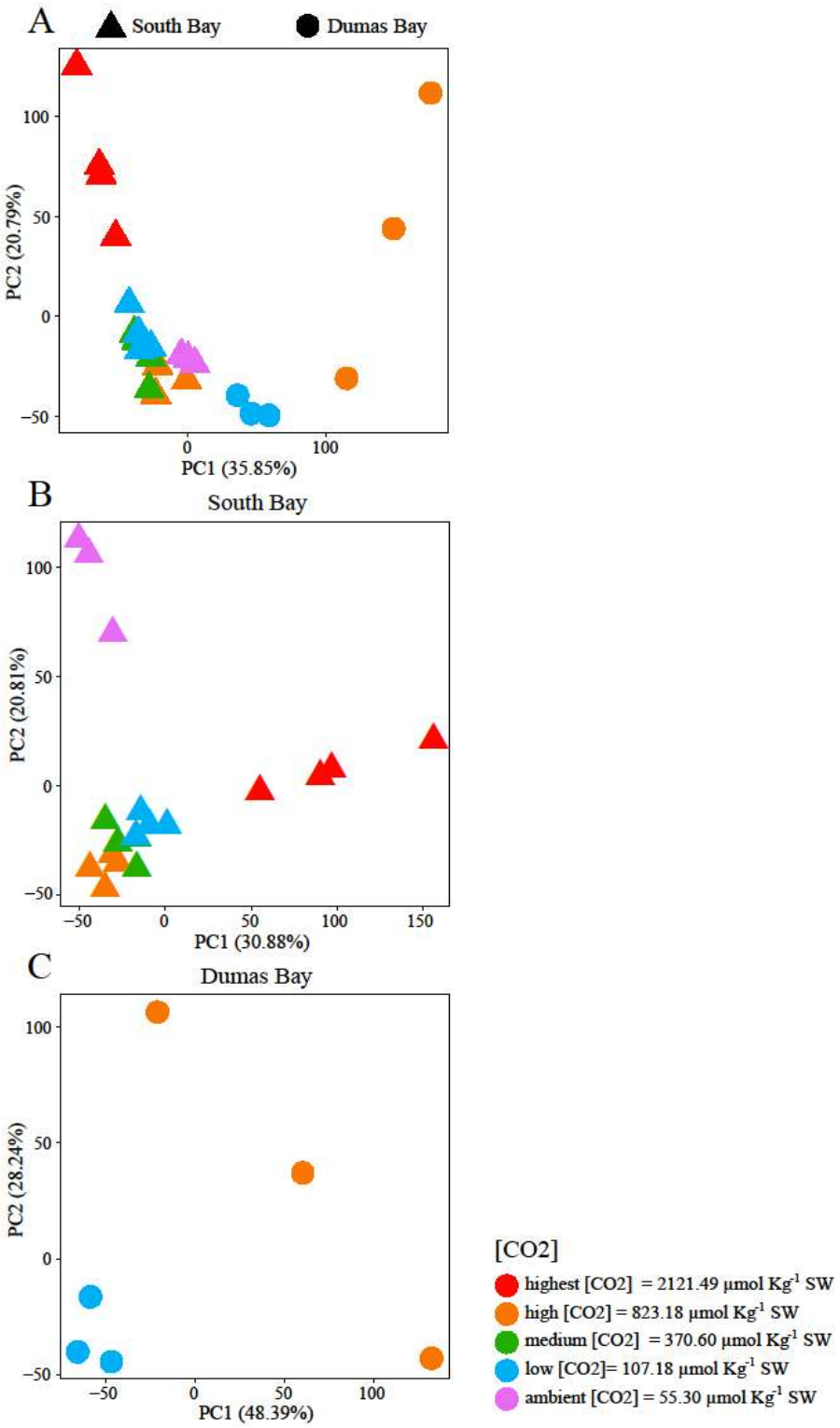

Figure 13. Principal Component Analyses of the metabolome fingerprints of eelgrass leaves from May 2014 growing at different CO_2 concentrations from South Bay, VA (triangles) and Dumas Bay (circles) (A) together, (B) South Bay separately, and (C) Dumas Bay separately. CO_2 treatment is indicated by color.

Examining the metabolomic response from the different eelgrass populations under high CO_2 5,476 metabolites were detected. Only 133 of those responsive metabolites have been identified and 32 were significantly different between the populations under high CO_2 (823 μmol CO_2 $Kg^{-1}SW$). Similarly, under low CO_2 (107 μmol CO_2 $Kg^{-1}SW$) 5,120 metabolites were detected from those 131 identified and 39 significantly different between the populations.

In general, DBW eelgrass had higher abundances of photorespiratory and stress-related compounds in the shikimate pathway regardless of the CO_2 treatment (Fig. 14 a,b, Table 9,10), while SBV plants had higher abundances of α-ketoglutaric acid (TCA Cycle) across CO_2 treatments (Fig 14a,b, Table 9,10). Higher abundance of 3-dehydroshikimate (Fig. 14 a, b, Table 9,10) observed in DBW leaves relative to SBV may indicate up-regulation of metabolic flux through the shikimate pathway (Singh & Christendat 2006) leading to the synthesis of polyphenols. Stress conditions such as high light and pathogens (Vergeer et al. 1995), and CO_2 limitation of seagrass photosynthesis (Arnold et al. 2012) appear to increase the abundance phenolic compounds in seagrasses, and the shikimic intermediates are known to respond to oxidative stress and copper pollution in some macrophytes (Zou et al. 2014, Kumari et al. 2015).

Proline and serine were more abundant in DBW eelgrass than in SBV at high [CO_2] (Fig 14a, Table 9). Proline is known to aid stress tolerance by acting as a metal chelator, by providing antioxidative defense and as a signaling molecule (Verbruggen & Hermans 2008, Hayat et al. 2012) to control mitochondrial functions, developmental processes and activate gene expression that may facilitate plant recovery from stress (Szabados & Savouré 2010). Serine has also been implicated in stress tolerance (e.g., low temperature and elevated salinity in *Arabidopsis thaliana* (Ho & Saito 2001) and references therein) and is synthesized (i) through the photorespiratory glycolate pathway, (ii) from Calvin Cycle intermediates (the

"phosphorylated" pathway) and/ or (iii) the glycerate pathway via cytosolic glycolysis (Bourguignon J et al. 1998). However, high [CO_2] is known to decrease photorespiration in eelgrass (Celebi 2016), suggesting that the elevated abundance of serine observed here were likely being driven by non-photorespiratory pathways.

Table 9. ANOVA population comparison of leaf metabolites relative abundance (i.e., MS peak area) and standard error on high [CO_2] (823 μmol CO_2 $Kg^{-1}SW$) treatment.

Metabolite	KEGG ID	Dumas Bay WA Mean ± SE MS Peak Area	South Bay VA Mean ± SE MS Peak Area	*F*	*p*	Higher concentration
L-Serine	C00716	16.83E+04 ± 70.83E+02	8.60E+04 ± 30.00E+02	141.81	< 0.01	Dumas Bay, WA
Guanosine	C00387	3.00E+04 ± 24.28E+02	48.08E+02 ± 6.92E+02	132.18	< 0.01	Dumas Bay, WA
S-1-Phenylethanol	C07112	74.09E+04 ± 3.37E+04	23.77E+04 ± 2.94E+04	126.42	< 0.01	Dumas Bay, WA
Cytosine	C00380	41.57E+04 ± 3.66E+04	7.83E+04 ± 40.62E+02	118.45	< 0.01	Dumas Bay, WA
Guanine	C00242	54.94E+04 ± 2.76E+04	17.85E+04 ± 2.61E+04	92.37	< 0.01	Dumas Bay, WA
4-Hydroxy-L-Proline	C01157	10.72E+04 ± 71.02E+02	5.26E+04 ± 34.93E+02	56.91	< 0.01	Dumas Bay, WA
Uracil	C00106	16.81E+04 ± 91.72E+02	7.61E+04 ± 1.00E+04	42.35	< 0.01	Dumas Bay, WA
Sugars, Alcohol, Hexoses		96.95E+02 ± 13.34E+02	21.64E+02 ± 4.18E+02	38.09	< 0.01	Dumas Bay, WA
L-Proline	C16435	79.17E+06 ± 2.13E+06	61.69E+06 ± 1.88E+06	37.67	< 0.01	Dumas Bay, WA
Nicotinamide	C00153	1.11E+06 ± 6.34E+04	69.68E+04 ± 4.33E+04	31.87	< 0.01	Dumas Bay, WA
D-Arabinose	C00216	78.30E+04 ± 62.38E+02	27.09E+04 ± 8.16E+04	28.08	< 0.01	Dumas Bay, WA
Shikimate	C00493	66.48E+04 ± 7.94E+04	32.14E+04 ± 2.15E+04	23.31	< 0.01	Dumas Bay, WA
Glyceraldehyde	C02154	40.84E+04 ± 5.64E+04	10.28E+04 ± 3.79E+04	22.04	0.01	Dumas Bay, WA
3.Dehydroshikimate	C02637	73.98E+02 ± 16.20E+02	14.08E+02 ± 4.92E+02	16.48	0.01	Dumas Bay, WA
Pyridoxine	C00314	16.31E+04 ± 1.99E+04	7.91E+04 ± 1.13E+04	15.39	0.01	Dumas Bay, WA
5-Methylcytosine Hydrochloride	C02376	5.16E+04 ± 89.69E+02	2.06E+04 ± 21.03E+02	15.35	0.01	Dumas Bay, WA
4-Acetamidobutanoate	C02946	11.80E+04 ± 2.17E+04	4.35E+04 ± 62.86E+02	14.37	0.01	Dumas Bay, WA
Galactitol	C01697	84.07E+02 ± 20.09E+02	31.34E+02 ± 1.59E+02	9.72	0.03	Dumas Bay, WA
5-Methylthioadenosine	C00170	4.48E+04 ± 22.82E+02	2.57E+04 ± 51.65E+02	8.87	0.03	Dumas Bay, WA
Deoxy-Hexoses		60.58E+02 ± 13.94E+02	21.70E+02 ± 5.35E+02	8.59	0.03	Dumas Bay, WA
Adenine	C00147	7.66E+06 ± 56.81E+04	3.66E+06 ± 1.14E+06	7.80	0.04	Dumas Bay, WA
Hypoxanthine	C00262	15.34E+04 ± 6.12E+04	1.39E+04 ± 16.83E+02	7.41	0.04	Dumas Bay, WA
Naringenin	C00509	22.80E+02 ± 9.49E+02	1.40E+02 ± 4.21E+00	7.26	0.04	Dumas Bay, WA
Thymine	C00178	7.87E+04 ± 76.41E+02	4.30E+04 ± 1.06E+04	6.46	0.05	Dumas Bay, WA
Arabitol	C01904	56.96E+04 ± 5.56E+04	36.96E+04 ± 5.39E+04	6.42	0.05	Dumas Bay, WA

Table 9 continued

Metabolite	KEGG ID	Dumas Bay WA Mean ± SE MS Peak Area	South Bay VA Mean ± SE MS Peak Area	*F*	*p*	Higher concentration
Rs-Mevalonic Acid	C00418	51.14E+02 ± 4.67E+02	25.29E+02 ± 8.45E+02	5.80	0.06	Dumas Bay, WA
Eriodictyol	C05631	11.96E+02 ± 5.42E+02	1.30E+02 ± 14.68E+00	5.53	0.07	Dumas Bay, WA
D-Pantothenic Acid	C00864	10.41E+04 ± 3.41E+04	3.71E+04 ± 27.40E+02	5.45	0.07	Dumas Bay, WA
Diethanolamine	C06772	6.78E+04 ± 3.31E+04	33.73E+02 ± 7.08E+02	5.39	0.07	Dumas Bay, WA
Pyruvate	C00022	5.69E+04 ± 20.32E+02	3.14E+04 ± 96.51E+02	4.91	0.08	Dumas Bay, WA
L-Threonine	C00188	18.64E+04 ± 3.22E+04	11.14E+04 ± 2.03E+04	4.31	0.09	Dumas Bay, WA
L-Pipecolic Acid	C00408	1.49E+06 ± 37.59E+04	83.29E+04 ± 8.45E+04	3.95	0.10	Dumas Bay, WA
Creatine	C00300	81.76E+04 ± 47.44E+04	4.86E+04 ± 67.21E+02	3.75	0.11	Dumas Bay, WA
2-Aminophenol	C01987	72.94E+04 ± 5.98E+04	59.72E+04 ± ± 4.30E+04	3.43	0.12	Dumas Bay, WA
Palmitic Acid	C00249	2.45E+06 ± ± 4.92E+04	1.93E+06 ± 23.60E+04	3.36	0.13	Dumas Bay, WA
D-3-Phosphoglyceric Acid	C00597	95.48E+02 ± 53.36E+02	16.63E+02 ± 3.09E+02	3.10	0.14	Dumas Bay, WA
3-Amino-5-Hydroxybenzoic-Acid	C12107	3.48E+04 ± 18.80E+02	2.85E+04 ± 27.33E+02	3.07	0.14	Dumas Bay, WA
Monoshaccharides, Hexoses		1.86E+06 ± 77.52E+04	69.53E+04 ± 13.23E+04	3.04	0.14	Dumas Bay, WA
L-Valine	C00183	13.72E+06 ± 7.03E+06	3.67E+06 ± 72.09E+04	2.86	0.15	Dumas Bay, WA
Acetoacetate	C00164	6.94E+04 ± 17.89E+02	5.51E+04 ± 70.97E+02	2.80	0.15	Dumas Bay, WA
D-Mannose	C00159	1.85E+06 ± 72.02E+04	85.30E+04 ± 8.80E+04	2.67	0.16	Dumas Bay, WA
L-Arginine	C00062	1.00E+04 ± 24.94E+02	50.09E+02 ± 17.13E+02	2.79	0.17	Dumas Bay, WA
4.Guanidinobutanoate	C01035	22.37E+04 ± 11.96E+04	6.23E+04 ± 1.60E+04	2.51	0.17	Dumas Bay, WA
Glutaric Acid	C00489	11.32E+04 ± 2.64E+04	6.64E+04 ± 1.85E+04	2.26	0.19	Dumas Bay, WA
Mandelic Acid	C01984	2.10E+04 ± 85.77E+02	88.28E+02 ± 34.07E+02	2.18	0.20	Dumas Bay, WA
S-Malate	C00711	5.36E+06 ± 2.48E+06	2.08E+06 ± 68.49E+04	2.16	0.20	Dumas Bay, WA
Succinate Semialdehyde	C00232	1.16E+04 ± 30.63E+02	58.28E+02 ± 26.05E+02	2.09	0.21	Dumas Bay, WA
D-Lyxosylamine		1.91E+06 ± 31.60E+04	1.43E+06 ± 17.49E+04	2.03	0.21	Dumas Bay, WA
Histamine	C00388	4.76E+04 ± 59.27E+02	3.89E+04 ± 31.78E+02	1.96	0.22	Dumas Bay, WA
Pyruvic Aldehyde	C00546	20.55E+04 ± 9.51E+04	9.25E+04 ± 2.49E+04	1.77	0.24	Dumas Bay, WA
Gallic Acid	C01424	69.77E+02 ± 8.10E+02	44.02E+02 ± 16.46E+02	1.56	0.27	Dumas Bay, WA

Table 9 continued

Metabolite	KEGG ID	Dumas Bay WA Mean ± SE MS Peak Area	South Bay VA Mean ± SE MS Peak Area	*F*	*p*	Higher concentration
Fumarate	C00122	15.47E+04 ± 5.17E+04	9.48E+04 ± 2.38E+04	1.35	0.30	Dumas Bay, WA
Sucrose	C00089	1.26E+08 ± 6.37E+06	1.11E+08 ± 10.27E+06	1.30	0.31	Dumas Bay, WA
D-Gulonic Acid, Gama Lactone	C01040	3.69E+04 ± 1.04E+04	2.25E+04 ± 80.38E+02	1.25	0.31	Dumas Bay, WA
4-Hydroxy-L-Phenylglycine	CA1445	18.83E+04 ± 7.99E+04	10.82E+04 ± 2.20E+04	1.25	0.31	Dumas Bay, WA
Pyridoxal Creatinine	C00791	11.50E+04 ± 5.92E+04	6.34E+04 ± 57.68E+02	1.07	0.35	Dumas Bay, WA
L-Alanine	C00041	60.19E+04 ± 4.15E+04	47.35E+04 ± 10.33E+04	1.02	0.36	Dumas Bay, WA
3-Methoxytyramine	C05587	5.19E+04 ± 9.72E+02	4.49E+04 ± 57.89E+02	1.02	0.36	Dumas Bay, WA
Phloroglucinol	C02183	7.62E+06 ± 1.29E+06	5.94E+06 ± 1.20E+06	0.90	0.39	Dumas Bay, WA
Leucine	C16439	54.55E+04 ± 16.48E+04	40.77E+04 ± 5.74E+04	0.80	0.41	Dumas Bay, WA
Urocanate	C00785	3.73E+04 ± 34.12E+02	3.46E+04 ± 11.16E+02	0.76	0.42	Dumas Bay, WA
α Aminoadipate	C00956	10.57E+04 ± 89.31E+02	9.17E+04 ± 1.28E+04	0.68	0.45	Dumas Bay, WA
Adenosine Monophosphate	C00020	12.59E+04 ± 2.09E+04	10.92E+04 ± 93.03E+02	0.65	0.46	Dumas Bay, WA
Hexoses, Phosphate		4.67E+04 ± 2.50E+04	2.76E+04 ± 1.36E+04	0.52	0.50	Dumas Bay, WA
Pyridoxamine	C00534	3.63E+04 ± 9.68E+02	3.08E+04 ± 64.99E+02	0.51	0.51	Dumas Bay, WA
4.Aminobutanoate (GABA)	C00334	35.74E+04 ± 1.62E+04	29.46E+04 ± 7.55E+04	0.48	0.52	Dumas Bay, WA
1.Methyladenine	C02216	3.62E+04 ± 93.22E+02	3.03E+04 ± 28.45E+02	0.48	0.52	Dumas Bay, WA
Uridine	C00299	4.03E+04 ± 1.17E+04	3.27E+04 ± 46.63E+02	0.46	0.53	Dumas Bay, WA
L-Sorbose	C00247	38.14E+06 ± 13.90E+06	29.10E+06 ± 5.62E+06	0.46	0.53	Dumas Bay, WA
D-Malic Acid	C00497	3.48E+06 ± 1.49E+06	2.63E+06 ± 18.19E+04	0.45	0.53	Dumas Bay, WA
Luteolin	C01514	6.77E+06 ± 3.80E+06	4.90E+06 ± 1.30E+06	0.28	0.62	Dumas Bay, WA
D-Fructose	C00095	56.19E+06 ± 22.86E+06	45.86E+06 ± 9.37E+06	0.22	0.66	Dumas Bay, WA
D-Glucuronolactone	C00191	8.65E+04 ± 2.41E+04	7.27E+04 ± 2.42E+04	0.15	0.71	Dumas Bay, WA
Disaccharides		3.44E+06 ± 49.72E+04	2.95E+06 ± 1.04E+06	0.14	0.72	Dumas Bay, WA
Phenylacetic Acid	C07086	41.63E+02 ± 23.39E+02	33.73E+02 ± 13.24E+02	0.10	0.77	Dumas Bay, WA
N-ε-N-ε–N-εTrimethyl Lysine	C03793	13.64E+02 ± 46.86E+00	12.63E+02 ± 2.76E+02	0.09	0.77	Dumas Bay, WA
Succinate	C00042	6.40E+04 ± 38.40E+02	5.68E+04 ± 2.15E+04	0.08	0.79	Dumas Bay, WA

Table 9 continued

Metabolite	KEGG ID	Dumas Bay WA Mean ± SE MS Peak Area	South Bay VA Mean ± SE MS Peak Area	*F*	*p*	Higher concentration
L-Tyrosine	C01536	35.30E+04 ± 4.75E+04	33.45E+04 ± 5.96E+04	0.05	0.83	Dumas Bay, WA
O-Succinyl-L-Homoserine	C01118	22.50E+04 ± 2.74E+04	22.07E+04 ± 3.78E+04	0.01	0.94	Dumas Bay, WA
Caffeic Acid	C01197	87.49E+04 ± 20.75E+04	87.38E+04 ± 9.72E+04	0.00	1.00	Dumas Bay, WA
α Ketoglutaric Acid	C00026	1.09E+04 ± 29.89E+02	11.25E+04 ± 1.30E+04	57.84	< 0.01	South Bay, VA
N-Acetyl-D-Tryptophan	C03137	63.51E+02 ± 68.60E+00	1.75E+04 ± 23.78E+02	15.57	0.01	South Bay, VA
1-Aminocyclopropane-1-Carboxylate	C01234	2.29E+06 ± 12.23E+04	14.03E+06 ± 2.68E+06	13.66	0.01	South Bay, VA
2,6-Dihydroxypyridine	C03056	5.05E+04 ± 50.38E+02	8.77E+04 ± 88.83E+02	10.77	0.02	South Bay, VA
Azelaic Acid	C08261	34.55E+02 ± 8.16E+02	71.23E+02 ± 9.09E+02	8.29	0.03	South Bay, VA
Galactonic Acid	C00880	48.72E+04 ± 15.57E+04	90.02E+04 ± 6.29E+04	7.58	0.04	South Bay, VA
3-Amino-4-Hydroxybenzoic Acid	C12115	4.23E+04 ± 96.25E+02	7.19E+04 ± 60.89E+02	7.53	0.04	South Bay, VA
N-α-Acetyl-L-Lysine	C12989	3.50E+04 ± 84.95E+02	5.62E+04 ± 27.03E+02	7.42	0.04	South Bay, VA
L-Isoleucine	C16434	1.97E+06 ± 55.89E+04	3.29E+06 ± 20.96E+04	6.20	0.06	South Bay, VA
4.Hydroxybenzaldehyde	C00633	41.61E+02 ± 1.88E+02	2.41E+04 ± 69.12E+02	5.92	0.06	South Bay, VA
Rosmarinic Acid	C01850	57.90E+04 ± 33.30E+04	1.79E+06 ± 34.93E+04	5.88	0.06	South Bay, VA
Turanose	C19636	1.60E+06 ± 18.61E+04	2.44E+06 ± 26.06E+04	5.85	0.06	South Bay, VA
N-Acetyl-L-Alanine	C01073	2.98E+04 ± 3.52E+02	3.66E+04 ± 27.71E+02	4.23	0.09	South Bay, VA
N-Acetyl-D-l-Glutamic Acid	C00624	2.06E+06 ± 34.20E+04	10.89E+06 ± 3.74E+06	3.98	0.10	South Bay, VA
5-Oxo-L-Proline	C01879	8.52E+06 ± 96.91E+04	24.63E+06 ± 6.86E+06	3.90	0.11	South Bay, VA
L-Glutamine	C00303	14.20E+06 ± 2.30E+06	46.62E+06 ± 13.88E+06	3.84	0.11	South Bay, VA
L-DOPA	C00355	52.57E+04 ± 23.02E+04	96.88E+04 ± 11.11E+04	3.61	0.12	South Bay, VA
L-Asparagine	C16438	11.44E+04 ± 1.79E+04	32.37E+04 ± 10.81E+04	2.64	0.17	South Bay, VA
Maleamate	C01596	3.00E+04 ± 51.71E+02	4.12E+04 ± 47.14E+02	2.52	0.17	South Bay, VA
Salicylate	C00805	55.13E+02 ± 8.60E+02	4.59E+04 ± 2.23E+04	2.33	0.19	South Bay, VA
Adenosine	C00212	23.58E+04 ± 13.25E+04	4.48E+06 ± 2.36E+06	2.31	0.19	South Bay, VA
Citrate	C00158	2.11E+06 ± 87.25E+04	3.33E+06 ± 28.77E+04	2.30	0.19	South Bay, VA

Table 9 continued

Metabolite	KEGG ID	Dumas Bay WA Mean ± SE MS Peak Area	South Bay VA Mean ± SE MS Peak Area	*F*	*p*	Higher concentration
Formononetin	C00858	3.47E+02 ± 89.93E+00	13.71E+02 ± 6.21E+02	1.92	0.22	South Bay, VA
Trigonelline	C01004	6.00E+06 ± 1.24E+06	8.89E+06 ± 1.57E+06	1.86	0.23	South Bay, VA
Glutamic Acid	C00025	3.90E+06 ± 45.34E+04	10.35E+06 ± 4.00E+06	1.85	0.23	South Bay, VA
3,2-Hydroxyphenyl Propanoate	C01198	59.96E+02 ± 5.67E+02	72.65E+02 ± 7.10E+02	1.73	0.25	South Bay, VA
D-Trehalose	C01083	1.79E+06 ± 25.93E+04	2.21E+06 ± 20.94E+04	1.61	0.26	South Bay, VA
Salsolinol	C09642	3.05E+04 ± 17.30E+02	3.46E+04 ± 28.81E+02	1.22	0.32	South Bay, VA
L-Phenylalanine	C02057	75.89E+04 ± 14.95E+04	1.39E+06 ± 52.67E+04	0.99	0.37	South Bay, VA
Resorcinol Monoacetate	C12064	88.44E+02 ± 29.12E+02	1.56E+04 ± 54.21E+02	0.96	0.37	South Bay, VA
Sugars, Alcohol, Pentoses		37.90E+02 ± 9.48E+02	46.92E+02 ± 6.38E+02	0.68	0.45	South Bay, VA
3-Hydroxykynurenine	C02794	8.44E+04 ± 3.04E+04	10.45E+04 ± 74.54E+02	0.56	0.49	South Bay, VA
Myoinositol	C00137	47.75E+06 ± 5.72E+06	51.73E+06 ± 2.97E+06	0.45	0.53	South Bay, VA
Glycerol-3-Phosphate	C00093	68.27E+04 ± 15.36E+04	88.96E+04 ± 26.73E+04	0.37	0.57	South Bay, VA
Monosaccharides, Pentoses		12.64E+04 ± 1.84E+04	14.06E+04 ± 1.55E+04	0.35	0.58	South Bay, VA
3-Aminoisobutanoate	C05145	1.72E+04 ± 44.18E+02	2.19E+04 ± 59.68E+02	0.35	0.58	South Bay, VA
6-Phosphogluconic-Acid	C00345	7.33E+04 ± 2.22E+04	9.44E+04 ± 3.17E+04	0.25	0.64	South Bay, VA
Fisetin	C10041	1.19E+08 ± 13.65E+06	1.25E+08 ± 6.21E+06	0.23	0.65	South Bay, VA
Nicotinate Picolinic Acid	C00253	4.84E+04 ± 61.66E+02	5.37E+04 ± 93.59E+02	0.19	0.68	South Bay, VA
N-Acetylglycine	CA1212	6.57E+04 ± 86.22E+02	7.16E+04 ± 99.85E+02	0.18	0.69	South Bay, VA
Tyramine	C00483	4.08E+04 ± 95.01E+02	4.40E+04 ± 52.00E+02	0.10	0.76	South Bay, VA
Quinoline	C06413	3.37E+04 ± 75.35E+02	3.62E+04 ± 41.50E+02	0.10	0.77	South Bay, VA
Xylitol	C00379	10.81E+04 ± 2.55E+04	11.53E+04 ± 1.15E+04	0.08	0.79	South Bay, VA
Aspartate	C00049	1.27E+06 ± 47.44E+04	1.42E+06 ± 31.77E+04	0.07	0.80	South Bay, VA
2-Hydroxypyridine	C02502	77.64E+04 ± 7.79E+04	82.81E+04 ± 16.38E+04	0.06	0.81	South Bay, VA
Linoleic Acid	C01595	18.06E+04 ± 5.69E+04	19.69E+04 ± 2.91E+04	0.06	0.81	South Bay, VA
6-Hydroxynicotinate	C01020	4.87E+04 ± 48.38E+02	5.03E+04 ± 43.36E+02	0.06	0.82	South Bay, VA
1,2-Phenylenediamine	C14402	4.87E+04 ± 1.21E+04	5.19E+04 ± 87.65E+02	0.05	0.83	South Bay, VA

Table 9 continued

Metabolite	KEGG ID	Dumas Bay WA Mean ± SE MS Peak Area	South Bay VA Mean ± SE MS Peak Area	*F*	*p*	Higher concentration
Glyceric Acid	C00258	18.83E+04 ± 3.55E+04	19.27E+04 ± 1.51E+04	0.02	0.90	South Bay, VA
Dehydroascorbate	C05422	56.00E+04 ± 26.29E+04	58.46E+04 ± 16.30E+04	0.01	0.94	South Bay, VA
Amino-Sugars		5.63E+04 ± 3.52E+04	5.86E+04 ± 38.16E+02	0.01	0.94	South Bay, VA

Table 10. ANOVA population comparison of leaf metabolites relative abundance (i.e., MS peak area) and standard error on low CO_2 (107 μmol CO_2 $Kg^{-1}SW$) treatment.

Metabolite	KEGG ID	Dumas Bay WA Mean ± SE MS Peak Area	South Bay VA Mean ± SE MS Peak Area	*F*	*p*	Higher concentration
Glycerate 3P	C00597	7.63E+04 ± 78.57E+02	57.89E+02 ± 30.88E+02	87.91	<0.01	Dumas Bay, WA
Adenine	C00147	9.48E+06 ± 1.24E+06	1.66E+06 ± 5.26E+04	56.09	<0.01	Dumas Bay, WA
O-Succinyl-L-Homoserine	C01118	1.03E+06 ± 17.17E+04	14.11E+04 ± 1.18E+04	38.04	<0.01	Dumas Bay, WA
3-Dehydroshikimate	C02637	1.16E+04 ± 11.51E+02	57.56E+02 ± 3.81E+02	29.73	<0.01	Dumas Bay, WA
Disaccharides		4.03E+06 ± 55.30E+04	1.52E+06 ± 7.17E+04	28.44	<0.01	Dumas Bay, WA
4-Acetamidobutanoate	C02946	11.89E+04 ± 80.55E+02	7.25E+04 ± 48.58E+02	27.49	<0.01	Dumas Bay, WA
Uracil	C00106	25.08E+04 ± 4.78E+04	3.66E+04 ± 70.89E+02	27.43	<0.01	Dumas Bay, WA
Guanosine	C00387	5.57E+04 ± 1.11E+04	1.01E+04 ± 8.27E+02	24.03	<0.01	Dumas Bay, WA
4-Hydroxy-L-Proline	C01157	12.54E+04 ± 1.18E+04	7.58E+04 ± 30.81E+02	22.13	0.01	Dumas Bay, WA
Glutaric Acid	C00489	10.32E+04 ± 52.65E+02	7.62E+04 ± 37.02E+02	18.86	0.01	Dumas Bay, WA
Succinate Semialdehyde	C00232	62.22E+02 ± 5.92E+02	19.83E+02 ± 6.06E+02	25.06	0.01	Dumas Bay, WA
Glyceric Acid (Glycerate)	C00258	19.75E+04 ± 1.13E+04	15.54E+04 ± 34.57E+02	16.74	0.01	Dumas Bay, WA
Phloroglucinol	C02183	5.25E+06 ± 45.37E+04	3.06E+06 ± 32.92E+04	16.26	0.01	Dumas Bay, WA
D-Arabinose	C00216	69.28E+04 ± 3.15E+04	26.05E+04 ± 10.75E+04	11.08	0.02	Dumas Bay, WA
Hypoxanthine	C00262	6.68E+04 ± 1.33E+04	3.09E+04 ± 29.52E+02	9.44	0.03	Dumas Bay, WA
Cytosine	C00380	60.80E+04 ± 14.70E+04	23.99E+04 ± 2.93E+04	8.30	0.03	Dumas Bay, WA
Quinoline	C06413	4.99E+04 ± 16.23E+02	3.03E+04 ± 61.21E+02	7.10	0.04	Dumas Bay, WA
α-Aminoadipate	C00956	13.83E+04 ± 2.92E+04	6.99E+04 ± 1.05E+04	6.24	0.05	Dumas Bay, WA
1-Methyladenine	C02216	7.93E+04 ± 52.28E+02	4.84E+04 ± 1.00E+04	5.97	0.06	Dumas Bay, WA
5-Methylcytosine-Hydrocloride	C02376	4.92E+04 ± 43.70E+02	2.79E+04 ± 67.57E+02	5.89	0.06	Dumas Bay, WA
Aspartate	C00049	1.43E+06 ± 9.70E+04	1.14E+06 ± 7.57E+04	5.82	0.06	Dumas Bay, WA
Urocanate	C00785	14.66E+04 ± 6.40E+04	2.94E+04 ± 38.16E+02	4.75	0.08	Dumas Bay, WA
L-Serine	C00716	24.18E+04 ± 7.67E+04	10.13E+04 ± 2.15E+04	4.15	0.10	Dumas Bay, WA
Histamine	C00388	6.39E+04 ± 95.39E+02	4.01E+04 ± 74.54E+02	4.01	0.10	Dumas Bay, WA
Sucrose	C00089	1.03E+08 ± 9.44E+06	85.07E+06 ± 4.28E+06	3.70	0.11	Dumas Bay, WA
Pyruvate	C00022	7.38E+04 ± 69.77E+02	5.78E+04 ± 51.92E+02	3.55	0.12	Dumas Bay, WA

Table 10 continued

Metabolite	KEGG ID	Dumas Bay WA Mean ± SE MS Peak Area	South Bay VA Mean ± SE MS Peak Area	*F*	*p*	Higher concentration
Glycerate 3P	C00597	7.63E+04 ± 78.57E+02	57.89E+02 ± 30.88E+02	87.91	<0.01	Dumas Bay, WA
Hexoses, Phosphate		11.35E+04 ± 2.73E+04	5.82E+04 ± 1.60E+04	3.47	0.12	Dumas Bay, WA
Glyceraldehyde	C02154	44.02E+04 ± 4.72E+04	32.40E+04 ± 4.47E+04	3.11	0.14	Dumas Bay, WA
Guanine	C00242	92.49E+04 ± 26.23E+04	49.42E+04 ± 9.82E+04	3.01	0.14	Dumas Bay, WA
N-α-Acetyl-Lysine	C12989	7.55E+04 ± 95.55E+02	6.16E+04 ± 18.15E+02	2.81	0.15	Dumas Bay, WA
Thymine	C00178	8.34E+04 ± 1.38E+04	5.86E+04 ± 92.14E+02	2.44	0.18	Dumas Bay, WA
Rs-Mevalonic Acid	C00418	46.72E+02 ± 12.80E+02	29.90E+02 ± 2.90E+02	2.24	0.19	Dumas Bay, WA
Pyridoxamine	C00534	5.83E+04 ± 1.37E+04	4.14E+04 ± 44.95E+02	1.77	0.24	Dumas Bay, WA
Creatine	C00300	7.15E+04 ± 3.75E+04	2.05E+04 ± 2.78E+02	1.85	0.25	Dumas Bay, WA
Naringenin	C00509	22.46E+02 ± 16.78E+02	4.11E+02 ± 1.21E+02	1.69	0.25	Dumas Bay, WA
2.Hydroxypyridine	C02502	1.27E+06 ± 19.79E+04	93.81E+04 ± 16.30E+04	1.69	0.25	Dumas Bay, WA
L-Alanine	C00041	76.48E+04 ± 14.37E+04	54.61E+04 ± 11.31E+04	1.48	0.28	Dumas Bay, WA
Eriodictyol	C05631	26.31E+02 ± 20.88E+02	5.54E+02 ± 1.24E+02	1.40	0.29	Dumas Bay, WA
N-Acetyl-L-Alanine	C01073	3.65E+04 ± 36.02E+02	3.21E+04 ± 20.54E+02	1.31	0.30	Dumas Bay, WA
Palmitic Acid	C00249	3.25E+06 ± 99.43E+04	2.37E+06 ± 14.78E+04	1.07	0.35	Dumas Bay, WA
Nicotinamide	C00153	1.09E+06 ± 15.29E+04	91.81E+04 ± 8.78E+04	1.07	0.35	Dumas Bay, WA
Amino-Sugars		6.37E+04 ± 2.19E+04	4.28E+04 ± 86.20E+02	1.00	0.36	Dumas Bay, WA
Galactitol	C01697	60.72E+02 ± 24.15E+02	42.59E+02 ± 10.01E+02	0.60	0.47	Dumas Bay, WA
D-Pantothenic Acid	C00864	6.96E+04 ± 1.51E+04	5.53E+04 ± 1.32E+04	0.51	0.51	Dumas Bay, WA
Turanose	C19636	1.41E+06 ± 30.46E+04	1.23E+06 ± 8.04E+04	0.45	0.53	Dumas Bay, WA
1,2-Phenylenediamine	C14402	5.86E+04 ± 1.49E+04	4.49E+04 ± 1.39E+04	0.45	0.53	Dumas Bay, WA
Acetoacetate	C00164	5.17E+04 ± 15.66E+02	4.98E+04 ± 21.79E+02	0.43	0.54	Dumas Bay, WA
4-Hydroxy-L-Phenylglycine	CA1445	12.21E+04 ± 47.18E+02	10.51E+04 ± 2.23E+04	0.40	0.55	Dumas Bay, WA
Pyridoxal N-Acetylglycine	CA1212	9.12E+04 ± 1.71E+04	7.94E+04 ± 1.12E+04	0.37	0.57	Dumas Bay, WA
Nicotinate Picolinic Acid	C00253	4.96E+04 ± 52.35E+02	4.43E+04 ± 66.49E+02	0.35	0.58	Dumas Bay, WA
Tyramine	C00483	5.21E+04 ± 1.42E+04	4.38E+04 ± 66.93E+02	0.34	0.58	Dumas Bay, WA
L-Threonine	C00188	24.26E+04 ± 5.02E+04	21.51E+04 ± 3.01E+04	0.25	0.64	Dumas Bay, WA
Salsolinol	C09642	4.47E+04 ± 1.12E+04	3.92E+04 ± 53.76E+02	0.23	0.65	Dumas Bay, WA

Table 10 continued

Metabolite	KEGG ID	Dumas Bay WA Mean ± SE MS Peak Area	South Bay VA Mean ± SE MS Peak Area	*F*	*p*	Higher concentration
D-Glucuronolactone	C00191	12.34E+04 ± 42.83E+02	11.61E+04 ± 1.27E+04	0.23	0.65	Dumas Bay, WA
Shikimate	C00493	28.77E+04 ± 2.28E+04	26.43E+04 ± 4.10E+04	0.20	0.67	Dumas Bay, WA
Maleamate	C01596	8.13E+04 ± 2.14E+04	7.40E+04 ± 73.35E+02	0.13	0.73	Dumas Bay, WA
2-Aminophenol	C01987	74.03E+04 ± 12.21E+04	69.14E+04 ± 11.78E+04	0.08	0.79	Dumas Bay, WA
Linoleic Acid	C01595	29.20E+04 ± 21.40E+04	25.24E+04 ± 3.91E+04	0.08	0.80	Dumas Bay, WA
Azelaic Acid	C08261	64.63E+02 ± 18.57E+02	56.31E+02 ± 26.40E+02	0.06	0.82	Dumas Bay, WA
6-Hydroxynicotinate	C01020	5.34E+04 ± 75.80E+02	5.09E+04 ± 91.03E+02	0.04	0.85	Dumas Bay, WA
3-Methoxytyramine	C05587	4.69E+04 ± 67.02E+02	4.57E+04 ± 49.92E+02	0.02	0.89	Dumas Bay, WA
Citrate	C00158	3.54E+06 ± 66.92E+04	3.42E+06 ± 44.11E+04	0.02	0.89	Dumas Bay, WA
Pyruvic Aldehyde	C00546	10.21E+04 ± 1.06E+04	10.17E+04 ± 2.96E+04	0.00	0.99	Dumas Bay, WA
Glycerol-3-Phosphate	C00093	76.28E+04 ± 13.98E+04	1.74E+06 ± 8.31E+04	41.28	<0.01	South Bay, VA
Rosmarinic Acid	C01850	4.21E+04 ± 2.40E+04	3.01E+06 ± 39.52E+04	40.24	<0.01	South Bay, VA
Caffeic Acid	C01197	65.42E+04 ± 4.94E+04	1.46E+06 ± 10.44E+04	38.67	<0.01	South Bay, VA
Resorcinol Monoacetate	C12064	74.55E+02 ± 23.71E+02	4.24E+04 ± 57.48E+02	24.27	<0.01	South Bay, VA
Dehydroascorbate	C05422	72.58E+04 ± 2.23E+04	1.50E+06 ± 13.47E+04	23.41	<0.01	South Bay, VA
4-Hydroxybenzaldehyde	C00633	11.03E+02 ± 3.06E+02	9.77E+04 ± 33.48E+02	591.92	0.00	South Bay, VA
Adenosine	C00212	7.69E+04 ± 1.04E+04	8.28E+06 ± 43.48E+04	253.90	0.00	South Bay, VA
Myoinositol	C00137	32.52E+06 ± 3.90E+06	56.09E+06 ± 3.34E+06	21.15	0.01	South Bay, VA
N-Acetyl-D-l-Glutamic Acid	C00624	1.40E+06 ± 37.90E+04	5.97E+06 ± 84.76E+04	18.90	0.01	South Bay, VA
1-Aminocyclopropane-1-Carboxylate	C01234	1.87E+06 ± 51.08E+04	6.70E+06 ± 87.71E+04	18.47	0.01	South Bay, VA
N-ε--Trimethyl Lysine	C03793	34.27E+02 ± 14.85E+02	76.21E+02 ± 3.70E+02	15.49	0.02	South Bay, VA
Formononetin	C00858	6.55E+02 ± 2.59E+02	40.87E+02 ± 8.71E+02	10.63	0.02	South Bay, VA
L-Proline	C16435	46.84E+06 ± 8.59E+06	74.92E+06 ± 4.57E+06	9.74	0.03	South Bay, VA
Adenosine-5-Monophosphate	C00020	5.87E+04 ± 2.20E+04	32.22E+04 ± 6.97E+04	9.73	0.03	South Bay, VA
L-Asparagine	C16438	14.46E+04 ± 7.41E+04	50.54E+04 ± 8.46E+04	9.40	0.03	South Bay, VA

Table 10 continued

Metabolite	KEGG ID	Dumas Bay WA Mean ± SE MS Peak Area	South Bay VA Mean ± SE MS Peak Area	*F*	*p*	Higher concentration
L-Isoleucine	C16434	1.41E+06 ± 18.19E+04	2.77E+06 ± 35.80E+04	9.21	0.03	South Bay, VA
L-Tyrosine	C01536	28.04E+04 ± 43.56E+02	47.13E+04 ± 5.62E+04	8.22	0.04	South Bay, VA
L.DOPA	C00355	39.15E+04 ± 10.68E+04	3.69E+06 ± 72.90E+04	9.05	0.04	South Bay, VA
3-Hydroxykynurenine	C02794	7.02E+04 ± 1.69E+04	19.42E+04 ± 3.83E+04	6.82	0.05	South Bay, VA
α-Ketoglutaric Acid	C00026	6.06E+04 ± 27.71E+02	11.03E+04 ± 1.65E+04	6.41	0.05	South Bay, VA
L-Sorbose	C00247	8.06E+06 ± 88.34E+04	18.85E+06 ± 3.73E+06	5.83	0.06	South Bay, VA
Salicylate	C00805	25.02E+02 ± 7.96E+02	6.99E+04 ± 2.37E+04	5.78	0.06	South Bay, VA
Fructose	C00095	13.02E+06 ± 1.54E+06	32.97E+06 ± 7.02E+06	5.64	0.06	South Bay, VA
L-Glutamine	C00303	18.46E+06 ± 9.55E+06	54.51E+06 ± 11.13E+06	5.47	0.07	South Bay, VA
Monoshaccharides, Hexoses		61.80E+04 ± 4.49E+04	98.34E+04 ± 13.27E+04	5.12	0.07	South Bay, VA
5-Oxo-L-Proline	C01879	11.23E+06 ± 4.36E+06	27.71E+06 ± 5.33E+06	5.11	0.07	South Bay, VA
Fisetin	C10041	80.10E+06 ± 5.36E+06	98.82E+06 ± 5.89E+06	5.10	0.07	South Bay, VA
Glutamic Acid	C00025	8.71E+06 ± 1.20E+06	15.68E+06 ± 2.57E+06	4.73	0.08	South Bay, VA
Sugars, Alcohol, Pentoses		83.83E+02 ± 18.06E+02	1.39E+04 ± 18.22E+02	4.42	0.09	South Bay, VA
Gallic Acid	C01424	23.49E+02 ± 7.62E+02	52.66E+02 ± 10.73E+02	4.21	0.10	South Bay, VA
Succinate	C00042	13.28E+04 ± 1.81E+04	20.83E+04 ± 2.86E+04	4.15	0.10	South Bay, VA
5-Methylthioadenosine	C00170	2.62E+04 ± 1.08E+04	8.08E+04 ± 2.14E+04	4.11	0.10	South Bay, VA
S--Phenylethanol	C07112	48.96E+04 ± 3.52E+04	80.18E+04 ± 13.17E+04	3.88	0.11	South Bay, VA
L-Pipecolic Acid	C00408	95.68E+04 ± 6.52E+04	1.38E+06 ± 18.17E+04	3.71	0.11	South Bay, VA
Luteolin	C01514	3.72E+06 ± 1.47E+06	7.19E+06 ± 1.29E+06	3.12	0.14	South Bay, VA
D-Malic-Acid	C00497	2.43E+06 ± 85.22E+04	5.12E+06 ± 1.23E+06	2.73	0.16	South Bay, VA
D-Mannose	C00159	53.57E+04 ± 3.74E+04	75.02E+04 ± 10.90E+04	2.61	0.17	South Bay, VA
Pyridoxine	C00314	11.70E+04 ± 2.41E+04	15.62E+04 ± 1.17E+04	2.56	0.17	South Bay, VA
S-Malate	C00711	3.31E+06 ± 1.07E+06	6.95E+06 ± 1.86E+06	2.34	0.19	South Bay, VA
Trigonelline	C01004	7.09E+06 ± 2.27E+06	10.31E+06 ± 99.40E+04	2.08	0.21	South Bay, VA
Mandelic Acid	C01984	1.82E+04 ± 41.11E+02	3.52E+04 ± 1.01E+04	1.89	0.23	South Bay, VA
D-Lyxosylamine		1.33E+06 ± 12.64E+04	1.70E+06 ± 22.23E+04	1.67	0.25	South Bay, VA

Table 10 continued

Metabolite	KEGG ID	Dumas Bay WA Mean ± SE MS Peak Area	South Bay VA Mean ± SE MS Peak Area	*F*	*p*	Higher concentration
3-Aminoisobutanoate	C05145	2.32E+04 ± 27.27E+02	3.49E+04 ± 74.17E+02	1.67	0.25	South Bay, VA
N-Acetyl-D-Tryptophan	C03137	1.12E+04 ± 39.55E+02	22.26E+04 ± 14.67E+04	1.48	0.28	South Bay, VA
3-Amino-5-Hydroxybenzoic Acid	C12107	3.78E+04 ± 60.36E+02	5.52E+04 ± 1.20E+04	1.33	0.30	South Bay, VA
Xylitol	C00379	7.99E+04 ± 1.90E+04	10.07E+04 ± 1.03E+04	1.08	0.35	South Bay, VA
L-Valine	C00183	4.33E+06 ± 2.19E+06	7.29E+06 ± 1.92E+06	1.03	0.36	South Bay, VA
Leucine	C16439	44.94E+04 ± 8.92E+04	53.67E+04 ± 4.00E+04	0.98	0.37	South Bay, VA
Uridine	C00299	5.69E+04 ± 99.28E+02	7.03E+04 ± 93.64E+02	0.93	0.38	South Bay, VA
Galactonic Acid	C00880	59.85E+04 ± 26.28E+04	79.71E+04 ± 4.46E+04	0.77	0.42	South Bay, VA
3-Amino-4-Hydroxybenzoic Acid	C12115	4.66E+04 ± 2.06E+04	6.38E+04 ± 87.54E+02	0.73	0.43	South Bay, VA
L-Phenylalanine	C02057	73.54E+04 ± 7.22E+04	99.61E+04 ± 26.35E+04	0.67	0.45	South Bay, VA
6-Phosphogluconic Acid	C00345	5.00E+04 ± 58.99E+02	6.33E+04 ± 1.60E+04	0.46	0.53	South Bay, VA
2-6-Dihydroxypyridine	C03056	6.49E+04 ± 1.26E+04	8.19E+04 ± 2.24E+04	0.35	0.58	South Bay, VA
Fumarate	C00122	18.25E+04 ± 3.90E+04	20.79E+04 ± 2.70E+04	0.31	0.60	South Bay, VA
Monosaccharides Pentoses		9.74E+04 ± 90.09E+02	10.81E+04 ± 1.81E+04	0.22	0.66	South Bay, VA
Deoxy-Hexoses		70.73E+02 ± 10.30E+02	82.95E+02 ± 23.56E+02	0.18	0.69	South Bay, VA
4-Aminobutanoate (GABA)	C00334	32.04E+04 ± 49.08E+02	39.00E+04 ± 14.84E+04	0.16	0.71	South Bay, VA
4-Guanidinobutanoate	C01035	5.41E+04 ± 2.22E+04	6.27E+04 ± 1.31E+04	0.13	0.73	South Bay, VA
Arabitol	C01904	42.47E+04 ± 3.60E+04	45.17E+04 ± 6.94E+04	0.10	0.77	South Bay, VA
Sugars, Alcohol, Hexoses		75.83E+02 ± 17.26E+02	80.87E+02 ± 8.58E+02	0.08	0.79	South Bay, VA
D-Trehalose	C01083	1.13E+06 ± 31.01E+04	1.18E+06 ± 8.40E+04	0.03	0.88	South Bay, VA
Creatinine	C00791	3.48E+04 ± 67.41E+02	3.62E+04 ± 1.14E+04	0.01	0.93	South Bay, VA
3-2-Hydroxyphenyl Propanoate	C01198	80.47E+02 ± 18.64E+02	82.21E+02 ± 14.71E+02	0.01	0.94	South Bay, VA
D-Gulonic Acid, γ-Lactone	C01040	2.92E+04 ± 42.98E+02	2.95E+04 ± 69.92E+02	0.00	0.97	South Bay, VA
L-Arginine	C00062	1.07E+04 ± 43.58E+02	1.07E+04 ± 31.86E+02	0.00	0.99	South Bay, VA

Metabolites involved in biotic/abiotic stress responses were elevated in both populations at low [CO_2] (107 μmol $CO_2 \cdot Kg^{-1}SW$). However, the abundance of the photorespiratory metabolites glycerate, glycerate 3-P and succinate semialdehyde (GABA shunt) were higher in DBW leaves than in SBV leaves (Fig. 14 B, Table 10). The increase in succinate semialdehyde abundance under low [CO_2] in DBW could represent another potential stress response as the GABA shunt may help prevent the accumulation of reactive oxygen intermediates (Vergeer et al. 1995, Shelp et al. 1999, Bouché et al. 2003, Singh & Christendat 2006). SBV plants growing under low [CO_2] (107 μmol $CO_2 \cdot Kg^{-1}$ SW) had higher abundance of proline and the sugar alcohol myo-inositol (Fig.14b, Table 10) which are known to generate protein stabilizing osmolytes, such as di-myo-inositol phosphate that may help protect this population from heat stress (Gu et al. 2012).

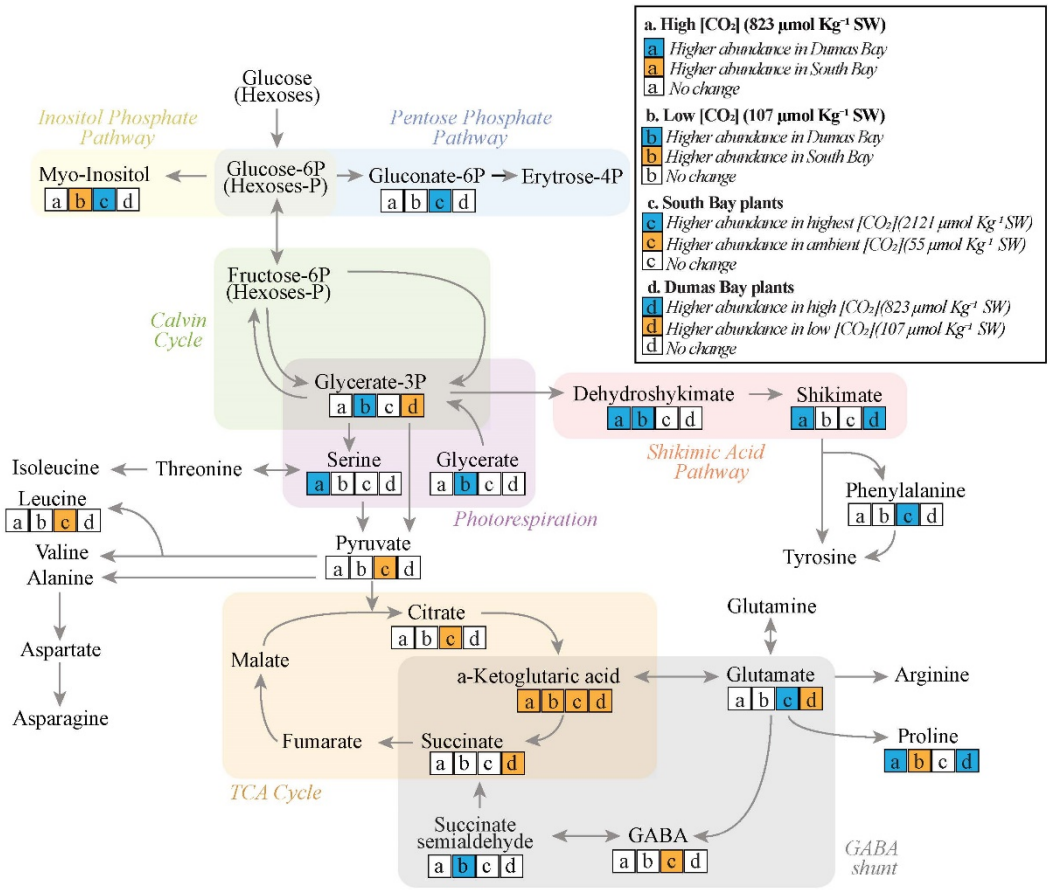

Figure 14. Representation of the main metabolic pathways of *Z. marina* from South Bay VA and Dumas Bay WA in response to high and low CO_2 concentrations. Only identified metabolites are represented in the diagram. Significant changes in any of the metabolite comparisons are represented in **bold typeface**. Colored boxes below metabolite names represent the result of each of the comparisons after one-way ANOVA. Each letter within each box represent a different comparison: (a) South Bay vs. Dumas Bay plants growing at high CO_2 (823 μmol CO_2 $Kg^{-1}SW$). (b) South Bay vs. Dumas Bay plants growing at low CO_2 (107 μmol CO_2 $Kg^{-1}SW$). For a and b, blue and orange colors indicate higher relative abundance in Dumas Bay and South Bay plants, respectively. (c) Highest vs. ambient CO_2 conditions (2121vs 55 μmol CO_2 $Kg^{-1}SW$) plants from South Bay. (d) High vs. low CO_2 conditions (823vs 107 μmol CO_2 $Kg^{-1}SW$) plants from Dumas Bay. For (c) and (d), blue and orange color indicate higher relative abundance of metabolites in plants growing at high CO_2 [2121μmol CO_2 $Kg^{-1}SW$ in (c), 823μmol CO_2 $Kg^{-1}SW$in (d)] and ambient or low CO_2 (55μmol CO_2 $Kg^{-1}SW$in (c), pH 107μmol CO_2 $Kg^{-1}SW$ in (d), respectively.

Metabolomic Response of Eelgrass: South Bay comparison across CO_2 treatments

The SBV plants were grown in three plastic containers in each aquarium, enabling the examination of their metabolomic responses to different [CO_2] in some detail. Of the approximately 5,000 metabolites detected, 455 (9%) were positively correlated to [CO_2] and 408 (8.1%) were negatively correlated to [CO_2]. To date, only 131 of those responsive metabolites have been positively identified. Experimental CO_2 enrichment elevated the concentration of intermediates associated with carbon fixation and amino acid synthesis, as well as sucrose, the latter which is consistent with prior experimental findings (Palacios & Zimmerman 2007, Zimmerman et al. 2017). PCA clustered the SBV plants growing at the highest [CO_2] (2121 μmol $CO_2 \cdot Kg^{-1}$ SW) well away from the rest along PC1 which explained 30% of the total variability (Fig. 13B) and these differences were statistically significant (PERMANOVA $p<$ 0.05, Table 8). The other CO_2 enrichment treatments all clustered near the lower left corner of the PCA space (Fig. 13B), although the ambient CO_2 treatment (no CO_2 addition) was separated from the rest along PC2. The most drastic overall metabolome change was between the highest (2121 μmol $CO_2 \cdot Kg^{-1}$ SW) and the ambient (55μmol $CO_2 \cdot Kg^{-1}$ SW) [CO_2] (Figure 15), consistent with the negative log-linear relationship between [CO_2] and whole plant performance (Figs. 4 to 7). We detected higher abundance of glutamate in SBV plants under highest [CO_2] (Fig.14c, Table 12) which is involved in nitrogen assimilation (Forde & Lea 2007) required for growth. In addition, CO_2 enhancement of gluconate 6-P (Fig. 14c, Table 12) suggests activation of the pentose phosphate pathway (Tabita & McFadden 1972) that leads to the synthesis of aromatic amino acids such as phenylalanine; another critical compound in protein synthesis as well as the formation of cell wall components, including lignin (Bonawitz & Chapple 2010).

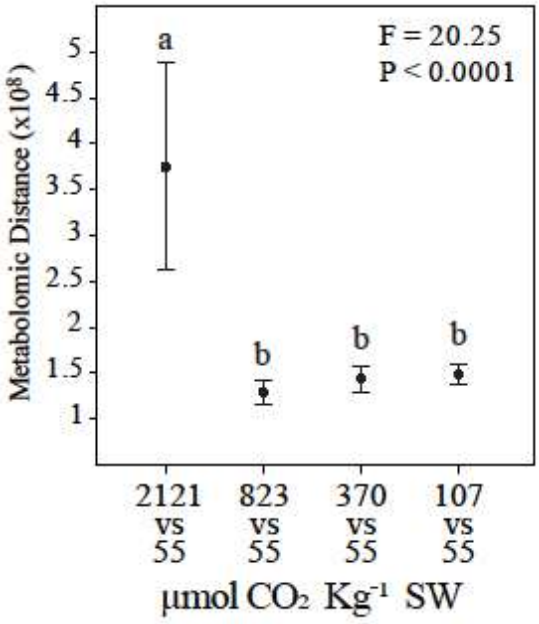

Figure 15. South Bay metabolomic distances (Mean ± Confidence Intervals 95%) between plants growing at ambient CO_2 (55μmol $CO_2 \cdot Kg^{-1}SW$) and plants higher CO_2 concentrations (2121,823, 370, and 107μmol $CO_2 \cdot Kg^{-1}SW$). Fisher's *F* and *p* value of the one-way ANOVA comparing the distances are indicated.

Table 11. Summary PERMANOVA results for effects of [CO_2] on leaf metabolites for South Bay VA and Dumas Bay WA separately.

	Source	*df*	Sum of Squares	Mean Square	*F*	*p*
All CO_2 SBV	[CO_2]	1	1.59×10^{17}	1.59×10^{17}	5.53	<0.001*
All CO_2DB	[CO_2]	1	7.77×10^{16}	7.77×10^{16}	4.03	0.1

Table 12. ANOVA CO_2 treatment comparison of relative abundance (i.e., MS peak area) and standard error of South Bay eelgrass. Highest CO_2 (2121 μmol CO_2 $Kg^{-1}SW$), Ambient CO_2 (55 μmol CO_2 $Kg^{-1}SW$).

Metabolite	KEGG ID	Highest CO2 Mean ± SE MS Peak Area	Ambient CO2 Mean ± SE MS Peak Area	*F*	*p*	Higher concentration
L.DOPA	C00355	5.13E+06 ± 47.79E+04	1.07E+06 ± 5.46E+04	51.16	< 0.01	Highest CO_2
Monosaccharides, Pentoses		16.82E+04 ± 52.20E+02	12.91E+04 ± 28.38E+02	35.02	< 0.01	Highest CO_2
Linoleic Acid	C01595	26.87E+04 ± 1.92E+04	11.49E+04 ± 1.68E+04	33.28	< 0.01	Highest CO_2
Caffeic Acid	C01197	2.27E+06 ± 11.85E+04	1.08E+06 ± 19.73E+04	30.12	< 0.01	Highest CO_2
Galactonic Acid	C00880	1.21E+06 ± 6.58E+04	73.40E+04 ± 5.07E+04	28.53	< 0.01	Highest CO_2
Rosmarinic Acid	C01850	7.14E+06 ± 94.33E+04	1.42E+06 ± 33.84E+04	24.66	< 0.01	Highest CO_2
Myo-Inositol	C00137	78.23E+06 ± 6.55E+06	42.65E+06 ± 1.17E+06	20.75	0.01	Highest CO_2
D-Mannose	C00159	1.58E+06 ± 19.49E+04	83.71E+04 ± 1.93E+04	10.42	0.02	Highest CO_2
L-Phenylalanine	C02057	8.82E+06 ± 1.72E+06	2.61E+06 ± 8.03E+04	9.30	0.03	Highest CO_2
L-Sorbose	C00247	46.69E+06 ± 7.63E+06	20.50E+06 ± 1.33E+06	8.30	0.03	Highest CO_2
Glutamic Acid (Glutamate)	C00025	29.48E+06 ± 6.07E+06	8.98E+06 ± 1.10E+06	8.02	0.04	Highest CO_2
Fructose	C00095	76.32E+06 ± 11.71E+06	36.77E+06 ± 2.67E+06	7.94	0.04	Highest CO_2
Xylitol	C00379	22.79E+04 ± 3.26E+04	11.71E+04 ± 1.47E+04	7.48	0.04	Highest CO_2
D-Arabinose	C00216	31.37E+04 ± 5.80E+04	12.54E+04 ± 97.67E+02	7.42	0.04	Highest CO_2
Trigonelline	C01004	14.13E+06 ± 1.02E+06	7.81E+06 ± 2.43E+06	7.17	0.04	Highest CO_2
6.Phosphogluconic.Acid (Gluconate 6P)	C00345	72.25E+04 ± 20.81E+04	7.51E+04 ± 3.12E+04	6.84	0.05	Highest CO_2
Luteolin	C01514	8.12E+06 ± 1.51E+06	3.38E+06 ± 53.98E+04	6.60	0.05	Highest CO_2
Creatine	C00300	4.31E+04 ± 1.31E+04	55.22E+02 ± 15.97E+02	5.88	0.06	Highest CO_2
N-ε-N-ε-N-ε-Trimethyl Lysine	C03793	4.58E+04 ± 82.91E+02	1.84E+04 ± 97.15E+02	4.61	0.08	Highest CO_2
N-Acetyl-D-Tryptophan	C03137	2.86E+04 ± 45.99E+02	1.78E+04 ± 9.11E+02	3.87	0.11	Highest CO_2
Resorcinol Monoacetate	C12064	3.84E+04 ± 29.14E+02	2.75E+04 ± 53.68E+02	3.73	0.11	Highest CO_2
5-Oxo-L-Proline	C01879	24.76E+06 ± 6.37E+06	10.12E+06 ± 3.43E+06	3.30	0.13	Highest CO_2
1-Aminocyclopropane-1-Carboxylate	C01234	8.02E+06 ± 2.74E+06	2.21E+06 ± 1.05E+06	3.00	0.14	Highest CO_2
L-Proline	C16435	1.31E+08 ± 33.30E+06	62.48E+06 ± 7.49E+06	2.98	0.14	Highest CO_2

Table 12 continued

Metabolite	KEGG ID	Highest CO2 Mean ± SE MS Peak Area	Ambient CO2 Mean ± SE MS Peak Area	*F*	*p*	Higher concentration
D-Trehalose	C01083	2.52E+06 ± 58.08E+04	1.37E+06 ± 9.53E+04	2.73	0.16	Highest CO_2
L-Glutamine	C00303	40.99E+06 ± 10.35E+06	18.69E+06 ± 8.50E+06	2.48	0.18	Highest CO_2
Deoxy-Hexoses		1.56E+04 ± 29.60E+02	99.06E+02 ± 16.73E+02	2.29	0.19	Highest CO_2
Creatinine	C00791	4.13E+04 ± 81.63E+02	2.71E+04 ± 6.14E+02	2.17	0.20	Highest CO_2
L-Threonine	C00188	17.80E+04 ± 1.02E+04	15.95E+04 ± 59.01E+02	2.00	0.22	Highest CO_2
4-Hydroxybenzaldehyde	C00633	10.41E+04 ± 3.44E+04	5.41E+04 ± 1.99E+04	1.29	0.31	Highest CO_2
S-1-Phenylethanol	C07112	74.30E+04 ± 20.39E+04	48.61E+04 ± 5.36E+04	1.10	0.34	Highest CO_2
L-Valine	C00183	4.71E+06 ± 1.00E+06	3.49E+06 ± 29.82E+04	1.02	0.36	Highest CO_2
Turanose	C19636	2.56E+06 ± 75.49E+04	1.69E+06 ± 10.71E+04	0.95	0.37	Highest CO_2
L-Serine	C00716	42.49E+04 ± 15.27E+04	23.76E+04 ± 8.37E+04	0.93	0.38	Highest CO_2
Pyruvic Aldehyde	C00546	18.07E+04 ± 3.84E+04	13.58E+04 ± 1.61E+04	0.90	0.39	Highest CO_2
L-Asparagine	C16438	23.63E+04 ± 3.78E+04	16.61E+04 ± 7.39E+04	0.85	0.40	Highest CO_2
Arabitol	C01904	60.18E+04 ± 9.25E+04	52.83E+04 ± 1.93E+04	0.44	0.54	Highest CO_2
Shikimate	C00493	17.18E+04 ± 2.09E+04	14.15E+04 ± 5.84E+04	0.31	0.60	Highest CO_2
Monoshaccharides, Hexoses		1.13E+06 ± 25.53E+04	96.21E+04 ± 9.44E+04	0.27	0.62	Highest CO_2
Succinate Semialdehyde	C00232	42.20E+02 ± 3.68E+02	39.65E+02 ± 5.07E+02	0.18	0.69	Highest CO_2
Aspartate	C00049	81.66E+04 ± 13.85E+04	73.31E+04 ± 17.10E+04	0.15	0.72	Highest CO_2
Salicylate	C00805	2.03E+04 ± 52.65E+02	1.75E+04 ± 65.44E+02	0.12	0.75	Highest CO_2
3.Aminoisobutanoate	C05145	3.06E+04 ± 23.08E+02	2.93E+04 ± 78.47E+02	0.03	0.86	Highest CO_2
Succinate	C00042	17.01E+04 ± 43.32E+02	16.81E+04 ± 1.70E+04	0.02	0.90	Highest CO_2
L-Isoleucine	C16434	6.76E+06 ± 55.15E+04	6.63E+06 ± 1.03E+06	0.01	0.91	Highest CO_2
3,2-Hydroxyphenyl Propanoate	C01198	1.04E+04 ± 5.95E+02	1.03E+04 ± 8.24E+02	0.01	0.94	Highest CO_2
Cytosine	C00380	3.16E+04 ± 44.55E+02	30.85E+04 ± 82.01E+02	1024.49	< 0.01	Ambient CO_2
Guanosine	C00387	44.35E+02 ± 1.53E+02	3.45E+04 ± 5.54E+02	4324.15	< 0.01	Ambient CO_2

Table 12 continued

Metabolite	KEGG ID	Highest CO2 Mean ± SE MS Peak Area	Ambient CO2 Mean ± SE MS Peak Area	*F*	*p*	Higher concentration
Thymine	C00178	1.50E+04 ± 20.81E+02	8.47E+04 ± 39.04E+02	290.69	< 0.01	Ambient CO_2
D-Glucuronolactone	C00191	4.05E+04 ± 29.29E+02	10.25E+04 ± 23.42E+02	242.38	< 0.01	Ambient CO_2
2-Aminophenol	C01987	19.60E+04 ± 5.29E+04	1.13E+06 ± 21.53E+02	224.37	< 0.01	Ambient CO_2
Urocanate	C00785	55.89E+02 ± 14.91E+02	4.67E+04 ± 25.17E+02	223.84	< 0.01	Ambient CO_2
Adenosine	C00212	31.89E+04 ± 16.43E+04	10.61E+06 ± 79.52E+04	220.62	< 0.01	Ambient CO_2
2-Hydroxypyridine	C02502	19.71E+04 ± 3.44E+04	1.31E+06 ± 7.92E+04	204.94	< 0.01	Ambient CO_2
Guanine	C00242	5.34E+04 ± 38.76E+02	55.92E+04 ± 4.55E+04	174.26	< 0.01	Ambient CO_2
3-Amino-4-Hydroxybenzoic Acid	C12115	1.34E+04 ± 39.38E+02	10.72E+04 ± 65.62E+02	169.69	< 0.01	Ambient CO_2
5-Methylthioadenosine	C00170	2.70E+04 ± 6.58E+02	22.55E+04 ± 1.10E+04	575.99	< 0.01	Ambient CO_2
Pyridoxine	C00314	7.89E+04 ± 1.21E+04	24.94E+04 ± 1.04E+04	103.07	< 0.01	Ambient CO_2
D-Pantothenic-Acid	C00864	1.43E+04 ± 33.91E+02	9.83E+04 ± 89.01E+02	98.50	< 0.01	Ambient CO_2
Eriodictyol	C05631	1.54E+02 ± 9.27E+00	6.90E+02 ± 27.38E+00	513.31	< 0.01	Ambient CO_2
N-Acetyl-L-Alanine	C01073	1.12E+04 ± 14.02E+02	3.91E+04 ± 28.20E+02	94.20	< 0.01	Ambient CO_2
Nicotinamide	C00153	67.28E+04 ± 3.45E+04	1.23E+06 ± 4.90E+04	93.67	< 0.01	Ambient CO_2
4-Hydroxy-L-Phenylglycine Pyridoxal	CA1445	7.51E+04 ± 1.65E+04	25.55E+04 ± 59.20E+02	80.58	< 0.01	Ambient CO_2
Hypoxanthine	C00262	66.08E+02 ± 19.69E+02	3.32E+04 ± 22.32E+02	79.25	< 0.01	Ambient CO_2
Tyramine	C00483	4.37E+04 ± 41.78E+02	10.22E+04 ± 56.21E+02	73.64	< 0.01	Ambient CO_2
Histamine	C00388	1.69E+04 ± 44.53E+02	9.10E+04 ± 15.14E+02	120.80	< 0.01	Ambient CO_2
Salsolinol	C09642	2.12E+04 ± 35.26E+02	6.81E+04 ± 50.90E+02	61.97	< 0.01	Ambient CO_2
Maleamate	C01596	2.58E+04 ± 12.88E+02	4.86E+04 ± 30.21E+02	59.59	< 0.01	Ambient CO_2
Glyceraldehyde	C02154	25.41E+04 ± 1.13E+04	49.55E+04 ± 3.70E+04	51.31	< 0.01	Ambient CO_2
Glutaric Acid	C00489	6.24E+04 ± 55.75E+02	12.46E+04 ± 76.44E+02	45.90	< 0.01	Ambient CO_2
1,2-Phenylenediamine	C14402	2.57E+04 ± 84.42E+02	10.08E+04 ± 83.99E+02	37.78	< 0.01	Ambient CO_2
Naringenin	C00509	1.60E+02 ± 71.44E+00	6.76E+02 ± 13.09E+00	36.53	< 0.01	Ambient CO_2
3-Amino-5-Hydroxybenzoic Acid	C12107	2.12E+04 ± 22.92E+02	4.87E+04 ± 45.66E+02	34.24	< 0.01	Ambient CO_2
Sugars, Alcohol, Hexoses		22.31E+02 ± 3.69E+02	77.14E+02 ± 9.93E+02	34.13	< 0.01	Ambient CO_2

Table 12 continued

Metabolite	KEGG ID	Highest CO2 Mean ± SE MS Peak Area	Ambient CO2 Mean ± SE MS Peak Area	*F*	*p*	Higher concentration
Adenosine-5-Monophosphate	C00020	6.31E+04 ± 1.86E+04	23.51E+04 ± 2.44E+04	32.89	< 0.01	Ambient CO_2
6-Hydroxynicotinate	C01020	94.13E+02 ± 23.22E+02	5.99E+04 ± 1.02E+04	31.92	< 0.01	Ambient CO_2
1-Methyladenine	C02216	2.68E+04 ± 55.05E+02	6.86E+04 ± 48.00E+02	29.85	< 0.01	Ambient CO_2
D-Gulonic Acid, γ-Lactone	C01040	2.17E+04 ± 14.34E+02	3.13E+04 ± 9.96E+02	25.68	< 0.01	Ambient CO_2
Sugars, Alcohol, Pentoses		33.23E+02 ± 5.33E+02	1.14E+04 ± 17.49E+02	25.60	< 0.01	Ambient CO_2
Amino-Sugars		1.77E+04 ± 60.08E+02	8.69E+04 ± 1.43E+04	24.61	< 0.01	Ambient CO_2
Citrate	C00158	1.88E+06 ± 25.22E+04	3.93E+06 ± 35.57E+04	23.57	< 0.01	Ambient CO_2
Leucine	C16439	48.82E+04 ± 5.98E+04	89.47E+04 ± 6.07E+04	21.76	0.01	Ambient CO_2
Glycerol-3-Phosphate	C00093	63.35E+04 ± 18.22E+04	1.53E+06 ± 3.40E+04	16.93	0.01	Ambient CO_2
5-Methylcytosine-Hydrocloride	C02376	47.54E+02 ± 10.19E+02	3.37E+04 ± 92.60E+02	13.66	0.01	Ambient CO_2
4-Acetamidobutanoate (GABA)	C02946	5.77E+04 ± 1.41E+04	12.22E+04 ± 92.67E+02	12.23	0.02	Ambient CO_2
α-Ketoglutaric Acid	C00026	5.85E+04 ± 53.78E+02	11.31E+04 ± 1.84E+04	10.79	0.02	Ambient CO_2
Pyruvate	C00022	4.19E+04 ± 61.45E+02	6.68E+04 ± 28.93E+02	10.59	0.02	Ambient CO_2
Mandelic Acid	C01984	78.07E+02 ± 11.74E+02	2.11E+04 ± 46.46E+02	10.30	0.02	Ambient CO_2
4-Guanidinobutanoate	C01035	1.27E+04 ± 78.72E+02	4.33E+04 ± 24.89E+02	10.27	0.02	Ambient CO_2
Pyridoxamine	C00534	2.61E+04 ± 1.10E+04	7.83E+04 ± 1.20E+04	10.17	0.02	Ambient CO_2
N-Acetylglycine	CA1212	4.90E+04 ± 1.34E+04	9.87E+04 ± 51.12E+02	9.12	0.03	Ambient CO_2
Nicotinate Picolinic Acid	C00253	2.28E+04 ± 15.19E+02	4.77E+04 ± 98.05E+02	8.82	0.03	Ambient CO_2
α-Aminoadipate	C00956	4.69E+04 ± 1.16E+04	15.62E+04 ± 4.35E+04	7.90	0.04	Ambient CO_2
4-Aminobutanoate (GABA)	C00334	80.28E+04 ± 24.67E+04	2.48E+06 ± 63.52E+04	7.61	0.04	Ambient CO_2
Acetoacetate	C00164	3.74E+04 ± 35.81E+02	5.55E+04 ± 64.98E+02	6.92	0.05	Ambient CO_2
Galactitol	C01697	49.38E+02 ± 5.95E+02	1.52E+04 ± 49.40E+02	5.95	0.06	Ambient CO_2
O-Succinyl-L-Homoserine	C01118	18.84E+04 ± 1.98E+04	49.28E+04 ± 15.12E+04	5.59	0.06	Ambient CO_2
Hexoses, Phosphate		2.15E+04 ± 12.30E+02	5.16E+04 ± 1.54E+04	5.42	0.07	Ambient CO_2
Phloroglucinol	C02183	3.32E+06 ± 44.64E+04	4.64E+06 ± 25.71E+04	5.38	0.07	Ambient CO_2

Table 12 continued

Metabolite	KEGG ID	Highest CO2 Mean ± SE MS Peak Area	Ambient CO2 Mean ± SE MS Peak Area	*F*	*p*	Higher concentration
3-Dehydroshikimate	C02637	43.51E+02 ± 8.57E+02	72.92E+02 ± 10.74E+02	4.71	0.08	Ambient CO_2
Fumarate	C00122	18.37E+04 ± 2.16E+04	26.64E+04 ± 3.39E+04	4.69	0.08	Ambient CO_2
Uracil	C00106	8.64E+04 ± 2.49E+04	15.17E+04 ± 87.87E+02	4.62	0.08	Ambient CO_2
D-Lyxosylamine		1.58E+06 ± 22.53E+04	2.26E+06 ± 20.14E+04	4.56	0.09	Ambient CO_2
Rs-Mevalonic Acid	C00418	21.90E+02 ± 2.27E+02	1.01E+04 ± 45.29E+02	4.34	0.09	Ambient CO_2
2-6-Dihydroxypyridine	C03056	3.85E+04 ± 1.26E+04	7.14E+04 ± 61.08E+02	4.33	0.09	Ambient CO_2
Disaccharides		1.49E+06 ± 28.29E+04	2.21E+06 ± 12.14E+04	4.30	0.09	Ambient CO_2
L-Tyrosine	C01536	42.20E+04 ± 4.82E+04	90.44E+04 ± 30.01E+04	3.51	0.12	Ambient CO_2
4-Hydroxy-L-Proline	C01157	2.26E+04 ± 50.59E+02	3.48E+04 ± 66.18E+02	2.24	0.19	Ambient CO_2
L-Alanine	C00041	98.89E+04 ± 5.06E+04	1.09E+06 ± 4.54E+04	2.06	0.21	Ambient CO_2
Quinoline	C06413	6.69E+04 ± 1.94E+04	10.29E+04 ± 1.59E+04	1.84	0.23	Ambient CO_2
D-Malic Acid	C00497	1.88E+06 ± 13.19E+04	2.93E+06 ± 97.64E+04	1.60	0.26	Ambient CO_2
Uridine	C00299	54.42E+02 ± 16.16E+02	1.15E+04 ± 54.23E+02	1.51	0.27	Ambient CO_2
Fisetin	C10041	84.56E+06 ± 6.70E+06	93.98E+06 ± 4.67E+06	1.14	0.34	Ambient CO_2
Glyceric Acid	C00258	14.12E+04 ± 3.54E+04	18.07E+04 ± 2.06E+04	0.76	0.42	Ambient CO_2
Dehydroascorbate	C05422	1.33E+06 ± 19.49E+04	1.49E+06 ± 11.31E+04	0.42	0.54	Ambient CO_2
L-Pipecolic Acid	C00408	93.99E+04 ± 13.27E+04	1.12E+06 ± 26.31E+04	0.42	0.54	Ambient CO_2
Adenine	C00147	1.59E+06 ± 47.21E+04	1.92E+06 ± 26.07E+04	0.30	0.60	Ambient CO_2
3-Hydroxykynurenine	C02794	6.24E+04 ± 2.10E+04	7.81E+04 ± 2.37E+04	0.24	0.64	Ambient CO_2
3-Methoxytyramine	C05587	4.04E+04 ± 63.19E+02	4.56E+04 ± 1.24E+04	0.17	0.70	Ambient CO_2
Azelaic Acid	C08261	49.95E+02 ± 22.87E+02	57.68E+02 ± 3.73E+02	0.08	0.79	Ambient CO_2
N-Acetyl-D-l-Glutamic Acid	C00624	2.53E+06 ± 51.14E+04	2.82E+06 ± 1.05E+06	0.08	0.80	Ambient CO_2
N-α-Acetyl-L-Lysine	C12989	4.15E+04 ± 1.32E+04	4.57E+04 ± 67.02E+02	0.06	0.81	Ambient CO_2
Gallic Acid	C01424	46.84E+02 ± 10.44E+02	49.65E+02 ± 6.04E+02	0.04	0.84	Ambient CO_2
L-Arginine	C00062	2.68E+04 ± 16.85E+02	2.82E+04 ± 94.34E+02	0.03	0.87	Ambient CO_2

Table 12 continued

Metabolite	KEGG ID	Highest CO2 Mean ± SE MS Peak Area	Ambient CO2 Mean ± SE MS Peak Area	*F*	*p*	Higher concentration
Sucrose	C00089	1.16E+08 ± 15.23E+06	1.18E+08 ± 9.18E+06	0.00	0.95	Ambient CO_2
Formononetin	C00858	19.92E+02 ± 2.86E+02	20.15E+02 ± 7.69E+02	0.00	0.98	Ambient CO_2
Palmitic Acid	C00249	2.34E+06 ± 33.78E+04	2.34E+06 ± 5.60E+04	0.00	1.00	Ambient CO_2
S-Malate	C00711	3.59E+06 ± 60.23E+04	3.59E+06 ± 98.41E+04	0.00	1.00	Ambient CO_2

SBV plants exposed to ambient [CO_2] produced higher abundance of TCA cycle intermediates (Fig. 14c) such as citrate, α-ketoglutarate, pyruvate and GABA (Table 12). However, no differences were found in dark respiration rates across different [CO_2] treatments or between eelgrass populations (Fig. 9, Table 4), suggesting that the increases of TCA Cycle metabolites in plants under ambient [CO_2] may have been diverted to other metabolic pathways (e.g. Shikimate) rather than enhancing respiratory ATP production. Although depriving the plant of potential energy for growth, such diversion leads to the synthesis of secondary compounds with diverse physiological roles, such as cell signaling, production of stress-related compounds and the formation of metabolites associated with the biosynthesis of polyphenols (Weaver & Herrmann 1997). Studies have reported accumulation of α-ketoglutarate under oxidative stress in *Z. marina* (Hasler-Sheetal et al. 2015) and rice (Miro & Ismail 2013). Exposing the Mediterranean seagrass *Cymodocea nodosa* to a small range of CO_2 conditions revealed up-regulation of genes coding for respiratory metabolism, increasing energetic demand for biosynthesis and stress-related processes under similar ambient [CO_2] (pH 7.8/ [CO_2] 43 μmol Kg^{-1} SW) (Ruocco et al. 2017). Quantifying this diversion of respiratory intermediates to other pathways may provide a means for calculating the energetic cost of the physiological stress response to growth and reproductive output.

Metabolomic Response of Eelgrass: Dumas Bay comparison between high and low CO_2

The two [CO_2] treatments for DBW plants clustered in different regions along PC1 (Fig. 13C) but PERMANOVA suggests the differences were not significant (Table 11). Of the approximately 5,000 metabolites detected in DBW, individual ANOVAS showed 1167 metabolic features that changed significantly between [CO_2]. So far, 132 metabolites were identified, 8 (6.06%) were upregulated under high [CO_2] (823 μmol CO_2 Kg^{-1}SW) and 7 (5.3%)

were upregulated under low [CO_2] (107 μmol CO_2 Kg^{-1}SW). Under low [CO_2], DBW plants accumulated α-ketoglutarate, succinate, glutamate and glycerate 3-P (Fig. 14d, Table 13) again suggesting activation of the GABA shunt as a way to mitigate stress (Hasler-Sheetal et al. 2015). High [CO_2] (823 μmol $CO_2 \cdot Kg^{-1}$ SW) stimulated the abundance of shikimate and proline (Fig 14d, Table 13), consistent with increased growth and stress tolerance under elevated [CO_2].

Table 13. ANOVA CO_2 treatment comparison of relative abundance (i.e., MS peak area) and standard error of Dumas Bay eelgrass. High CO_2 (823 μmol CO_2 $KgSW^{-1}$), Low CO_2 (107 μmol CO_2 $KgSW^{-1}$).

Metabolite	KEGG ID	High CO2 Mean ± SE MS Peak Area	Low CO2 Mean ± SE MS Peak Area	*F*	*p*	Higher concentration
D-Glucosamine-6-Suflate	C02827	5.31E+04 ± 4.74E+02	77.86E+02 ± 1.80E+02	7969.16	<0.01	High CO_2
4-Hydroxybenzaldehyde	C00633	41.61E+02 ± 1.88E+02	11.03E+02 ± 3.06E+02	72.33	<0.01	High CO_2
Acetoacetate	C00164	6.94E+04 ± 17.89E+02	5.17E+04 ± 15.66E+02	55.09	<0.01	High CO_2
S-1-Phenylethanol	C07112	74.09E+04 ± 3.37E+04	48.96E+04 ± 3.52E+04	26.59	0.01	High CO_2
Shikimate	C00493	66.48E+04 ± 7.94E+04	28.77E+04 ± 2.28E+04	20.85	0.01	High CO_2
Gallic Acid	C01424	69.77E+02 ± 8.10E+02	23.49E+02 ± 7.62E+02	17.31	0.01	High CO_2
L-Proline	C16435	79.17E+06 ± 2.13E+06	46.84E+06 ± 8.59E+06	13.33	0.02	High CO_2
D-Arabinose	C00216	78.30E+04 ± 62.38E+02	69.28E+04 ± 3.15E+04	7.88	0.05	High CO_2
Fisetin	C10041	1.19E+08 ± 13.65E+06	80.10E+06 ± 5.36E+06	6.95	0.06	High CO_2
Salicylate	C00805	55.13E+02 ± 8.60E+02	25.02E+02 ± 7.96E+02	6.60	0.06	High CO_2
Adenosine-5-Monophosphate	C00020	12.59E+04 ± 2.09E+04	5.87E+04 ± 2.20E+04	4.88	0.09	High CO_2
Myo-Inositol	C00137	47.75E+06 ± 5.72E+06	32.52E+06 ± 3.90E+06	4.84	0.09	High CO_2
Arabitol	C01904	56.96E+04 ± 5.56E+04	42.47E+04 ± 3.60E+04	4.79	0.09	High CO_2
4-Aminobutanoate (GABA)	C00334	35.74E+04 ± 1.62E+04	32.04E+04 ± 49.08E+02	4.78	0.09	High CO_2
L.-sorbose	C00247	38.14E+06 ± 13.90E+06	8.06E+06 ± 88.34E+04	4.67	0.10	High CO_2
Sucrose	C00089	1.26E+08 ± 6.37E+06	1.03E+08 ± 9.44E+06	4.19	0.11	High CO_2
Fructose	C00095	56.19E+06 ± 22.86E+06	13.02E+06 ± 1.54E+06	3.55	0.13	High CO_2
D-Mannose	C00159	1.85E+06 ± 72.02E+04	53.57E+04 ± 3.74E+04	3.33	0.14	High CO_2
Diethanolamine	C06772	6.78E+04 ± 3.31E+04	75.22E+02 ± 39.43E+02	3.26	0.15	High CO_2
Phloroglucinol	C02183	7.62E+06 ± 1.29E+06	5.25E+06 ± 45.37E+04	3.02	0.16	High CO_2
Succinate Semialdehyde	C00232	1.16E+04 ± 30.63E+02	62.22E+02 ± 5.92E+02	2.99	0.16	High CO_2
D-Lyxosylamine		1.91E+06 ± 31.60E+04	1.33E+06 ± 12.64E+04	2.85	0.17	High CO_2
5-Methylthioadenosine	C00170	4.48E+04 ± 22.82E+02	2.62E+04 ± 1.08E+04	2.85	0.17	High CO_2
D-Trehalose	C01083	1.79E+06 ± 25.93E+04	1.13E+06 ± 31.01E+04	2.63	0.18	High CO_2

Table 13 continued

Metabolite	KEGG ID	High CO2 Mean ± SE MS Peak Area	Low CO2 Mean ± SE MS Peak Area	*F*	*p*	Higher concentration
Rosmarinic Acid	C01850	57.90E+04 ± 33.30E+04	4.21E+04 ± 2.40E+04	2.59	0.18	High CO_2
Monoshaccharides, Hexoses		1.86E+06 ± 77.52E+04	61.80E+04 ± 4.49E+04	2.55	0.19	High CO_2
Creatine	C00300	81.76E+04 ± 47.44E+04	7.15E+04 ± 3.75E+04	2.46	0.19	High CO_2
L-Tyrosine	C01536	35.30E+04 ± 4.75E+04	28.04E+04 ± 43.56E+02	2.32	0.20	High CO_2
Pyridoxine	C00314	16.31E+04 ± 1.99E+04	11.70E+04 ± 2.41E+04	2.17	0.21	High CO_2
Monosaccharides Pentoses		12.64E+04 ± 1.84E+04	9.74E+04 ± 90.09E+02	2.00	0.23	High CO_2
4.Guanidinobutanoate	C01035	22.37E+04 ± 11.96E+04	5.41E+04 ± 2.22E+04	1.94	0.24	High CO_2
L-Pipecolic-Acid	C00408	1.49E+06 ± 37.59E+04	95.68E+04 ± 6.52E+04	1.94	0.24	High CO_2
Hypoxanthine	C00262	15.34E+04 ± 6.12E+04	6.68E+04 ± 1.33E+04	1.91	0.24	High CO_2
Creatinine	C00791	11.50E+04 ± 5.92E+04	3.48E+04 ± 67.41E+02	1.81	0.25	High CO_2
N-Acetyl-D-l-Glutamic Acid	C00624	2.06E+06 ± 34.20E+04	1.40E+06 ± 37.90E+04	1.69	0.26	High CO_2
L-Valine	C00183	13.72E+06 ± 7.03E+06	4.33E+06 ± 2.19E+06	1.63	0.27	High CO_2
Adenosine	C00212	23.58E+04 ± 13.25E+04	7.69E+04 ± 1.04E+04	1.43	0.30	High CO_2
Pyruvic Aldehyde	C00546	20.55E+04 ± 9.51E+04	10.21E+04 ± 1.06E+04	1.17	0.34	High CO_2
Caffeic Acid	C01197	87.49E+04 ± 20.75E+04	65.42E+04 ± 4.94E+04	1.07	0.36	High CO_2
6-Phosphogluconic Acid	C00345	7.33E+04 ± 2.22E+04	5.00E+04 ± 58.99E+02	1.03	0.37	High CO_2
Sugars, Alcohol, Hexoses		96.95E+02 ± 13.34E+02	75.83E+02 ± 17.26E+02	0.94	0.39	High CO_2
L-Isoleucine	C16434	1.97E+06 ± 55.89E+04	1.41E+06 ± 18.19E+04	0.93	0.39	High CO_2
D-Pantothenic Acid	C00864	10.41E+04 ± 3.41E+04	6.96E+04 ± 1.51E+04	0.86	0.41	High CO_2
Xylitol	C00379	10.81E+04 ± 2.55E+04	7.99E+04 ± 1.90E+04	0.78	0.43	High CO_2
4-Hydroxy-L-Phenylglycine	CA1445	18.83E+04 ± 7.99E+04	12.21E+04 ± 47.18E+02	0.69	0.45	High CO_2
Pyridoxal 1-Aminocyclopropane-1-Carboxylate	C01234	2.29E+06 ± 12.23E+04	1.87E+06 ± 51.08E+04	0.63	0.47	High CO_2
S-Malate	C00711	5.36E+06 ± 2.48E+06	3.31E+06 ± 1.07E+06	0.57	0.49	High CO_2
Luteolin	C01514	6.77E+06 ± 3.80E+06	3.72E+06 ± 1.47E+06	0.56	0.50	High CO_2

Table 13 continued

Metabolite	KEGG ID	High CO2 Mean ± SE MS Peak Area	Low CO2 Mean ± SE MS Peak Area	*F*	*p*	Higher concentration
Galactitol	C01697	84.07E+02 ± 20.09E+02	60.72E+02 ± 24.15E+02	0.55	0.50	High CO_2
3-Methoxytyramine	C05587	5.19E+04 ± 9.72E+02	4.69E+04 ± 67.02E+02	0.53	0.51	High CO_2
D-Gulonic Acid, γ-Lactone	C01040	3.69E+04 ± 1.04E+04	2.92E+04 ± 42.98E+02	0.47	0.53	High CO_2
D-Malic Acid	C00497	3.48E+06 ± 1.49E+06	2.43E+06 ± 85.22E+04	0.38	0.57	High CO_2
Turanose	C19636	1.60E+06 ± 18.61E+04	1.41E+06 ± 30.46E+04	0.28	0.63	High CO_2
Leucine	C16439	54.55E+04 ± 16.48E+04	44.94E+04 ± 8.92E+04	0.26	0.63	High CO_2
L.DOPA	C00355	52.57E+04 ± 23.02E+04	39.15E+04 ± 10.68E+04	0.19	0.69	High CO_2
Phenylacetic Acid	C07086	41.63E+02 ± 23.39E+02	27.12E+02 ± 26.01E+02	0.17	0.70	High CO_2
3.Hydroxykynurenine	C02794	8.44E+04 ± 3.04E+04	7.02E+04 ± 1.69E+04	0.17	0.70	High CO_2
Glutaric Acid	C00489	11.32E+04 ± 2.64E+04	10.32E+04 ± 52.65E+02	0.14	0.73	High CO_2
Resorcinol Monoacetate	C12064	88.44E+02 ± 29.12E+02	74.55E+02 ± 23.71E+02	0.14	0.73	High CO_2
Rs-Mevalonic Acid	C00418	51.14E+02 ± 4.67E+02	46.72E+02 ± 12.80E+02	0.11	0.76	High CO_2
Mandelic Acid	C01984	2.10E+04 ± 85.77E+02	1.82E+04 ± 41.11E+02	0.09	0.78	High CO_2
5-Methylcytosine Hydrochloride	C02376	5.16E+04 ± 89.69E+02	4.92E+04 ± 43.70E+02	0.05	0.83	High CO_2
Nicotinamide	C00153	1.11E+06 ± 6.34E+04	1.09E+06 ± 15.29E+04	0.02	0.89	High CO_2
L-Phenylalanine	C02057	75.89E+04 ± 14.95E+04	73.54E+04 ± 7.22E+04	0.02	0.89	High CO_2
Naringenin	C00509	22.80E+02 ± 9.49E+02	22.46E+02 ± 16.78E+02	0.00	0.99	High CO_2
α-Ketoglutaric Acid	C00026	1.09E+04 ± 29.89E+02	6.06E+04 ± 27.71E+02	148.52	<0.01	Low CO_2
D-3-Phosphoglyceric.Acid (Glycerate 3P)	C00597	95.48E+02 ± 53.36E+02	7.63E+04 ± 78.57E+02	49.41	<0.01	Low CO_2
O-Succinyl-L-Homoserine	C01118	22.50E+04 ± 2.74E+04	1.03E+06 ± 17.17E+04	21.50	0.01	Low CO_2
1-Methyladenine	C02216	3.62E+04 ± 93.22E+02	7.93E+04 ± 52.28E+02	16.24	0.02	Low CO_2
Glutamic Acid (Glutamate)	C00025	3.90E+06 ± 45.34E+04	8.71E+06 ± 1.20E+06	14.10	0.02	Low CO_2
Succinate	C00042	6.40E+04 ± 38.40E+02	13.28E+04 ± 1.81E+04	13.82	0.02	Low CO_2

Table 13 continued

Metabolite	KEGG ID	High CO2 Mean ± SE MS Peak Area	Low CO2 Mean ± SE MS Peak Area	*F*	*p*	Higher concentration
N-α-Acetyl-L-Lysine	C12989	3.50E+04 ± 84.95E+02	7.55E+04 ± 95.55E+02	10.04	0.03	Low CO_2
Maleamate	C01596	3.00E+04 ± 51.71E+02	8.13E+04 ± 2.14E+04	5.42	0.08	Low CO_2
2-Hydroxypyridine	C02502	77.64E+04 ± 7.79E+04	1.27E+06 ± 19.79E+04	5.36	0.08	Low CO_2
Pyruvate	C00022	5.69E+04 ± 20.32E+02	7.38E+04 ± 69.77E+02	5.35	0.08	Low CO_2
Guanosine	C00387	3.00E+04 ± 24.28E+02	5.57E+04 ± 1.11E+04	5.18	0.09	Low CO_2
Sugars, Alcohol, Pentoses		37.90E+02 ± 9.48E+02	83.83E+02 ± 18.06E+02	5.07	0.09	Low CO_2
Quinoline	C06413	3.37E+04 ± 75.35E+02	4.99E+04 ± 16.23E+02	4.42	0.10	Low CO_2
3-Dehydroshikimate	C02637	73.98E+02 ± 16.20E+02	1.16E+04 ± 11.51E+02	4.37	0.10	Low CO_2
N-Acetyl-L-Alanine	C01073	2.98E+04 ± 3.52E+02	3.65E+04 ± 36.02E+02	3.45	0.14	Low CO_2
Hexoses. Phosphate		4.67E+04 ± 2.50E+04	11.35E+04 ± 2.73E+04	3.26	0.15	Low CO_2
N-ε-Trimethyl Lysine	C03793	13.64E+02 ± 46.86E+00	34.27E+02 ± 14.85E+02	3.46	0.16	Low CO_2
Urocanate	C00785	3.73E+04 ± 34.12E+02	14.66E+04 ± 6.40E+04	2.91	0.16	Low CO_2
Uracil	C00106	16.81E+04 ± 91.72E+02	25.08E+04 ± 4.78E+04	2.88	0.16	Low CO_2
Pyridoxamine	C00534	3.63E+04 ± 9.68E+02	5.83E+04 ± 1.37E+04	2.55	0.19	Low CO_2
D-Glucuronolactone	C00191	8.65E+04 ± 2.41E+04	12.34E+04 ± 42.83E+02	2.27	0.21	Low CO_2
Azelaic-Acid	C08261	34.55E+02 ± 8.16E+02	64.63E+02 ± 18.57E+02	2.20	0.21	Low CO_2
Histamine	C00388	4.76E+04 ± 59.27E+02	6.39E+04 ± 95.39E+02	2.12	0.22	Low CO_2
Guanine	C00242	54.94E+04 ± 2.76E+04	92.49E+04 ± 26.23E+04	2.03	0.23	Low CO_2
N-Acetylglycine	CA1212	6.57E+04 ± 86.22E+02	9.12E+04 ± 1.71E+04	1.78	0.25	Low CO_2
Adenine	C00147	7.66E+06 ± 56.81E+04	9.48E+06 ± 1.24E+06	1.76	0.25	Low CO_2
4-Hydroxy-L-Proline	C01157	10.72E+04 ± 71.02E+02	12.54E+04 ± 1.18E+04	1.73	0.26	Low CO_2
Citrate	C00158	2.11E+06 ± 87.25E+04	3.54E+06 ± 66.92E+04	1.69	0.26	Low CO_2
Cytosine	C00380	41.57E+04 ± 3.66E+04	60.80E+04 ± 14.70E+04	1.61	0.27	Low CO_2
Salsolinol	C09642	3.05E+04 ± 17.30E+02	4.47E+04 ± 1.12E+04	1.55	0.28	Low CO_2

Table 13 continued

Metabolite	KEGG ID	High CO2 Mean ± SE MS Peak Area	Low CO2 Mean ± SE MS Peak Area	*F*	*p*	Higher concentration
N-Acetyl-D-Tryptophan	C03137	63.51E+02 ± 68.60E+00	1.12E+04 ± 39.55E+02	1.52	0.29	Low CO_2
3-Aminoisobutanoate	C05145	1.72E+04 ± 44.18E+02	2.32E+04 ± 27.27E+02	1.31	0.32	Low CO_2
Formononetin	C00858	3.47E+02 ± 89.93E+00	6.55E+02 ± 2.59E+02	1.26	0.33	Low CO_2
L-Alanine	C00041	60.19E+04 ± 4.15E+04	76.48E+04 ± 14.37E+04	1.19	0.34	Low CO_2
Uridine	C00299	4.03E+04 ± 1.17E+04	5.69E+04 ± 99.28E+02	1.17	0.34	Low CO_2
α-Aminoadipate	C00956	10.57E+04 ± 89.31E+02	13.83E+04 ± 2.92E+04	1.14	0.35	Low CO_2
2-6-Dihydroxypyridine	C03056	5.05E+04 ± 50.38E+02	6.49E+04 ± 1.26E+04	1.13	0.35	Low CO_2
3-2-Hydroxyphenyl Propanoate	C01198	59.96E+02 ± 5.67E+02	80.47E+02 ± 18.64E+02	1.11	0.35	Low CO_2
L-Serine	C00716	16.83E+04 ± 70.83E+02	24.18E+04 ± 7.67E+04	0.91	0.39	Low CO_2
L-Threonine	C00188	18.64E+04 ± 3.22E+04	24.26E+04 ± 5.02E+04	0.89	0.40	Low CO_2
Palmitic Acid	C00249	2.45E+06 ± 4.92E+04	3.25E+06 ± 99.43E+04	0.65	0.47	Low CO_2
Disaccharides		3.44E+06 ± 49.72E+04	4.03E+06 ± 55.30E+04	0.63	0.47	Low CO_2
Eriodictyol	C05631	11.96E+02 ± 5.42E+02	26.31E+02 ± 20.88E+02	0.44	0.54	Low CO_2
Tyramine	C00483	4.08E+04 ± 95.01E+02	5.21E+04 ± 1.42E+04	0.44	0.54	Low CO_2
Dehydroascorbate	C05422	56.00E+04 ± 26.29E+04	72.58E+04 ± 2.23E+04	0.40	0.56	Low CO_2
Linoleic Acid	C01595	18.06E+04 ± 5.69E+04	29.20E+04 ± 21.40E+04	0.40	0.57	Low CO_2
5-Oxo-L-Proline	C01879	8.52E+06 ± 96.91E+04	11.23E+06 ± 4.36E+06	0.37	0.58	Low CO_2
Deoxy-Hexoses		60.58E+02 ± 13.94E+02	70.73E+02 ± 10.30E+02	0.34	0.59	Low CO_2
1-2-Phenylenediamine	C14402	4.87E+04 ± 1.21E+04	5.86E+04 ± 1.49E+04	0.27	0.63	Low CO_2
6-Hydroxynicotinate	C01020	4.87E+04 ± 48.38E+02	5.34E+04 ± 75.80E+02	0.27	0.63	Low CO_2
3-Amino-5-Hydroxybenzoic Acid	C12107	3.48E+04 ± 18.80E+02	3.78E+04 ± 60.36E+02	0.23	0.66	Low CO_2
L-Glutamine	C00303	14.20E+06 ± 2.30E+06	18.46E+06 ± 9.55E+06	0.19	0.69	Low CO_2
Glyceraldehyde	C02154	40.84E+04 ± 5.64E+04	44.02E+04 ± 4.72E+04	0.19	0.69	Low CO_2
Fumarate	C00122	15.47E+04 ± 5.17E+04	18.25E+04 ± 3.90E+04	0.18	0.69	Low CO_2
Trigonelline	C01004	6.00E+06 ± 1.24E+06	7.09E+06 ± 2.27E+06	0.18	0.70	Low CO_2

Table 13 continued

Metabolite	KEGG ID	High CO2 Mean ± SE MS Peak Area	Low CO2 Mean ± SE MS Peak Area	*F*	*p*	Higher concentration
L-Asparagine	C16438	11.44E+04 ± 1.79E+04	14.46E+04 ± 7.41E+04	0.16	0.71	Low CO_2
Glycerol-3-Phosphate	C00093	68.27E+04 ± 15.36E+04	76.28E+04 ± 13.98E+04	0.15	0.72	Low CO_2
Galactonic Acid	C00880	48.72E+04 ± 15.57E+04	59.85E+04 ± 26.28E+04	0.13	0.73	Low CO_2
Aspartate	C00049	1.27E+06 ± 47.44E+04	1.43E+06 ± 9.70E+04	0.11	0.76	Low CO_2
Thymine	C00178	7.87E+04 ± 76.41E+02	8.34E+04 ± 1.38E+04	0.09	0.78	Low CO_2
Glyceric Acid	C00258	18.83E+04 ± 3.55E+04	19.75E+04 ± 1.13E+04	0.06	0.82	Low CO_2
3-Amino-4-Hydroxybenzoic Acid	C12115	4.23E+04 ± 96.25E+02	4.66E+04 ± 2.06E+04	0.04	0.86	Low CO_2
Amino-Sugars		5.63E+04 ± 3.52E+04	6.37E+04 ± 2.19E+04	0.03	0.87	Low CO_2
Nicotinate Picolinic Acid	C00253	4.84E+04 ± 61.66E+02	4.96E+04 ± 52.35E+02	0.02	0.89	Low CO_2
L-Arginine	C00062	1.00E+04 ± 24.94E+02	1.07E+04 ± 43.58E+02	0.01	0.91	Low CO_2
2-Aminophenol	C01987	72.94E+04 ± 5.98E+04	74.03E+04 ± 12.21E+04	0.01	0.94	Low CO_2
4-Acetamidobutanoate	C02946	11.80E+04 ± 2.17E+04	11.89E+04 ± 80.55E+02	0.00	0.97	Low CO_2

Conclusion

These results revealed that eelgrass populations from very different thermal environments both exhibited increased thermal tolerance with enhanced photosynthetic energy capture, sucrose formation and growth under CO_2 enrichment that could counteract some climate warming impacts on this foundational species. Although similar whole plant responses to CO_2 in terms of leaf sucrose, leaf growth, and shoot numbers suggest common effects of CO_2 enrichment, differences in metabolite profiles hint at important genetic differences between these populations. Metabolomics analyses suggest that stress causes the diversion of carbon flow pathways from growth and energy (ATP) production to non-anabolic intermediates that may help elucidate important mechanisms responsible for stress tolerance and quantify the energetic cost of the stress response.

Although the differences in metabolite pools observed here in response to different [CO_2] point to shifts in the activities of metabolic pathways leading to whole plant responses to potential climate forcing, noting that metabolite pool sizes alone are insufficient to fully understand the physiological basis for whole-plant responses to climate-driven environmental change.In addition to making more detailed analyses of metabolite change over time, analyses of changes in the proteome and transcriptome will be necessary to fully understand key genomic functions and metabolic pathways, and those analyses are currently under way. However, the metabolite profiles generated here, in combination with analysis of whole-plant performance, provide a force multiplier for translating 'omic' approaches into a predictive understanding of the physiological response of seagrasses to an increasingly hot and sour sea, and the potential for populations to adapt to new environments. Such mechanistic knowledge will help predict earth

system interactions in the context of global cycles and help inform best practices for seagrass restoration.

CHAPTER 4

DIFFERENTIAL GENE EXPRESSION AMONG GEOGRAPHICALLY DISTINCT POPULATIONS OF *ZOSTERA MARINA* L (EELGRASS) IN RESPONSE TO SIMULATED CLIMATE CHANGE

Introduction

The transcriptome is the set of RNAs transcribed from an entire organism or a specific cell type mainly composed of messenger or coding RNAs and a variety of non-coding RNAs (Srivastava et al. 2019). Inherently the transcriptome is dynamic and provides direct knowledge of gene regulation and protein content information. There are two types of transcriptomic analysis: single gene expression (targeted) and whole transcriptome (untargeted). Most studies use RNA-sequence to examine changes in the whole transcriptome. RT-qPCR is a common method for measurements of gene expression in individual genes and had played an important role in molecular research of seagrasses (Winters et al. 2011, Dattolo et al. 2014, Lauritano et al. 2015, Salo et al. 2015, Olivé et al. 2017), absolute and relative quantification are employed to quantify single gene expression data. The absolute quantification method requires the use of an array of standard curves. In contrast, relative quantification enables the calculation of the difference between a reference gene and the gene of interest producing a ΔCt value as a proxy to compare between different groups/samples. Targeted genes analysis might help us understand how molecular changes of foundation species cope with increase in CO_2 and temperature leading to physiological responses (Gracey 2007, Evans & Hofmann 2012).

Gene expression plays a central role in organismal plasticity and adaptation to environmental change by synchronizing physiological changes and metabolic pathways at the genetic level (Pigliucci 1996, DeWitt et al. 1998). Thus, genetic differences among organisms

and/or populations can limit their responses to their immediate environment within a single generation often impacting productivity and survival (Raven & Geider 2003). Seagrasses are sessile organisms fully exposed to their surrounding environment and any fluctuation in it. Therefore, any change in their surrounding influence the plant biogeochemical processes thus mirroring environmental changes. Recent studies have used transcriptomes from populations of *Z. marina* (Franssen et al. 2011, Winters et al. 2011, Salo et al. 2015), *Posidonia oceanica* (Dattolo et al. 2014, Lauritano et al. 2015, Ruocco et al. 2019) and *Cymodocea nodosa* (Olivé et al. 2017, Ruocco et al. 2017) to contextualize physiological results from temperature, light and acidification experiments. In the case of *Z. marina*, geographically isolated eelgrass populations appear to be genetically distinct (Alberte et al. 1994, Williams & Orth 1998, Reusch et al. 1999), displaying high plasticity in leaf morphology, suggesting that populations may be adapted to different conditions (Reusch et al. 1999, Staehr & Borum 2011). These leaf phenotypic variations are the result of expression of genes and gene complexes induced in response to environmental change or during changes in physiological state (Gracey 2007).

Environmental changes such as the increase in ocean CO_2 availability can reduce seagrass light requirements and enhance productivity and thermal tolerance, providing some compensation for climate warming (Björk et al. 1997, Zimmerman et al. 1997, Touchette & Burkholder 2000, Palacios & Zimmerman 2007, Zimmerman et al. 2015, Zimmerman et al. 2017). Specifically, *Z. marina* populations from South Bay in the Chesapeake Bay, VA and Dumas Bay in Puget Sound, WA exposed to a gradient of CO_2 concentrations not only revealed a positive effect of high CO_2 concentration enhancing overall plant size, growth, survival and leaf sugar (Chapter 2) but also an increase in the abundance of Calvin Cycle and nitrogen assimilation metabolites while suppressing stress-related metabolites (Chapter 3). As a result,

plants encompassed several physiological and morphological adjustments. Therefore, the objective of this study was to compare the gene expression patterns of eelgrass from South Bay, Virginia (SBV) and Dumas Bay, Washington (DBW) in the context of the whole plant physiology and metabolomic studies reported in Chapters 2 and 3. In theory, increased CO_2 availability should increase the gene expression of carbon fixation and photosynthetic genes and decrease the expression of stress response genes involved in temperature. Differential responses among populations may help identify heritable traits that facilitate adaptation of eelgrass to changing climate conditions and improve our predictive capacity for restoration and conservation of these important ecosystem engineers.

Materials and Methods

Source of Plant Materials

As previously stated (Chapter 2), in April 2013 eelgrass shoots from South Bay, Virginia and Dumas Bay in southern Puget Sound, WA were carefully uprooted by hand, transported and planted in the experimental growth facility at the Virginia Aquarium & Marine Science Center, Virginia Beach, VA. The 20 outdoor aquaria were maintained at five CO_2 concentrations ranging from ambient (~55μmol CO_2 Kg^{-1} SW, pH ~8.0) to 2121 μmol CO_2 Kg^{-1} SW (pH 6) (Zimmerman et al. 2017). From the 20 aquaria only in 10 aquaria DBW and NBW were present, therefore, having up to two replicates per CO_2 treatment for these populations and up to 4 replicates for SBV. Parallel experiments were running in the aquaria limiting the space, therefore five seagrass containers were into each aquaria (three plastic containers for SBV, one for DBW, and one for NBW).

Then, in April 2014 a second set of freshly uprooted plants from South Bay VA and Dumas Bay WA were transplanted to the experimental facility. Two separate containers of these new plants from South Bay (i.e. 2nd-year transplants, NSB) were added next to the acclimated SBV shoots from 2013 in each aquarium. The Dumas Bay 1st-year transplants were discarded in April 2014 and one container of new plants was added into the tanks (i.e., 2nd-year transplants, NDB) due to space limitation.

Tissue Collection, Storage, RNA extraction and cDNA preparation

The 2nd youngest leaf (No. 1 was the youngest leaf) was collected monthly from a shoot at random from each plastic container. The reason for choosing 2nd youngest leaf is that the levels of activity (metabolism, protein content) of *Z. marina* leaves decrease from the youngest (number 1) to the oldest (Mazzella & Alberte 1986, Kraemer et al. 1998). Leaf-age related differences in plant responses at molecular, physiological and morphological levels are amplified therefore leaf tissues with approximately 14 days of age were chosen. Epiphytes were removed by gently scraping each leaf with a clean razor blade, followed by a brief rinse in 0.2 μm-filtered seawater. The clean leaves were patted dry with a tissue, flash frozen in liquid nitrogen and stored at -80° C until RNA extraction.

The set of samples analyzed for gene expression included South Bay (SBV) leaves from three CO_2 treatments (55.3, 107.81 and 823.15 $\mu molKg^{-1}SW$) and five months (September 2013, November 2013, January 2014, April 2014, and August 2014). For Dumas Bay (DBW) plants, a low number of replicates due to sample limitation only allowed the gene expression analysis of three CO_2 treatments (55.3, 107.81 and 823.15 $\mu molKg^{-1}SW$) and three months (November 2013, January 2014, and April 2014). Also plants transplanted from the field in April 2014 into the CO_2 treatments but sampled in August 2014 were analyzed representing the peak of thermal stress period of our long running experiment. This also enabled the comparison of plants acclimated for a year to short term (3 month) acclimated plants from South Bay (NSB) and Dumas Bay (NDB). Nisqually Bay WA (NBW) eelgrass was not included because plants did not survive the warm summer of 2013.

Frozen leaf samples were removed from freezer, immediately placed 10mL of in house prepared RNAlater and incubated overnight at 4° C. The leaves were then ground to a fine

powder with mortar and pestles containing liquid nitrogen. Nucleic acids (total RNA + DNA) were extracted using InviTrap Spin Plant RNA Mini Kit (Stratec Molecular GmbH, Berlin, Germany), according to the manufacturer's protocol. About 100-120 mg of powdered tissue was suspended in 900 μl of lysis solution (RP buffer supplemented with DDT). RNase-free DNase I (Qiagen) was used to eliminate any trace of genomic DNA, leaving behind the total RNA. The quantity and purity of the total RNA were analyzed using Nanodrop 2000 Spectrophotometer (Thermo Scientific, Waltham, MA, USA), and Qubit 2.0 Fluorometer (Invitrogen by Life Technologies). RNA was used when Abs 260 nm/Abs 280 nm varied between 1.9 and 2.1 and the Abs 260nm /Abs 230 nm was >2.0. RNA concentrations ranged between 2.64 and 600 ng/μl showing high variability between biological replicates that originated from different aquaria. The quality of the RNA samples was confirmed using an Agilent 2100 Bioanalyzer (RNA 6000 NanoKit); only high quality RNA was used in the subsequent analyses (RNA integrity number, RIN>6). RNA templates were diluted ranging from 1.22 to 10 ng/μl final concentration (i.e., RNA not normalized). RNA was reverse transcribed into complimentary DNA (cDNA) using QuantiTect Reverse Transcription Kit (Qiagen) following the manufacturer's protocol. The protocol consisted in genomic elimination reactions and reverse-transcription reactions. The total reaction volume of genomic DNA elimination reaction components was increased to17.5 μl. From this initial volume, 3.5 μl was sampled after incubation to be used as non-reverse-transcription control (NRTC).

Target gene selection and QPCR

Seven target genes previously identified by Bergmann et al. (2010), Salo et al. (2015), Winters et al (2011) and Kong et al. (2016) were chosen (Table 14). These genes are involved in temperature stress response, carbon fixation and photosynthesis selected to compare the

responses to CO_2 and temperature between the South Bay VA and Dumas Bay WA eelgrass populations. The mRNA products provided transcription information from

i) two proteins involved in the photosynthetic process: Photosystem II 22 kDa protein (PSBS) and a Light-Harvesting Chlorophyll a/b-Binding Protein (LHCB5)
ii) two genes involve in carbon metabolism: Rubisco, large subunit-binding protein subunit alpha (RBP) and sucrose synthase (SS)
iii) two antioxidant/stress genes: Catalase (CAT) and Superoxide dismutase (Mn) (SOD)
iv) Hsp70, a gene from the Heat shock proteins chaperone family, 70kDa

The eukaryotic initiation factor 4A (eIF4A) and TATA box were used as housekeeping genes (HKG) (Ransbotyn & Reusch 2006) under the assumption that they provide constant expression levels necessary for calibrating target gene expression levels and were analyzed for stability in the experimental CO_2 conditions.

RT-qPCR was performed in MicroAmpFast 96-well reaction plate (Applied Biosystems) with Optical Adhesive Covers (Applied Biosystems) on, to measure the abundance of target genes relative to the reference gene. Each plate included 3 samples in technical triplicates with housekeeping genes and target genes, in addition to two no-template controls (NTC) for each primer set using sterile water. The PCR reaction mix consisted of 10 μL Power SYBR® Green PCR Master Mix (Applied Biosystems), 2 μL cDNA template, 0.8 μ L of each primer and 6.4μL of RNase/DNase free water in a total volume of 20 μL. The thermal profile involved (i) an initial denaturation period for 20 min 95° C, (ii) 40 cycles of denaturation at 95° C and annealing at 54° C (duration 15 sec $cycle^{-1}$) and (iii) a final extension for 1min at 60° C.

Lastly, to explore the differential expression between populations, CO_2 conditions and compare expression over time −ΔCt (cycle threshold) values were used. The relative gene expression levels were calculated as:

$$-\Delta Ct = Ct\ (housekeeping\ gene) - Ct\ (target\ gene)$$

Statistical Analysis

The number of biological replicates varied between 1 to 4 per population per CO_2 treatment each month. Two-way analysis of variance (Two-Way ANOVA) was performed for all the −ΔCt values obtained from the different populations, implemented in the multivariate general linear model component of IBM SPSS Statistics 22 using log [CO_2] and month as factors. Following two-way ANOVA, a Tukey's HSD post hoc test was performed to assess significant differences ($p < 0.05$) in −ΔCt values in response to the different CO_2 treatments and months for each population. Principal component analysis (PCA) was performed with gene expression data (−ΔCt values) to explore general patterns along principal components (PC) 1 and PC2 that explained most variability. The datasets analyzed were SBV alone, DBW alone, NSBV alone, NDBW alone, SBV + DBW, SBV + NDBW+ SBV and then by month. PCAs were performed in R version 4.0.3 (R Core Team 2019) using the function prcomp found in “stats” package (R Core Team 2019).

The interacting effects of environmental parameters were analyzed by regressing −ΔCt values against temperature, light (PAR), and [CO_2] values averaged over the 2-week period preceding the leaf collection date. This period accounted the response time (short-term) of the plants adjust the photosynthetic apparatus that drive carbon assimilation under different CO_2 treatments (Celebi 2016), and noticeable changes in growth helping to determine the relative

significance of each environmental parameter to drive the gene expression changes. For each gene, a general multiple linear regression was performed against all three environmental predictors (temperature, PAR, [CO_2]) and simple linear regression against sucrose concentration and chlorophyll concentration, where data from all CO_2 treatments were aggregated. Additionally, for each CO_2 treatment, stepwise multiple linear regression was performed to discern the principal environmental predictor ([CO_2], temperature, PAR) among the different treatments. Each CO_2 treatment resulted in some temporal variability in [CO_2] due to the dependency of CO_2 solubility on water temperature and salinity/alkalinity. Therefore, during these treatments, specific multiple linear regression analysis and collinearity statistics between CO_2 and temperature were evaluated. Steps were taken to account for the variance inflation factor (VIF) of the index of collinearity statistics which should not exceed the threshold value of 2 (Help IBM SPSS Statistics). VIF quantifies the severity of multicollinearity in an ordinary least squares regression analysis, a low VIF index assured that multiple linear regression models between -ΔCt with CO_2, temperature and light as predictors to be a significant explanatory fit.

Table 14. *Zostera marina* genes and primer pairs used in the gene expression analysis and their function.

Gene name	**Abbreviation**	**Function**	**Primer sequence**	**Encoded**	**Synonyms**
Photosystem II, 22 kDa protein[d]	PSBS	Photosynthesis, chloroplast precursor	F: 5-TTC CCA AAA AGG TGG TAG TTA-3 R: 5-ATA AAG AAG CGG CAA AAC C-3	chloroplast	Psbs, CP22
Light-Harvesting Complex, Chlorophyll a/b-Binding Protein [e]	LHCB5	Photosynthesis, light-harvesting protein of photosystem II	F: 5-TGG AGA AGT CCC CGG AGA CT-3 R: 5-AAC GGC AAT GGA GCA GC-3	Nuclear	CP26, LHCIIc Light-harvesting complex II protein 5
Catalase[d]	CAT	Antioxidant	F: 5-ACA AAA TTC CGT CCG TCA-3 R: 5-GTC CTC AAG GAG TAT TGG TCC TC-3	Nuclear	CAT2
Superoxidase dismutase (Mn)[d]	SOD	Antioxidant	F: 5-ATG GGT GTG GCT TGC TTA-3 R: 5-ATG CAT GCT CCC ATA CAT CT-3	Nuclear	
Heat shock protein[a]	HSP70	Molecular chaperone	F: 5-CAC GAC CGT GTT GAG ATC AT-3 R: 5-ACC GCT TCG CAT CAA AGA C-3	Nuclear	

Table 14 continued

Rubisco, large subunit-binding protein subunit alpha[b]	RBP	Enzyme (in photosynthesis)	F: 5-CCA TCT CTA CCG CTA TCC CT-3 R: 5-GAC GAC CTC ACA ACA AAC CT-3	chloroplast	60 kDa chaperonin subunit alpha, CPN-60 alpha
Sucrose synthase[b]	SS	Enzyme (sucrose catabolism)	F: 5-TTA CCG TAT AAC TCG ACC AAA CC-3 R: 5-TAG CAA AGA AGA CAA CAC TGA G-3	Nuclear	
Eukaryotic initiation factor 4A[c]	eIF4A	Translation initiation factor (housekeeping gene)	F: 5-TCT TTC TGC GAT GCG AAC AG-3 R: 5-TGG ATG TAT CGG CAG AAA CG-3	Nuclear	
TATA Box binding protein[c]	TATA	General RNA polymerase II transcription factor	F: 5-CGG AGA GCT CAT TGA AAC AGC TA-3 R: 5-GGA ACT TTT CCT TCC AAC TTC AGA-3	Nuclear	

Genes previously researched by: [a]Bergmann et al. (2010), [b]Salo et al. (2015), [c]Ransbotyn and Reusch (2006), [d]Winters et al (2011),[e]Kong et al. (2016)

Results

Housekeeping genes across CO_2 treatments

Both the housekeeping genes eIF4A and TATA box showed a high level of expression with Ct values between 27.62 and 32.95 for EIF4A and 30.54 to 35.52 for TATA. Raw Ct data of housekeeping genes are reported in Fig. 16. High Ct variability was observed showing that the expression of both HKG vary among different CO_2 conditions and time (months) (Table 15). EIF4A was selected for normalizing expression data of the remaining genes as the Ct value was below the recommended upper threshold of 35 (de Kok et al. 2005) and had been used as reference gene in previous studies on *Z. marina* (Ransbotyn & Reusch 2006, Winters et al. 2011, Salo et al. 2015, Zang et al. 2018).

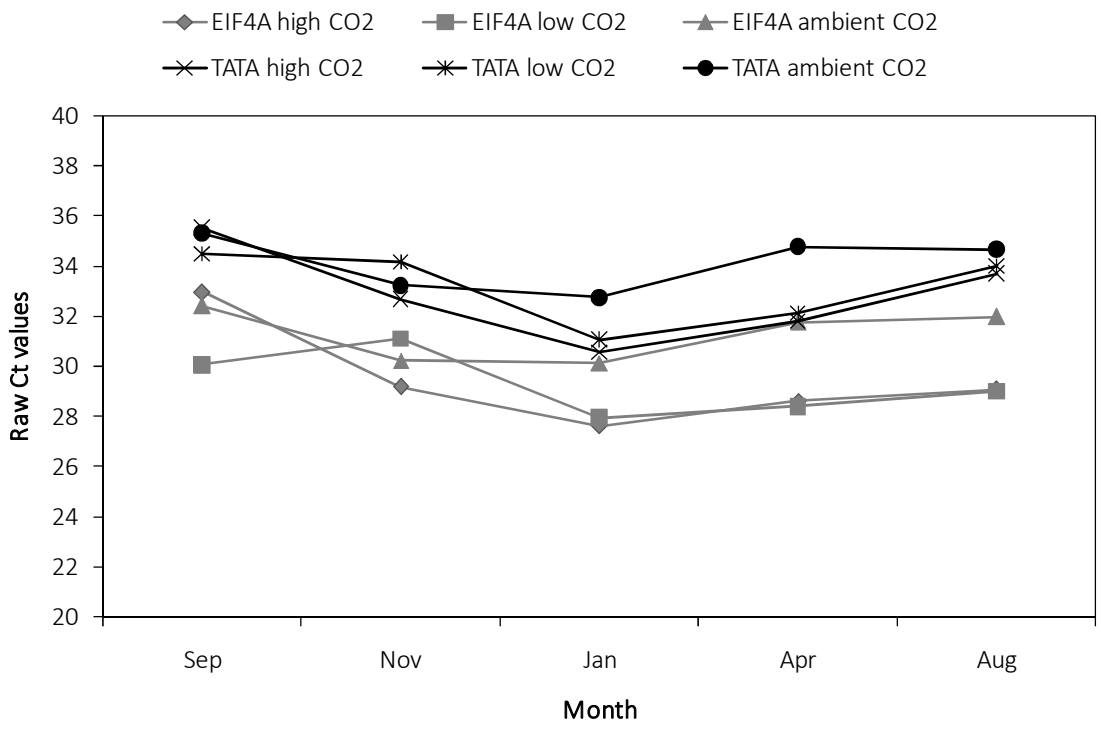

Figure 16. Ct values obtained for the candidate reference genes used on eelgrass leaves growing at different CO_2 concentrations during the five RNA sampling time points (months).

Table 15. Summary of two-way ANOVA results for comparison of Ct values across CO_2 treatments and time for the housekeeping genes used in this study. ANOVA table for Type III tests of fixed effects using the univariate general linear model routine implemented in SPSS. log [CO_2], month and housekeeping gene were treated as fixed factors.

Source	Type III Sum of Squares	*df*	Mean Square	*F*	*p*
HKG	441.42	1	441.42	128.86	<0.001*
log [CO_2]	67.89	2	33.95	9.91	<0.001*
month	185.76	4	46.44	13.56	<0.001*
HKG* log [CO_2]	5.19	2	2.59	0.76	0.47
HKG X month	8.51	4	2.13	0.62	0.65
log [CO_2] X month	74.40	8	9.30	2.72	0.01*
HKG X log [CO_2] $_X$ month	7.68	8	0.96	0.28	0.97

South Bay comparison across time and CO_2 treatments

Principal components analysis of SBV gene expression across time and CO_2 treatments showed a cluster of plants growing in November under the intermediate CO_2 treatment (pH 7.5, 107 μmol $CO_2 \cdot Kg^{-1}$ SW) along the PC1which explains over 28% of the total variability (Fig. 17) suggesting that plants growing at this CO_2 level in November experienced more changes in gene expression compared to other CO_2 treatments and months.

In general, two-way ANOVA of SBV gene expression showed clear statistical differences through time for six of the seven genes measured ($p < 0.05$, Table 16). Genes coding for PSBS, LHCB5, RBP and SS expression changed through time (Fig. 18-19) and showed a significant interaction between month and log [CO_2] ($p < 0.05$, Table 16) suggesting that the

effect of CO_2 on gene expression was modified by temporal responses where the mean for gene expression differ between CO_2 treatments for at least one month.

The relative quantity of PSBS transcripts changed through time (Fig.18a, Table 16) indicating significant differences between the depth of winter (January 2014) and the other time points and between November 2013 and April 2014. PSBS gene expression was expected to respond to light. However, linear regression analysis found no correlations between gene expression and light availability (Total daily PAR) as well as no correlations to other environmental features (CO_2 variability, temperature), chlorophyll or leaf sugar concentration under different CO_2 treatments (Table 17). Analyzing CO_2 treatments individually highlighted that the gene expression of PSBS under high CO_2 (pH 6.5, 823 μmol $CO_2 \cdot Kg^{-1}$ SW) responded to sucrose concentration (p= 0.025, Table 18) maybe suggesting a signaling function of sucrose on mRNA levels of PSBS.

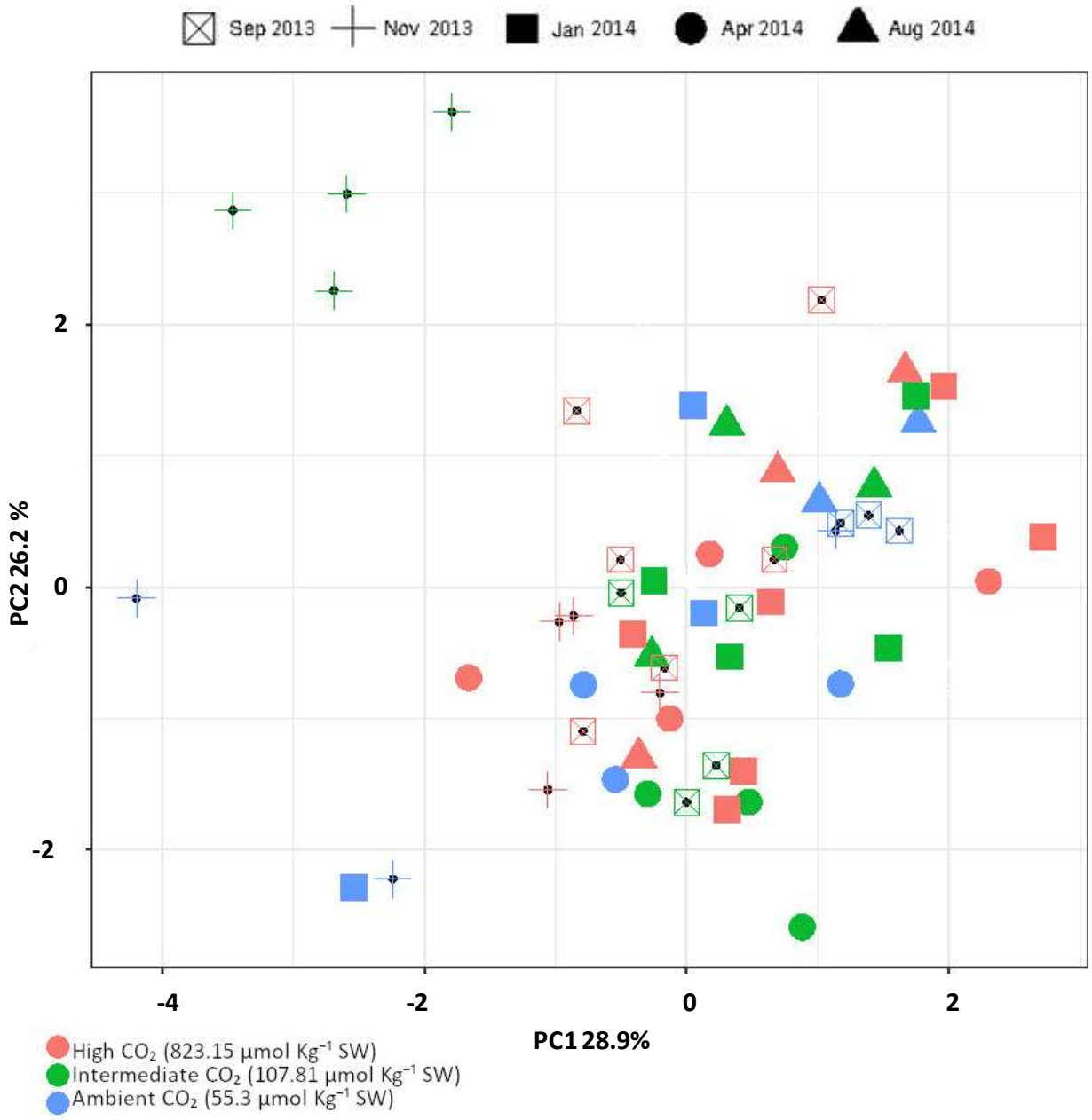

Figure 17. Principal Component Analyses of the −ΔCt values of eelgrass leaves growing at different CO_2 concentrations from South Bay, VA including three CO_2 treatments and five months (September 2013, November 2013, January 2014, April 2014 and August 2014). CO_2 treatments indicated by color.

Table 16. Summary of two-way ANOVA results for comparison of relative gene expression across CO_2 treatments for South Bay, VA eelgrass. ANOVA table for Type III tests of fixed effects using the multivariate general linear model routine implemented in SPSS. Log [CO_2] and month were treated as fixed factors.

GOI	Source	Type III Sum of Squares	*df*	Mean Square	*F*	*p*
PSBS	month	218.62	4	54.65	16.22	<0.001*
	log [CO_2]	5.87	2	2.93	0.87	0.43
	month X log [CO_2]	191.61	8	23.95	7.11	<0.001*
CAT	month	17.88	4	4.47	0.69	0.60
	log [CO_2]	9.05	2	4.53	0.70	0.50
	month X log [CO_2]	55.16	8	6.89	1.07	0.40
HSP70	month	46.55	4	11.64	3.04	0.03*
	log [CO_2]	1.75	2	0.88	0.23	0.80
	month X log [CO_2]	57.94	8	7.24	1.89	0.09
LHCB5	month	594.08	4	148.52	12.20	<0.001*
	log [CO_2]	13.83	2	6.92	0.57	0.57
	month X log [CO_2]	277.95	8	34.74	2.85	0.01*
RBP	month	51.56	4	12.89	8.77	<0.001*
	log [CO_2]	5.04	2	2.52	1.71	0.19
	month X log [CO_2]	58.29	8	7.29	4.96	<0.001*
SOD	month	29.42	4	7.35	7.53	<0.001*
	log [CO_2]	0.27	2	0.13	0.14	0.87
	month X log [CO_2]	10.47	8	1.31	1.34	0.25
SS	month	104.95	4	26.24	2.89	0.05*
	log [CO_2]	28.43	2	14.22	1.57	0.24
	month X log [CO_2]	264.43	8	33.05	3.64	0.01*

Table 17. South Bay linear regression analysis with their standardized coefficients.* indicate significance at $p \leq 0.05$.

	Multiple Linear Regression (3 predictors)				Simple Linear Regression (1 predictor)			
GOI	**Predictors**	**Beta**	***t***	***p***	**Predictors**	**Slope**	***t***	***p***
PSBS	Daily Average [CO_2]	0.17	0.64	0.54	[Suc] μmol g^{-1} DW	0.02	2.06	0.06
	Daily Average Temp	-0.68	-1.77	0.10	Total Chl per LA (μg Chl cm^{-2})	-0.13	-0.87	0.40
	Daily Total PAR	0.56	1.47	0.17				
CAT	Daily Average [CO_2]	-0.03	-0.13	0.90	[Suc] μmol g^{-1} DW	0.00	-0.45	0.66
	Daily Average Temp	-0.46	-1.15	0.28	Total Chl per LA (μg Chl cm^{-2})	-0.04	-0.55	0.59
	Daily Total PAR	0.66	1.67	0.12				
HSP70	Daily Average [CO_2]	-0.06	-0.20	0.85	[Suc] μmol g^{-1} DW	0.00	-0.19	0.85
	Daily Average Temp	0.53	1.30	0.22	Total Chl per LA (μg Chl cm^{-2})	0.11	1.40	0.19
	Daily Total PAR	-0.28	-0.69	0.50				
LHCB5	Daily Average [CO_2]	0.19	0.91	0.38	[Suc] μmol g^{-1} DW	-0.01	-0.90	0.38
	Daily Average Temp	-0.11	-0.39	0.71	Total Chl per LA (μg Chl cm^{-2})	0.06	0.28	0.78
	Daily Total PAR	0.82	2.77	0.02*				
RBP	Daily Average [CO_2]	0.03	0.13	0.90	[Suc] μmol g^{-1} DW	0.00	-0.25	0.81
	Daily Average Temp	0.79	2.36	0.04*	Total Chl per LA (μg Chl cm^{-2})	0.04	0.41	0.69
	Daily Total PAR	-0.96	-2.90	0.01*				
SOD	Daily Average [CO_2]	0.13	0.60	0.56	[Suc] μmol g^{-1} DW	0.00	-0.96	0.36
	Daily Average Temp	0.71	2.22	0.05*	Total Chl per LA (μg Chl cm^{-2})	0.08	1.68	0.12
	Daily Total PAR	-0.01	-0.03	0.98				
SS	Daily Average [CO_2]	-0.22	-0.79	0.45	[Suc] μmol g^{-1} DW	-0.02	-2.01	0.07
	Daily Average Temp	0.37	0.89	0.39	Total Chl per LA (μg Chl cm^{-2})	0.11	0.55	0.59
	Daily Total PAR	-0.17	-0.41	0.69				

Table 18. South Bay backward stepwise linear regression model results for effects of environmental and physiological parameters on the gene expression for each CO_2 treatment (exc.: defined by the stepping method criteria parameters were excluded from the model if the significance level of their *F* values >0.10, #: collinearity statistics VIF>2.0).

		High CO_2		Intermediate CO_2		Ambient CO_2			High CO_2		Intermediate CO_2		Ambient CO_2	
GOI	**Predictors**	**Beta**	***p***	**Beta**	***p***	**Beta**	***p***	**Predictors**	**Slope**	***p***	**Slope**	***p***	**Slope**	***p***
PSBS	Daily Average [CO_2]	0.840	0.075	exc.		exc.		[Suc] μmol g^{-1} DW	0.023	0.025*	0.037	0.182	-0.002	0.876
	Daily Average Temp	exc.		exc.		exc.		Total Chl per LA (μg Chl cm^{-2})	-0.205	0.344	-0.221	0.817	-0.032	0.912
	Daily Total PAR	exc.		exc.		exc.								
CAT	Daily Average [CO_2]	exc.		0.648	0.006*	0.989	0.001*	[Suc] μmol g^{-1} DW	0.004	0.147	0.008	0.033*	-0.011	0.348
	Daily Average Temp	-1.448	0.013*	exc.		exc.		Total Chl per LA (μg Chl cm^{-2})	-0.053	0.189	-0.156	0.285	-0.196	0.580
	Daily Total PAR	1.085	0.023*	-1.181	0.002*	exc.								
HSP70	Daily Average [CO_2]	exc.		1.177	0.058#	-2.12	0.044*#	[Suc] μmol g^{-1} DW	0.000	0.973	0.007	0.541	-0.006	0.659
	Daily Average Temp	exc.		1.824	0.073#	exc.		Total Chl per LA (μg Chl cm^{-2})	0.169	0.195	-0.025	0.937	0.319	0.315
	Daily Total PAR	exc.		-2.732	0.046*#	2.50	0.033*#							
LHCB5	Daily Average [CO_2]	exc.		exc.		0.824	0.005*	[Suc] μmol g^{-1} DW	0.003	0.892	-0.020	0.663	-0.025	0.148
	Daily Average Temp	exc.		exc.		0.288	0.037*	Total Chl per LA (μg Chl cm^{-2})	0.050	0.873	1.128	0.366	0.863	-0.096
	Daily Total PAR	exc.		0.820	0.089	exc.								
RBP	Daily Average [CO_2]	exc.		exc.		3.284	0.082#	[Suc] μmol g^{-1} DW	-0.003	0.697	0.000	0.983	-0.003	0.652
	Daily Average Temp	1.140	0.059	exc.		exc.		Total Chl per LA (μg Chl cm^{-2})	0.053	0.573	-0.040	0.941	0.232	0.162
	Daily Total PAR	-1.398	0.041*	exc.		-2.197	0.096#							
SOD	Daily Average [CO_2]	exc.		exc.		exc.		[Suc] μmol g^{-1} DW	-0.001	0.810	-0.003	0.610	-0.006	0.459
	Daily Average Temp	exc.		exc.		0.868	0.057	Total Chl per LA (μg Chl cm^{-2})	0.135	0.151	0.100	0.543	0.256	0.158
	Daily Total PAR	exc.		exc.		exc.								
SS	Daily Average [CO_2]	exc.		exc.		0.718	0.013*	[Suc] μmol g^{-1} DW	-0.005	0.730	-0.003	0.454	-0.020	0.105
	Daily Average Temp	exc.		exc.		0.421	0.035*	Total Chl per LA (μg Chl cm^{-2})	0.065	0.747	-0.154	0.896	0.011	0.977
	Daily Total PAR	exc.		exc.		exc.								

During the experiment, LHCB5 gene expression followed the temporal pattern in irradiance as confirmed by the positive correlation with irradiance (Table 17), while CO_2 (quasi-constant seasonally) and temperature, which lagged the solar signal by 43 days, had no significant impact. The LHCB5 gene expression differed in November 2013 across CO_2 treatments when intermediate CO_2 sample exhibited lower expression than the other CO_2 treatments. Also in August 2014 when irradiance started to decrease (Fig 2) LHCB5 expression under high CO_2 was lower than the other CO_2 treatments (Fig. 18b, Table 3). Correlating individual CO_2 treatments to the environmental features showed that gene expression of LHCB5 under ambient CO_2 responded positively to increasing temperature and seasonal variability of CO_2, whereas the irradiance at such a low CO_2 environment had no significant impact (Table 18). On the other hand, LHCB5 gene expression did not change under intermediate and high CO_2 treatments (i.e. pH 7.5, 107μmol $CO_2 \cdot Kg^{-1}$ SW and pH 6.5, 823 μmol $CO_2 \cdot Kg^{-1}$ SW) revealing no consistent pattern that can be relate to CO_2 treatment or seasonal variability in light and temperature (Fig.18b, Table 18).

CO_2 had no significant impact on RBP gene expression throughout the experiment, despite the fact that RBP responded to irradiance and temperature (Table 17). When analyzing each CO_2 treatment the RBP gene expression of plants under high and ambient CO_2 responded to increasing irradiance (Table 18) while RBP gene expression of plants under intermediate CO_2 concentrations (pH 7.5, 107 μmol $CO_2 \cdot Kg^{-1}$ SW) did not change in response to the environmental features (temperature, irradiance, CO_2 variability) (Table 18). ANOVA revealed that RBP gene expression changed through time and showed a significant interaction between month and log [CO_2] (Fig. 18c, $p < 0.05$, Table 16). CO_2 treatments only differed in November 2013 when plants experienced low light and cold temperatures (Fig. 18c, Table 16). However,

RBP expression decreased across CO_2 treatments during spring when the plants experienced optimal growth temperatures ($\geq$ 15º C) and irradiances ($\geq$ 18 mol quanta m^{-2} d^{-1}, Fig. 1), (Fig. 18c). Despite the decrease in RBP across CO_2 treatments, these conditions favored a differential response across CO_2 treatments increasing survival and sucrose concentrations under high CO_2 conditions (Fig. 4a and 7a).

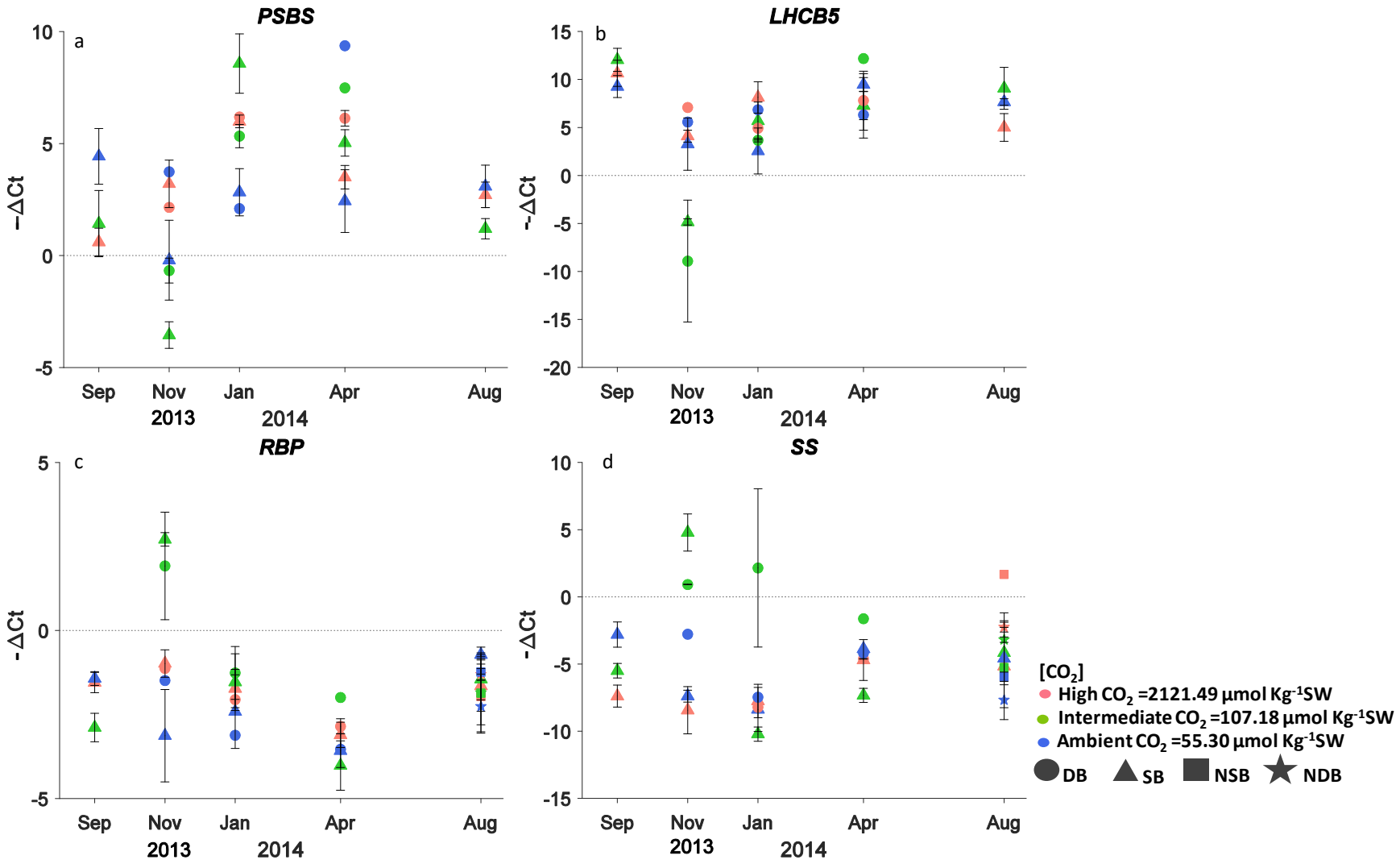

Figure 18. Effects of CO_2 and temperature on mean gene expression (–ΔCt) of eelgrass populations.–ΔCt values of 4 GOI (gene names Table 14) measured from different time points for plants from South Bay, VA (filled triangles), Dumas Bay, WA (filled circles), 2nd year transplants South Bay (filled squares) and 2nd year transplants Dumas Bay, VA (stars). CO_2 treatment is indicated by color. Means ± SE.

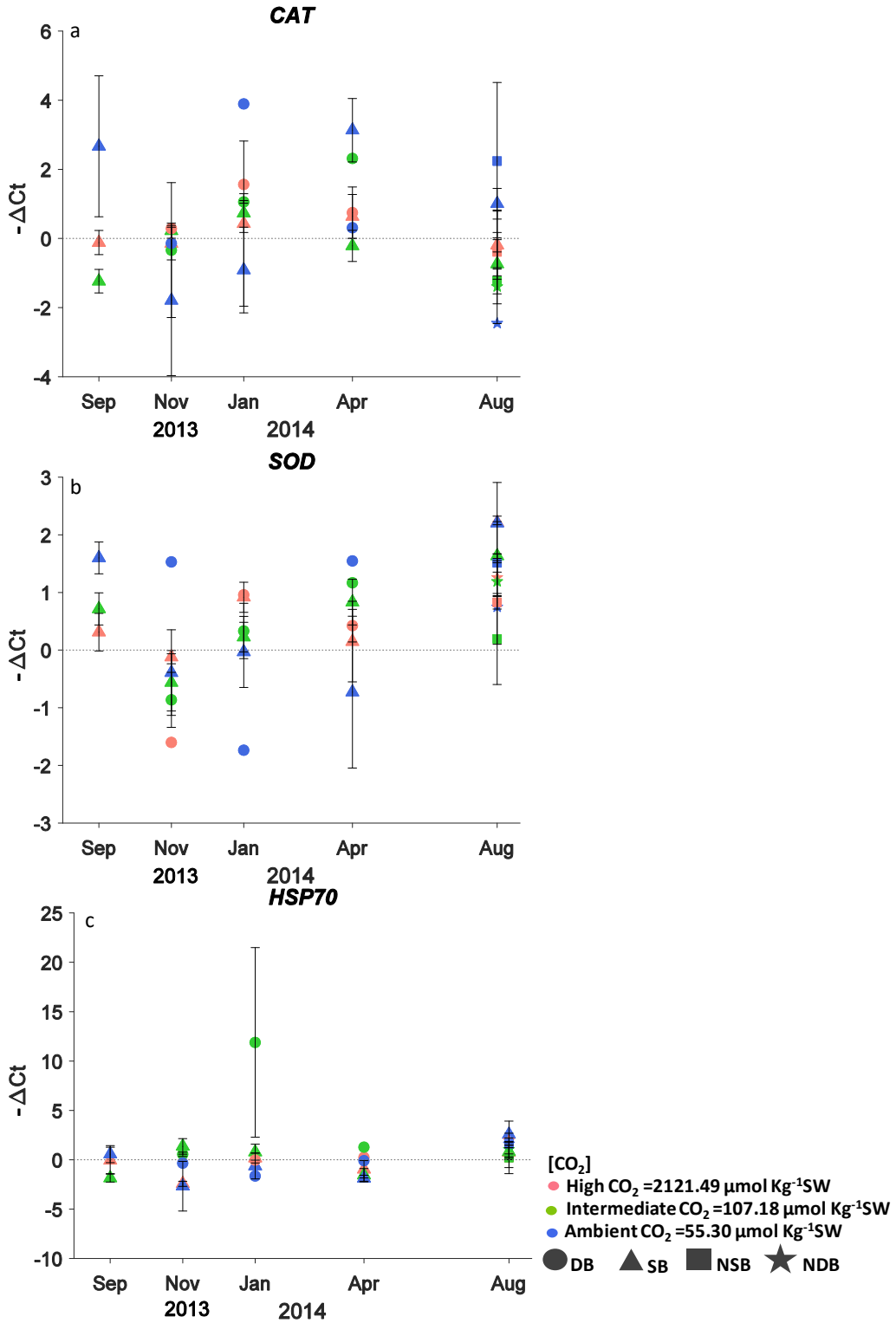

Figure 19. Effects of CO_2 and temperature on mean gene expression (–ΔCt) of eelgrass populations.–ΔCt values of 3 GOI (gene names Table 14) measured from different time points for plants from South Bay, VA (filled triangles), Dumas Bay, WA (filled circles), 2nd year transplants South Bay (filled squares) and 2nd year transplants Dumas Bay, VA (stars). CO_2 treatment is indicated by color. Means ± SE.

The gene coding for sucrose synthase (SS) changed through time and showed significant interaction between month and log [CO_2] (Fig. 18d, Table 16) suggesting that the CO_2 effect was modified by temporal responses. However, SS gene expression across CO_2 treatments did not respond independently to CO_2 treatment or seasonal variability in light or temperature (Table 17). Further, the relationship between SS gene expression and sucrose concentration was weak (p=0.07, Table 17). However, in September 2013 SS -ΔCt showed dissimilarity across CO_2 treatments (Fig. 18d) when leaf sucrose concentrations started to differentiated across CO_2 treatments (Chapter 2). Then, during winter when ambient temperature and growth rates were low, sugar concentrations peaked in all CO_2 treatments agreeing with a lower SS expression across CO_2 treatments (Fig. 18d). Subsequently during the summer of 2014 as sucrose reserves were mobilized to support shoot proliferation (Zimmerman et al. 2017), there were no differences in the expression of the SS gene among CO_2 treatments (Fig. 18d, Table 18).

According to the South Bay ANOVA the gene coding for the antioxidant enzyme CAT did not change in response to CO_2 treatments or time (Fig. 19a, Table 16). This was then confirmed by the multiple linear regression where CAT gene expression was not affected by temperature, irradiance or CO_2 variability (Table 17). However, similarly to SS during September 2013 and April 2014 CAT showed dissimilarity in -ΔCt across CO_2 treatments (Fig. 19a) when leaf sucrose concentrations across treatments were significantly different (Chapter 2). Analyzing individual CO_2 treatments, CAT expression was higher in plants exposed to low and intermediate CO_2 concentrations, suggesting that these plants might be under stress (Table 18) while CAT expression on plants under high CO_2 were affected by temperature and irradiance (Table 18).

In September 2013 SOD also showed dissimilarity in -ΔCt between ambient CO_2 and the other CO_2 treatments (Fig. 19b) when leaf sucrose concentrations differed across treatments

(Chapter 2) but sucrose concentration did not appear as a predictor in the regression analysis (Table 18). However, temperature had a significant impact on the expression of the antioxidant gene super oxidase dismutase [Mn] (SOD Mn) (Table 17), being highest in August 2014 when plants experienced high temperatures (Fig. 19b, Table 3). Within individual CO_2 treatments, temperature was the most significant environmental predictor of SOD for the ambient CO_2 treatment having a marginally significant relationship (p=0.057) (Fig. 19b, Table 18).

Although the expression of HSP70 changed through time, it was not significantly related to irradiance, temperature or CO_2 variability (Fig. 19c, Table 16). When analyzed by individual CO_2 treatments, HSP70 gene expression was, however, affected by irradiance in the intermediate and ambient CO_2 treatments (Table 17). Despite differences in survival and sucrose concentration particularly during April 2014 (Chapter 2) HSP70 transcripts did not differ across CO_2 treatments. The two-way ANOVA post hoc comparisons indicated significant differences in HSP70 expression between April 2014 and August 2014, with HSP70 expression being higher in August 2014 when plants experienced high irradiance and temperatures above their threshold and high irradiances (Fig. 19c).

When comparing only 2nd year transplants across CO_2 treatments in August 2014 no significant differences in the expression of the seven genes as assessed by RT-qPCR was detected (Fig. 18, 19, $p< 0.05$, Table 19). This result was unexpected as plants experienced approximately 67 days above their thermal threshold during this time period (Fig. 3) and differences in survival across CO_2 treatments (Zimmerman et al. 2017).

Table 19. Summary of two-way ANOVA results for comparison of relative gene expression in August 2014 across CO_2 treatments for new plants from South Bay, VA eelgrass. ANOVA table for Type III tests of fixed effects using the multivariate general linear model routine implemented in SPSS. log [CO_2] was treated as fixed factors.

GOI	Source	Type III Sum of Squares	*df*	Mean Square	*F*	*p*
PSBS	log [CO_2]	23.40	2	11.70	2.80	0.21
CAT		16.68	2	8.34	0.65	0.58
HSP70		2.12	2	1.06	0.10	0.91
LHCB5		9.56	2	4.78	0.58	0.61
RBP		1.59	2	0.79	0.22	0.81
SOD		1.70	2	0.85	0.54	0.63
SS		43.86	2	21.93	0.92	0.49

Dumas Bay comparison across CO_2 treatments

DBW plants had a low number of replicates across CO_2 concentrations and less time points than SBV due to sample limitation. However, PCA across CO_2 treatments for this population showed high correlation among CO_2 treatments and months (Fig. 20). Two-way ANOVA also demonstrated that CO_2 and months had no effect on expression of most of the genes of interest (Table 20). The only gene expression that changed significantly during the experiment was PSBS where months were significantly different (Fig. 18a, $p< 0.05$, Table 20) therefore changing through time in response to irradiance (Table 21). The post hoc comparisons indicated significant differences in PSBS expression between November 2013 and January 2014 (Fig. 18). In November 2013, DBW had more PSBS expression under high CO_2 (pH 6.5, 823

μmol $CO_2 \cdot Kg^{-1}$ SW) and ambient CO_2 (pH 8, 55 μmol $CO_2 \cdot Kg^{-1}$ SW) but intermediate CO_2 (pH 7.5, 107μmol $CO_2 \cdot Kg^{-1}$ SW) had a small change while in January 2014 when irradiance and temperature were low PSBS expression increased across CO_2 treatments (Fig. 18a). When analyzing each CO_2 treatment, the PSBS and LHCB5 gene expression responded positively to CO_2 under intermediate CO_2, whereas the temperature and irradiance in this treatment had no significant impact (Table 22). The RBP gene expression of Dumas Bay did not show differences across treatments or months (Fig. 18c, $p < 0.05$, Table 20) but had negative relationship with irradiance (*beta*= -0.81, Table 8).

Gene expression of DBW 2nd-year transplants measured in August 2014, were not affected by CO_2 treatment ($p < 0.05$, Table 23). However, the only genes showing low differential expression was SS under ambient CO_2 conditions (pH 8, 55 μmol $CO_2 \cdot Kg^{-1}$ SW) (Fig. 18d, $p < 0.05$, Table 10), perhaps responding to low sucrose concentration in this treatment (Chapter 2).

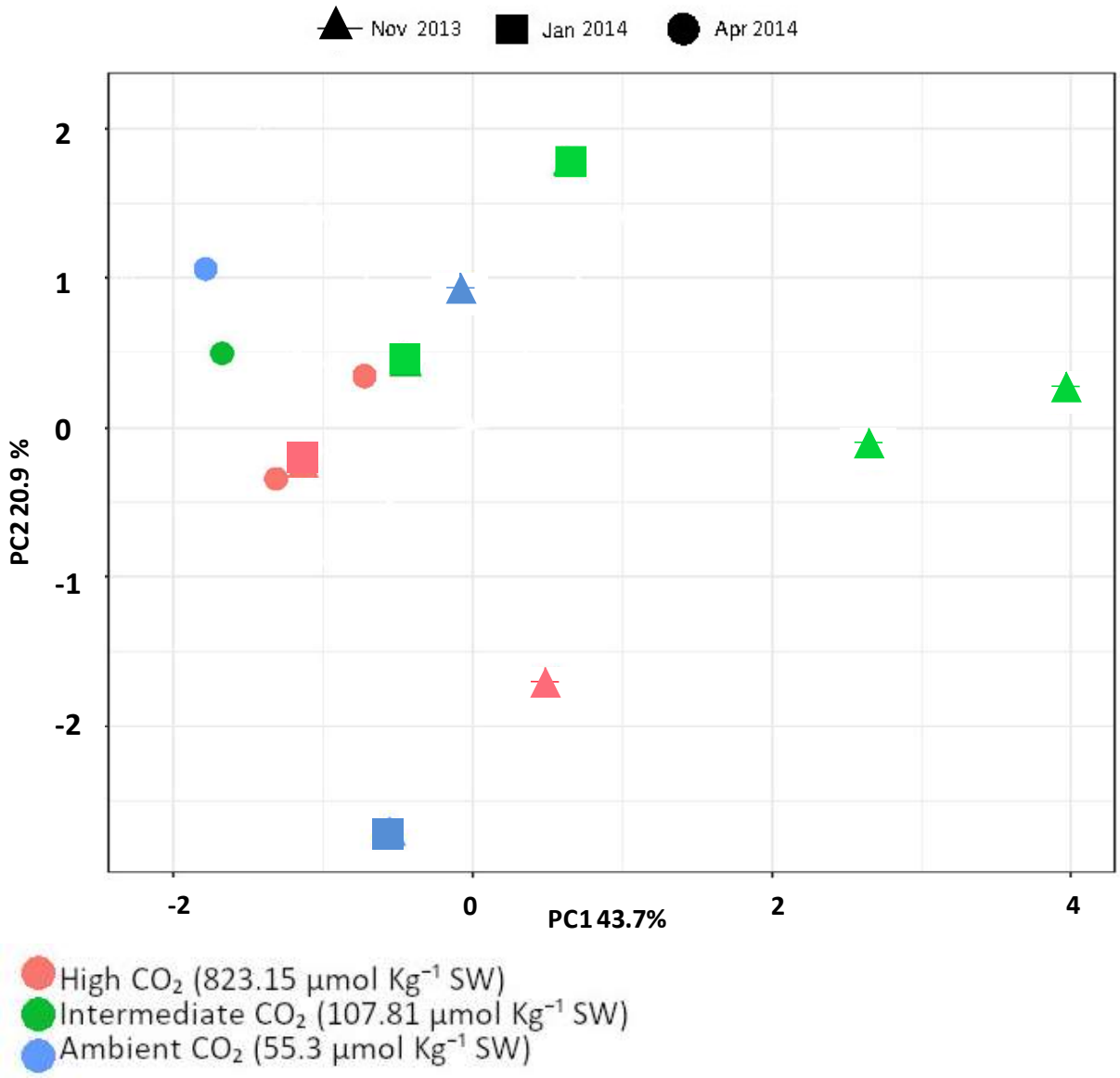

Figure 20. Principal Component Analyses of the −ΔCt values of eelgrass leaves growing at different CO_2 concentrations from Dumas Bay, WA including three CO_2 treatments and three months (November 2013, January 2014 and April 2014). CO_2 treatments are indicated by color.

Table 20. Summary of two-way ANOVA results for comparison of relative gene expression across CO_2 treatments for Dumas Bay, WA eelgrass. ANOVA table for Type III tests of fixed effects using the multivariate general linear model routine implemented in SPSS. Log [CO_2] and month were treated as fixed factors.

GOI	Source	Type III Sum of Squares	*df*	Mean Square	*F*	*p*
PSBS	month	63.16	2	31.58	68.14	<0.001*
	log [CO_2]	2.19	2	1.10	2.36	0.24
	month X log [CO_2]	28.75	4	7.19	15.51	0.02*
CAT	month	8.99	2	4.50	1.55	0.35
	log [CO_2]	0.41	2	0.20	0.07	0.93
	month X log [CO_2]	7.36	4	1.84	0.63	0.67
HSP70	month	28.71	2	14.35	0.16	0.87
	log [CO_2]	63.68	2	31.84	0.34	0.74
	month X log [CO_2]	78.86	3	26.29	0.28	0.84
LHCB5	month	101.79	2	50.89	1.53	0.35
	log [CO_2]	45.69	2	22.85	0.69	0.57
	month X log [CO_2]	190.47	4	47.62	1.43	0.40
RBP	month	12.77	2	6.38	2.97	0.19
	log [CO_2]	10.32	2	5.16	2.40	0.24
	month X log [CO_2]	2.56	4	0.64	0.30	0.86
SOD	month	3.96	2	1.98	5.50	0.10
	log [CO_2]	0.45	2	0.22	0.62	0.59
	month X log [CO_2]	10.07	4	2.52	7.00	0.07
SS	month	8.24	2	4.12	0.18	0.85
	log [CO_2]	78.00	2	39.00	1.69	0.32
	month X log [CO_2]	26.53	3	8.84	0.38	0.77

Table 21. Dumas Bay linear regression analysis with their standardized coefficients. * indicate significance at $p \leq 0.05$.

	Multiple Linear Regression (3 predictors)				Simple Linear Regression (1 predictor)			
GOI	**Predictors**	**Beta**	***t***	***p***	**Predictors**	**Slope**	***t***	***p***
PSBS	Daily Average [CO_2]	0.04	0.21	0.84	[Suc] μmol g^{-1} DW	0.00	-0.38	0.71
	Daily Average Temp	-0.49	-2.12	0.07				
	Daily Total PAR	0.98	4.21	0.00*				
CAT	Daily Average [CO_2]	-0.07	-0.25	0.81	[Suc] μmol g^{-1} DW	0.00	0.52	0.61
	Daily Average Temp	-0.67	-1.96	0.09				
	Daily Total PAR	0.49	1.40	0.20				
HSP70	Daily Average [CO_2]	-0.15	-0.38	0.72	[Suc] μmol g^{-1} DW	0.01	0.51	0.63
	Daily Average Temp	-0.43	-0.98	0.36				
	Daily Total PAR	0.10	0.23	0.83				
LHCB5	Daily Average [CO_2]	0.17	0.61	0.56	[Suc] μmol g^{-1} DW	-0.01	-0.56	0.59
	Daily Average Temp	-0.36	-1.09	0.31				
	Daily Total PAR	0.67	1.98	0.08				
RBP	Daily Average [CO_2]	-0.13	-0.54	0.61	[Suc] μmol g^{-1} DW	0.00	0.21	0.84
	Daily Average Temp	0.51	1.74	0.12				
	Daily Total PAR	-0.81	-2.72	0.03*				
SOD	Daily Average [CO_2]	-0.11	-0.37	0.72	[Suc] μmol g^{-1} DW	0.00	-0.23	0.82
	Daily Average Temp	-0.13	-0.34	0.74				
	Daily Total PAR	0.57	1.55	0.16				
SS	Daily Average [CO_2]	-0.43	-1.32	0.23	[Suc] μmol g^{-1} DW	-0.01	-0.50	0.63
	Daily Average Temp	0.18	0.48	0.65				
	Daily Total PAR	-0.26	-0.67	0.53				

Table 22. Dumas Bay backward stepwise linear regression model results for effects of environmental and physiological parameters on the gene expression for each CO_2 treatment (exc.: defined by the stepping method criteria parameters were excluded from the model if the significance level of their F values >0.10, #: collinearity statistics VIF > 2.0).

		High CO_2		**Intermediate CO_2**		**Ambient CO_2**			**High CO_2**		**Intermediate CO_2**		**Ambient CO_2**	
GOI	**Predictors**	**Beta**	***p***	**Beta**	***p***	**Beta**	***p***	**Predictors**	**Slope**	***p***	**Slope**	***p***	**Slope**	***p***
PSBS	Daily Average [CO_2]	exc.		0.927	0.011*	0.300		[Suc] μmol g^{-1} DW	0.014	0.267	-0.015	0.691	-0.046	0.140
	Daily Average Temp	exc.		-0.334	0.078	0.789								
	Daily Total PAR	exc.		exc.		exc.								
CAT	Daily Average [CO_2]	exc.		exc.		-1.161		[Suc] μmol g^{-1} DW	0.005	0.343	-0.008	0.627	0.021	0.452
	Daily Average Temp	exc.		exc.		0.318								
	Daily Total PAR	exc.		exc.		exc.								
HSP70	Daily Average [CO_2]	-0.001		exc.		1.010		[Suc] μmol g^{-1} DW	-	-	0.067	0.427	-0.009	0.298
	Daily Average Temp	exc.		exc.		-0.016								
	Daily Total PAR	exc.		exc.		exc.								
LHCB5	Daily Average [CO_2]	exc.		0.881	0.048*	-1.251		[Suc] μmol g^{-1} DW	-0.009	0.643	-0.057	0.559	0.003	0.784
	Daily Average Temp	exc.		exc.		0.883								
	Daily Total PAR	exc.		exc.		exc.								
RBP	Daily Average [CO_2]	exc.		exc.		0.930		[Suc] μmol g^{-1} DW	-0.003	0.671	0.005	0.817	0.004	0.822
	Daily Average Temp	exc.		exc.		1.240								
	Daily Total PAR	-0.140	0.098	exc.		exc.								
SOD	Daily Average [CO_2]	exc.		0.863	0.059	1.103		[Suc] μmol g^{-1} DW	0.009	0.153	-0.006	0.558	-0.019	0.385
	Daily Average Temp	exc.		exc.		-0.187								
	Daily Total PAR	exc.		exc.		exc.								
SS	Daily Average [CO_2]	-1.000	0.006*	exc.		1.234		[Suc] μmol g^{-1} DW	-0.023	0.006*	0.024	0.567	-0.019	0.577
	Daily Average Temp	exc.		exc.		-0.549								
	Daily Total PAR	exc.		exc.		exc.								

Table 23. Summary of two-way ANOVA results for comparison of relative gene expression in August 2014 across CO_2 treatments for new plants from Dumas Bay, WA eelgrass. ANOVA table for Type III tests of fixed effects using the multivariate general linear model routine implemented in SPSS. Log [CO_2] was treated as a fixed factor.

GOI	Source	Type III Sum of Squares	df	Mean Square	*F*	*p*
PSBS	log [CO_2]	11.59	2	5.80	4.42	0.18
CAT		3.25	2	1.63	5.44	0.16
HSP70		0.13	2	0.06	0.08	0.93
LHCB5		12.57	2	6.28	0.27	0.79
RBP		1.00	2	0.50	0.92	0.52
SOD		0.23	2	0.11	0.08	0.93
SS		20.49	2	10.24	47.70	0.02*

Gene expression comparison between populations

PCA of the entire gene expression including both populations, three CO_2 treatments and three months (November 2013, January 2014 and April 2014), did not separate the populations but showed a cluster indicating differences in November 2013 under intermediate CO_2 (Fig. 21a). Two-way ANOVA of the entire gene expression values (−ΔCt) did not show significant differences for most genes of interest between the SBV and DBW populations growing in the experimental aquaria (Table 24). The LHCB5 gene of both populations changed through time ($p < 0.05$, Table 24) and light appears to have been the primarily driver (Table 17 and Table 21). When comparing the gene expression of SOD between these populations, population x month x log [CO_2] and month x log [CO_2] interactions were highly significant ($p < 0.05$, Table 11),

indicating that differential effects of CO_2 on gene expression between the two populations depended on the month.

Two-Way ANOVA found no differences in the gene expression between populations during November 2013. At the same time, a cluster of the intermediate CO_2 treatment was evident as shown in the PCA (Fig. 21a, Table 12). During this month both populations demonstrated the same pattern under the intermediate CO_2 treatment where PSBS and LHCB5 gene expression was significantly lower and RBP and SS expression significantly higher than the other treatments (pH 7.5, 107μmol $CO_2 \cdot Kg^{-1}$ SW) (Fig. 18). At this time only SBV plant size showed a significant CO_2 effect in the physiological data (Chapter 2).

The two-way ANOVA for January 2014 including both populations only demonstrated a difference in the expression of the PSBS gene under intermediate CO_2 (pH 7.5, 107μmol $CO_2 \cdot Kg^{-1}$ SW) during this time (Fig. 18a, Table 13). The other genes were not different between populations.

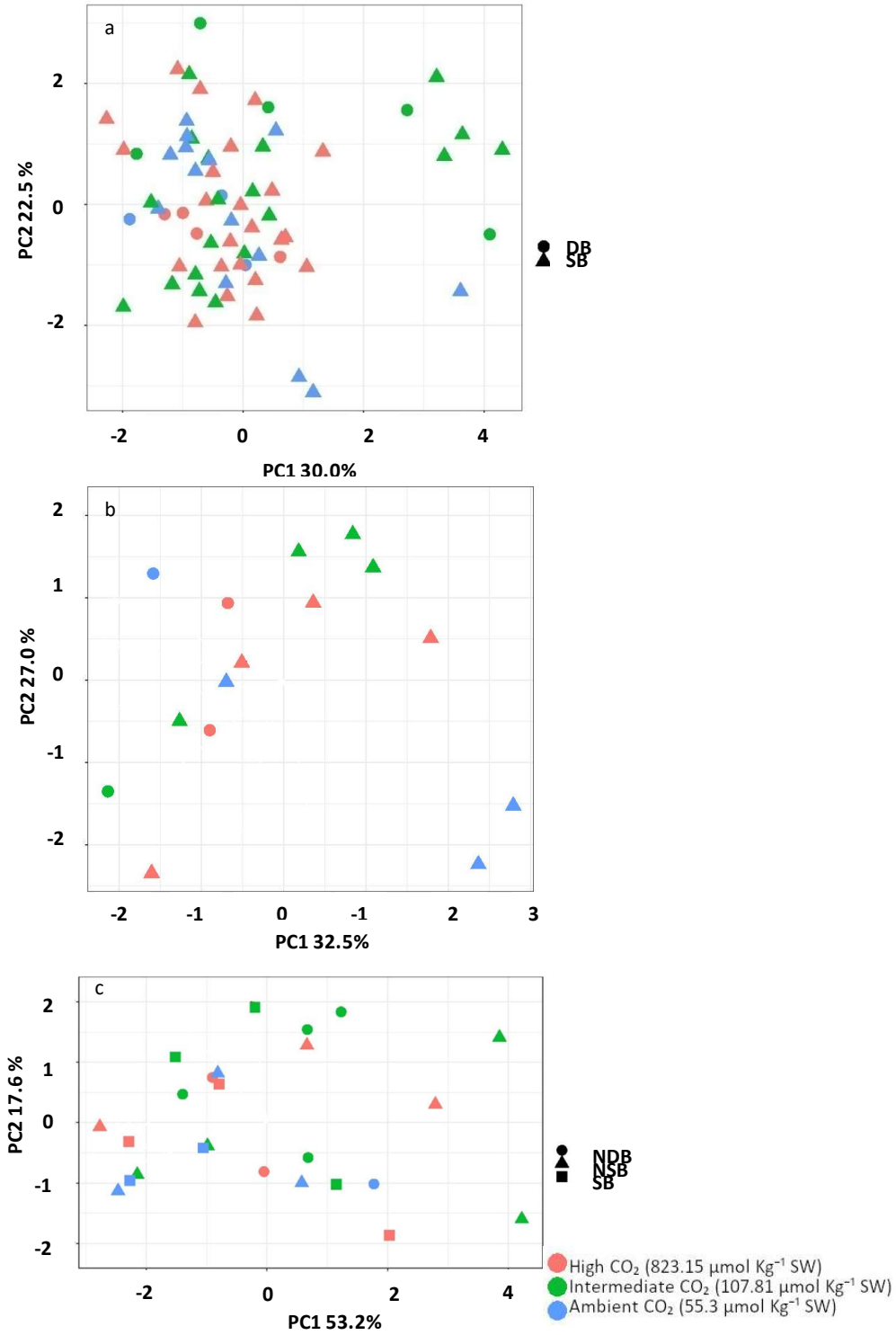

Figure 21. Principal Component Analyses of the −ΔCt values of eelgrass leaves growing at different CO_2 concentrations from South Bay, VA and Dumas Bay, WA (a) including both populations, three CO_2 treatments and three months (November 2013, January 2014 and April 2014) (b) including three CO_2 treatments and two populations in April 2014 (c) including three CO_2 treatments and three populations (1st and 2nd year transplanted SBV and 2nd year transplanted DBW) in August 2014. CO_2 treatments are indicated by color.

Table 24. Summary of two-way ANOVA results for comparison of relative gene expression during November 2013, January and April 2014 across eelgrass populations. ANOVA table for Type III tests of fixed effects using the multivariate general linear model routine implemented in SPSS. log [CO_2], populations and month were treated as fixed factors.

GOI	Source	Type III Sum of Squares	*df*	Mean Square	*F*	*p*
PSBS	Populations	19.27	1	19.27	2.37	0.14
	month	50.94	2	25.47	3.13	0.07
	log [CO_2]	7.36	2	3.68	0.45	0.64
	Pop X month	47.55	2	23.77	2.92	0.08
	Pop X log [CO_2]	5.99	2	3.00	0.37	0.70
	month X log [CO_2]	39.22	4	9.80	1.20	0.35
	Pop X Month X log [CO_2]	8.68	2	4.34	0.53	0.60
CAT	Populations	4.85	1	4.85	0.45	0.51
	month	10.98	2	5.49	0.50	0.61
	log [CO_2]	1.18	2	0.59	0.05	0.95
	Pop X month	9.24	2	4.62	0.42	0.66
	Pop X log [CO_2]	0.15	2	0.08	0.01	0.99
	month X log [CO_2]	1.47	4	0.37	0.03	1.00
	Pop X Month X log [CO_2]	23.19	2	11.60	1.07	0.37
HSP70	Populations	18.84	1	18.84	1.25	0.28
	month	45.73	2	22.87	1.52	0.25
	log [CO_2]	55.88	2	27.94	1.85	0.19
	Pop X month	4.25	2	2.12	0.14	0.87
	Pop X log [CO_2]	29.91	2	14.96	0.99	0.39
	month X log [CO_2]	78.01	4	19.50	1.29	0.31
	Pop X Month X log [CO_2]	28.75	2	14.37	0.95	0.41
LHCB5	Populations	3.07	1	3.07	0.10	0.76
	month	278.54	2	139.27	4.56	0.03*
	log [CO_2]	102.45	2	51.23	1.68	0.22
	Pop X month	3.45	2	1.73	0.06	0.95
	Pop X log [CO_2]	29.41	2	14.70	0.48	0.63
	month X log [CO_2]	125.49	4	31.37	1.03	0.42
	Pop X Month X log [CO_2]	72.11	2	36.06	1.18	0.33
RBP	Populations	1.03	1	1.03	0.18	0.68
	month	18.83	2	9.42	1.61	0.23
	log [CO_2]	21.15	2	10.57	1.81	0.20
	Pop X month	0.63	2	0.32	0.05	0.95
	Pop X log [CO_2]	0.15	2	0.07	0.01	0.99
	month X log [CO_2]	2.09	4	0.52	0.09	0.98
	Pop X Month X log [CO_2]	0.67	2	0.34	0.06	0.94

Table 24 continued

GOI	Source	Type III Sum of Squares	df	Mean Square	*F*	*p*
SOD	Populations	1.20	1	1.20	2.34	0.15
	month	0.83	2	0.42	0.81	0.46
	log [CO_2]	1.64	2	0.82	1.60	0.23
	Pop X month	2.15	2	1.08	2.09	0.16
	Pop X log [CO_2]	1.77	2	0.88	1.72	0.21
	month X log [CO_2]	11.00	4	2.75	5.34	0.01*
	Pop X Month X log [CO_2]	6.04	2	3.02	5.87	0.01*
SS	Populations	43.77	1	43.77	2.08	0.17
	month	40.25	2	20.12	0.96	0.41
	log [CO_2]	39.77	2	19.89	0.95	0.41
	Pop X month	24.19	2	12.10	0.57	0.57
	Pop X log [CO_2]	46.62	2	23.31	1.11	0.35
	month X log [CO_2]	6.66	4	1.67	0.08	0.99
	Pop X Month X log [CO_2]	34.44	2	17.22	0.82	0.46

Table 25. Summary of two-way ANOVA results for comparison of relative gene expression during November 2013 across eelgrass populations. ANOVA table for Type III tests of fixed effects using the multivariate general linear model routine implemented in SPSS. log [CO_2], populations and month were treated as fixed factors.

GOI	Source	Type III Sum of Squares	*df*	Mean Square	*F*	*p*
PSBS	Populations	12.92	1	12.92	2.62	0.16
	log [CO_2]	71.45	2	35.73	7.23	0.03*
	Pop* log [CO_2]	0.00	1	0.00	0.00	0.99
CAT	Populations	0.00	1	0.00	0.00	0.97
	log [CO_2]	0.00	2	0.00	0.00	1.00
	Pop* log [CO_2]	0.08	1	0.08	0.02	0.89
HSP70	Populations	0.90	1	0.90	0.27	0.62
	log [CO_2]	29.35	2	14.67	4.50	0.06
	Pop* log [CO_2]	2.69	1	2.69	0.83	0.40
LHCB5	Populations	5.93	1	5.93	0.32	0.59
	log [CO_2]	262.03	2	131.02	7.05	0.03*
	Pop* log [CO_2]	9.58	1	9.58	0.52	0.50
RBP	Populations	0.22	1	0.22	0.10	0.76
	log [CO_2]	36.44	2	18.22	8.28	0.02*
	Pop* log [CO_2]	2.59	1	2.59	1.18	0.32
SOD	Populations	0.04	1	0.04	0.18	0.68
	log [CO_2]	2.87	2	1.43	5.83	0.04*
	Pop* log [CO_2]	1.91	1	1.91	7.76	0.03*
SS	Populations	0.22	1	0.22	0.03	0.87
	log [CO_2]	202.58	2	101.29	13.43	0.01*
	Pop* log [CO_2]	28.74	1	28.74	3.81	0.10

Table 26. Summary of two-way ANOVA results for comparison of relative gene expression during January 2014 across eelgrass populations. ANOVA table for Type III tests of fixed effects using the multivariate general linear model routine implemented in SPSS. log [CO_2], populations and month were treated as fixed factors.

GOI	Source	Type III Sum of Squares	*df*	Mean Square	*F*	*p*
PSBS	Populations	3.34	1	3.34	2.03	0.20
	log [CO_2]	41.88	2	20.94	12.74	0.01*
	log [CO_2] X Pop	6.46	2	3.23	1.97	0.22
CAT	Populations	17.11	1	17.11	0.71	0.43
	log [CO_2]	0.65	2	0.33	0.01	0.99
	log [CO_2] X Pop	11.22	2	5.61	0.23	0.80
HSP70	Populations	24.84	1	24.84	0.77	0.41
	log [CO_2]	137.81	2	68.90	2.14	0.20
	log [CO_2] X Pop	63.57	2	31.78	0.99	0.43
LHCB5	Populations	0.02	1	0.02	0.00	0.97
	log [CO_2]	13.01	2	6.51	0.41	0.68
	log [CO_2] X Pop	29.81	2	14.91	0.94	0.44
RBP	Populations	0.03	1	0.03	0.01	0.91
	log [CO_2]	3.86	2	1.93	1.09	0.40
	log [CO_2] X Pop	0.19	2	0.10	0.05	0.95
SOD	Populations	0.20	1	0.20	0.30	0.60
	log [CO_2]	5.72	2	2.86	4.25	0.07
	log [CO_2] X Pop	1.58	2	0.79	1.18	0.37
SS	Populations	43.85	1	43.85	2.53	0.16
	log [CO_2]	36.70	2	18.35	1.06	0.40
	log [CO_2] X Pop	89.26	2	44.63	2.58	0.16

The PCA and two-way ANOVA for April 2014 did not reveal differences in mean gene expression between populations or CO_2 treatments for most genes of interest (Fig. 21b and Table 14). However, catalase (CAT) showed a significant interaction term, between population and log [CO_2], showing that the gene expression of CAT is different between the populations only under intermediate and ambient CO_2 during spring (Fig. 19a, Table14).

When comparing 2nd-year transplants from SBV, 2nd-year transplants from DBW and acclimated SBV in August 2014, PCA did not separate the populations or the CO_2 treatments suggesting that the populations experienced the same gene expression changes (Fig. 21c). August 2014 two-way ANOVA did not show significant differences in most of the GOI across populations (Table 15). However, populations showed differences in the gene expression of PSBS (Fig.18a, $p< 0.05$, Table 15) where 2nd-year transplants from DBW showed a lower expression under ambient CO_2 (pH 8, 55μmol $CO_2 \cdot Kg^{-1}$ SW) while 2nd-year transplants from SBV and acclimated SBV increased this gene expression under high light and heat stress of August 2014.

Table 27. Summary of two-way ANOVA results for comparison of relative gene expression during April 2014 across eelgrass populations. ANOVA table for Type III tests of fixed effects using the multivariate general linear model routine implemented in SPSS. log [CO_2], populations and month were treated as fixed factors.

GOI	Source	Type III Sum of Squares	*df*	Mean Square	*F*	*p*
PSBS	Populations	57.82	1	57.82	3.07	0.14
	log [CO_2]	1.07	2	0.53	0.03	0.97
	log [CO_2] X Pop	7.97	2	3.99	0.21	0.82
CAT	Populations	0.07	1	0.07	0.08	0.79
	log [CO_2]	1.51	2	0.76	0.80	0.50
	log [CO_2] X Pop	12.04	2	6.02	6.39	0.04*
HSP70	Populations	3.14	1	3.14	0.56	0.49
	log [CO_2]	4.74	2	2.37	0.42	0.68
	log [CO_2] X Pop	1.29	2	0.64	0.11	0.89
LHCB5	Populations	5.53	1	5.53	0.10	0.77
	log [CO_2]	17.57	2	8.78	0.16	0.86
	log [CO_2] X Pop	67.95	2	33.98	0.60	0.58
RBP	Populations	0.12	1	0.12	0.01	0.93
	log [CO_2]	6.11	2	3.06	0.22	0.81
	log [CO_2] X Pop	0.57	2	0.29	0.02	0.98
SOD	Populations	2.38	1	2.38	4.14	0.10
	log [CO_2]	1.22	2	0.61	1.06	0.41
	log [CO_2] X Pop	5.73	2	2.87	4.99	0.06
SS	Populations	0.08	1	0.08	0.00	0.96
	log [CO_2]	11.13	2	5.56	0.14	0.87
	log [CO_2] X Pop	0.48	2	0.24	0.01	0.99

Table 28. Summary of two-way ANOVA results for comparison of relative gene expression during August 2014 across eelgrass populations. ANOVA table for Type III tests of fixed effects using the multivariate general linear model routine implemented in SPSS. log [CO_2] and populations were treated as fixed factors.

GOI	Source	Type III Sum of Squares	*df*	Mean Square	*F*	*p*
PSBS	Populations	24.88	2	12.44	5.51	0.04*
	log [CO_2]	34.22	3	11.41	5.06	0.04*
	Pop X log [CO_2]	11.19	3	3.73	1.65	0.26
CAT	Populations	16.53	2	8.26	1.27	0.34
	log [CO_2]	6.55	3	2.18	0.33	0.80
	Pop X log [CO_2]	13.55	3	4.52	0.69	0.59
HSP70	Populations	4.57	2	2.28	0.42	0.67
	log [CO_2]	10.68	3	3.56	0.66	0.60
	Pop X log [CO_2]	1.36	3	0.45	0.08	0.97
LHCB5	Populations	1.66	2	0.83	0.05	0.95
	log [CO_2]	6.91	3	2.30	0.15	0.93
	Pop X log [CO_2]	41.71	3	13.90	0.92	0.48
RBP	Populations	2.23	2	1.12	0.37	0.71
	log [CO_2]	2.59	3	0.86	0.28	0.84
	Pop X log [CO_2]	1.74	3	0.58	0.19	0.90
SOD	Populations	1.93	2	0.96	0.53	0.61
	log [CO_2]	1.15	3	0.38	0.21	0.89
	Pop X log [CO_2]	1.20	3	0.40	0.22	0.88
SS	Populations	17.06	2	8.53	0.44	0.66
	log [CO_2]	48.70	3	16.23	0.83	0.52
	Pop X log [CO_2]	30.47	3	10.16	0.52	0.68

Discussion

The results revealed an agreement in the gene expression of two eelgrass populations to CO_2 availability and temperature. Both eelgrass populations revealed that photosynthetic gene expression changed through time in response to seasonal variation in light. Stress genes were affected by seasonal temperature but genes did not respond to CO_2 enrichment. For some genes the transcriptome profiles only differed across CO_2 treatments when the largest sucrose changes were observed. This implies that the differences observed at different time points, particularly during spring, under CO_2 enrichment in survival, chemical composition and plant performance were not reflected by the expression of all selected genes (Chapter 2). In general, six out of seven genes associated to temperature stress response, carbon fixation and photosynthesis changed during at least one time point when *Z. marina* was exposed to different seasons in the experimental facility.

Light played a major role where the expression patterns of the photosynthetic genes were regulated in the same direction across CO_2 treatments. LHCB5 gene, encoded by members of the nuclear LHC gene family and located between the PSII core and the major LHCII complex (Bassi et al., 1997), increased its expression during high light months and decreased in low light months. Simultaneously, expression of the PSBS gene, specifically coding for a protein involved in non-photochemical quenching rather than photosynthesis, increased during high light months and decreased in low light months. The changes in expression of the photosynthetic machinery during high light months suggests acclimation to maintain an efficient photosynthetic performance that enables the plants to process the high amount of harvested energy and to reduce damage of the photosynthetic apparatus (Walters, 2005). Plants acclimate to the light environment through modulation of LHCII however, regulating the amount of LHCII produces a

slower response to light, but regulating Chl-a/b binding proteins such as LHCB5 produces a quicker response to changes in light. Our gene expression data are consistent with short-term (2 weeks) seagrass studies, which suggest that environmental factors (salinity, temperature, light intensity and light quality) other than increased CO_2, may be at a play affecting photosynthetic metabolism (Kong et al. 2016, Olivé et al. 2017).

Eelgrass populations under CO_2 enrichment presented morphological acclimation increasing shoot numbers, growth, plant size and sucrose concentration resulted from improved photosynthetic capacity (Chapter 2 (Invers et al. 2001, Celebi 2016, Zimmerman et al. 2017). However, the photosynthetic genes (PSBS and LHCB5) representing two of many photosynthetic proteins did not reflect the physiological changes previously observed where CO_2 availability increased photosynthesis and affected the photosynthetic pigments. Under ambient CO_2 (pH 8, 55μmol $CO_2 \cdot Kg^{-1}$ SW) chlorophyll concentration decreased and increased under high CO_2 treatments (pH 6.5, 823μmol $CO_2 \cdot Kg^{-1}$ SW) (Zimmerman et al. 2017, Celebi et al. 2021). For example, in winter and spring a large contrast of chlorophyll concentrations across CO_2 treatments was observed (Zimmerman et al. 2017), however PSBS show significant differences among CO_2 treatments in winter but not during spring and LHCB5 did not show differences across treatments during this time but showed differences in late summer when plants experienced high light.

Carbohydrate metabolism transcripts, RBP and SS, were expected to respond to CO_2 enrichment. The Rubisco large subunit-binding protein subunit alpha, binds the small and large subunits of Rubisco, assist in the assembly of the enzyme oligomer and support folding. The effects of temperature and irradiance during spring on the low expression of RBP agree with optimal temperatures (below 25° C) for photosynthesis for *Z marina* and suggest a protective role

during hight light and high temperature months, i.e., August 2014, where an increase across CO_2 treatments was observed. These carbon metabolism genes were similar across CO_2 treatments but changed their expression through time and appeared to be opposite to the light reaction genes. A similar response between carbon metabolism genes and light reaction genes expression was observed under different light treatments in a previous experiment with European coast eelgrass but without CO_2 or thermal manipulations (Salo et al. 2015). Also, *Arabidopsis sp.* which shows lower expression of Rubisco interacting proteins genes under CO_2 treatments had presented an opposite response to genes coding for PS2 proteins (Kaplan et al. 2012). Conversely, Rubisco decreases across different plant species under CO_2 availability (Moore et al. 1998). This protein is regulated by the small subunit protein levels therefore measuring the gene expression of the Rubisco small subunit could better represent the changes in Rubisco under CO_2 availability (Moore et al. 1998, Moore et al. 1999). Using large-scale gene expression changes under similar ambient CO_2 conditions the seagrass *Cymodocea nodosa* demonstrated upregulation of the small subunit of Rubisco (Ruocco et al. 2017). This differential response between transcripts and proteins involved in Rubisco synthesis suggests a complicated combination of transcriptional and protein processes to determine the final amount of leaf Rubisco protein under different CO_2 conditions (Cheng et al. 1998). However, in today's ocean CO_2 is a limited substrate for seagrasses resulting in higher total protein content maintaining high metabolic capacity (Piro et al. 2020). Although it may seem wasteful in terms of nitrogen to retain high and stable levels of metabolic enzymes under ambient/low CO_2, it may give seagrass a huge buffer capacity to grab and process photosynthetic carbon when available. The instantaneous photosynthetic response to CO_2 exhibited by seagrass leaves indicates that even the plants growing under ambient conditions have all the light harvesting, electron transport,

carbon fixation and sucrose formation capacity to operate at much higher rates when CO_2 is available (Chapter 2 (Celebi 2016, Zimmerman et al. 2017). The lack of a differential response in the transcriptome under ambient/low CO_2 agrees with that potential capacity.

The SS gene plays a key role in carbon metabolism encoded by a small multigene family for a protein that catalyzes sucrose cleavage in the presence of a nucleoside diphosphate (Winter & Huber 2000, Xu et al. 2019)(EC 2.4.1.13). This gene shows distinct patterns of expression in different organs in angiosperms and has been found to be highly variable between genotypes of *Z. marina* in light experiments (Salo et al. 2015, Xu et al. 2019). Moreover, in experiments of *Z. marina* under temperature stress with no CO_2 subsidy, the SS gene has shown downregulation and increase in sucrose metabolites while presenting upregulation and a decrease in growth under anoxia (Gu et al. 2012, Zhang et al. 2021). Sucrose is a critical factor that controls SS gene expression serving as a strong inducer for this gene (Avigad & Dey 1997). Sucrose accumulation resulting from elevated CO_2 availability in *Z. marina* (Chapter 2, (Zimmerman et al. 2017) did not result in SS gene expression differences across treatments except in September 2013 and April 2014 when sucrose differences across the CO_2 treatments were very pronounced, when leaf sugar concentration in the high CO_2 treatment was 2 to 3 fold higher for SBV. However, when the differences of sucrose content across treatments were smaller, the SS gene expression did not differ across CO_2 treatments but changed with the seasons. Sugar concentrations increased in all CO_2 treatments during January and February 2014 for both populations (Chapter 2), is during that time that the SS gene expression decreased across CO_2 treatments. Thus, sugar levels may modify relative expression of the SS genes for *Z. marina* leaves as has been found in maize roots and rice scutellum (Karrer & Rodriguez 1992, Koch et al. 1992).

Previous studies suggest that elevated CO_2 decreases oxidative stress, therefore decreasing the activity of antioxidant enzymes such as CAT and SOD (Azevedo et al. 1998). CAT is indispensable for reactive oxygen species (ROS) detoxification during stress, when the level of hydrogen peroxide gets too high (Mittler, 2002). The CAT gene did not respond to CO_2 or seasons suggesting that *Z. marina* plants are not activating this protective mechanism, similarly to the response of *Posidonia oceanica* under elevated CO_2 growing in the vicinity of submarine volcanic vents (Lauritano et al. 2015). Specific responses of *Arabidopsis thaliana* and soybean plants also showed that the activities and gene transcription expression levels of ROS scavenging enzymes at elevated CO_2 did not change (Casteel et al. 2008, Zinta et al. 2014). However, experiments of sucrose deprive cell cultures resulted in the increase of catalase transcripts (Contento et al. 2004, Contento & Bassham 2010) suggesting how carbon reserves influence its activity. Eelgrass from SBV showed sucrose accumulation under intermediate and high CO_2 in *Z. marina* (Chapter 2) resulting in a differential CAT gene expression across CO_2 treatments in September 2013 and April 2014 when leaf sucrose concentrations across treatments were significantly different. As SS expression, CAT gene expression only differed across CO_2 treatments when the differences of sucrose content across treatments were large. This also suggests that shoots with low carbon reserves as *Z. marina* under ambient CO_2 might increase the catalase activity to support metabolic repair maybe negatively impacting their performance resulting in low survival, growth and smaller sizes (Chapter 2).

Although SOD did not respond to CO_2, it increased significantly in summer, potentially increasing thermal stress tolerance. This may be a common response of Z. *marina* under thermal stress where the only antioxidant gene activated is SOD possibly being among the first antioxidants to be activated in the cells (Bergmann et al. 2010, Winters et al. 2011). Warming

during late summer also induced the high expression of HSP70 in the two eelgrass populations across CO_2 treatments in accordance with their role to re-establish normal protein conformation and thus cellular homeostasis (Wang et al. 2004). Heat stress experiments performed on eelgrass populations without a CO_2 subsidy revealed significant up-regulation of HSPs genes in line with shoot losses (Reusch et al. 2008, Bergmann et al. 2010, Winters et al. 2011, Gu et al. 2012, Franssen et al. 2014). Despite differences in survival during the experiment across CO_2 treatments particularly during January and April 2014 (Chapter 2), HSP70 did not respond to the CO_2 treatments.

In this experiment both eelgrass populations showed the same gene expression response to CO_2 even though differed in physiological and metabolomic responses. Therefore, transcriptome profiles by themselves did not predict how gene expression translates into physiological (i.e. survival) and metabolic consequences because the regulation is multifaceted from genes, proteins to metabolites (Kaplan et al. 2012). Further, the totality of these results leading to an integrated whole-plant responses suggests non-transcriptomic controls on protein activity/function; in particular the concentrations of sucrose and other carbon metabolic intermediates may be more influential than the transcriptome in determining the response of eelgrass to environmental stress such as low CO_2 where seagrasses present low survival and lower photosynthetic rates (Chapter 2, (Zimmerman et al. 1995, Celebi 2016, Zimmerman et al. 2017).

CHAPTER 5

CONCLUSIONS

In today's ocean seagrasses are carbon limited and experience increases in temperature stress, poor water quality and physical destruction (Zimmerman et al. 1997). However, seagrasses photosynthesis and growth are demonstrably stimulated by increasing CO_2 concentration (Beer 1989, Durako 1993, Zimmerman et al. 1995, Koch & Beer 1996, Zimmerman et al. 2017). Exploring the impacts of CO_2 availability and temperature on the widely distributed *Z. marina* showed the degree of morphological and physiological plasticity between geographically isolated populations. Long term growth under high CO_2 conditions produced significant positive effects on photosynthesis and leaf sucrose on all populations, but the Cheasepeake Bay population, South Bay (SBV), was most responsive to CO_2 availability in terms of whole plant survival, shoot size and growth. CO_2 also helped eelgrass from the cool waters of Puget Sound, Dumas Bay (DBW), to survive summer temperatures exceeding the 25° C threshold increasing their shoot numbers, growth, plant size and sucrose concentration, but did not respond as well as SBV. On the other hand, the Nisqually Bay (NBW) plants experienced mass mortality regardless of CO_2 treatment even though plants did not show metabolic stress and a similar performance as the other eelgrass populations. Differences in population survival responses to CO_2 availability observed here point to differences in the acclimation ability of the populations, some of which may be related to carbon balance but some of which are related to other processes.

SBV and DBW showed similar whole plant responses to CO_2 in terms of leaf sucrose, growth, and shoot numbers suggest common effects of CO_2 enrichment however, differences in metabolite pools between CO_2 conditions and populations hint to shifts in the activities of

metabolic pathways leading to whole plant responses. During spring DBW showed higher abundances of photorespiratory and stress-related compounds than SBV regardless of CO_2 treatments. While under low CO_2 both populations demonstrated elevated metabolites involved in biotic/abiotic stress responses. However, the abundance of the photorespiratory metabolites were higher in DBW leaves than in SBV leaves under low CO_2. Metabolomics analyses revealed that CO_2 enrichment increased the abundance of metabolites involved carbon fixation and nitrogen assimilation metabolites while suppressing the abundance of stress-related metabolites. Similarly, gene expression analyses under CO_2 enrichment during spring showed lower expression of stress genes (CAT) demonstrating an agreement between transcripts and metabolites involved in stress response.

Both eelgrass populations revealed that gene expression changed through time responding to changes in light availability and temperature but the effect of CO_2 on gene expression was season dependent. This implies that all the differences observed on the leaves under CO_2 enrichment in growth rate and plant performance were not reflected by the gene expression of all selected genes. The results showed that photosynthetic genes changed in response to light and some stress genes were affected by temperature while others affected by sucrose concentration. This outcome suggests non-transcriptomic controls on protein activity/function, especially the concentrations of carbon metabolism substrates, i.e. sugars, may be more influential than the transcriptome in determining the response of eelgrass under low CO_2 where seagrasses present low survival and lower photosynthetic rates. Previous studies suggest future ocean warming will be a foremost determinant stressor influencing seagrass survival and physiological performance (Repolho et al. 2017, Collier et al. 2018) and that may well be the case for NBW eelgrass. However, increases in CO_2 could counteract thermal stress if the plants

accumulate sufficient carbon reserves to support growth and modify stress-related metabolites and genes.

One limitation of this research was the ability to capture the early molecular response to better relate transcriptional and metabolite changes to the physiological effects. However, to detect early responses maybe frequent sampling of biochemical indicators such as sugars varieties or proteins might be adequate to provide a good measure of seagrass response under climate change since morphological measurements are not dynamic enough (Govers et al. 2015, Roca et al. 2015, Soerensen 2020). For example, *Z. marina* biochemical changes under CO_2 availability were noticeable after 2-3 months in which pigments and sucrose concentration increased (Chapter 2, (Celebi 2016, Zimmerman et al. 2017).

Previous studies had shown that seagrasses decrease their total protein content where nitrogen became diluted as biomass increased with CO_2 availability (Jiang et al. 2010, Alexandre et al. 2012, Procaccini et al. 2017, Piro et al. 2020). Since CO_2 availability influences sucrose dynamics and other metabolic pathways; research is needed to explore metabolic pathways of nitrogen and the interaction between carbon and nitrogen under CO_2 availability. Therefore, future studies of seagrasses should explore the differences in the nitrogen assimilation ability of the populations under CO_2 availability.

The wide distribution of *Z. marina* is evidence of the high plasticity and acclimation capacity of this angiosperm. The findings of this dissertation tried to provide a holistic examination of how the environment (CO_2 and temperature) influences performance features linked to plant survival. The metabolite and gene expression profiles generated here, in combination with analysis of whole-plant performance, offer a new understanding into the seagrass ability to adapt to future changes in their respective environments. To effectively manage seagrass ecosystems

will depend in the clear understanding of multivariate stress responses (nutrients limitation, light availability, pathogens, invasive species) under CO_2 enrichment and their role in seagrass populations acclimation ability.

REFERENCES

Alberte RS, Suba GK, Procaccini G, Zimmerman RC, Fain SR (1994) Assessment of genetic diversity of seagrass populations using DNA fingerprinting: implications for population stability and management. Proceedings of the National Academy of Sciences 91:1049-1053

Alexandre A, Silva J, Buapet P, Björk M, Santos R (2012) Effects of CO2 enrichment on photosynthesis, growth, and nitrogen metabolism of the seagrass *Zostera noltii*. Ecology and Evolution 2:2625-2635

Arnold T, Mealey C, Leahey H, Miller AW, Hall-Spencer JM, Milazzo M, Maers K (2012) Ocean acidification and the loss of phenolic substances in marine plants. PLOS One 7:e35107

Avigad G, Dey PM (1997) 4 - Carbohydrate Metabolism: Storage Carbohydrates. In: Dey PM, Harborne JB (eds) Plant Biochemistry. Academic Press, London

Azevedo RA, Alas RM, Smith RJ, Lea PJ (1998) Response of antioxidant enzymes to transfer from elevated carbon dioxide to air and ozone fumigation, in the leaves and roots of wild-type and a catalase-deficient mutant of barley. Physiologia Plantarum 104:280-292

Backman TWH (1991) Genotypic and phenotypic variability of *Zostera marina* on the west coast of North America. Canadian Journal of Botany 59:1361-1371

Beardmore JA (1983) Extinction, survival and genetic variation. Genetics and conservation: a reference for managing wild animal and plant populations:125-151

Beca-Carretero P, Olesen B, Marbà N, Krause-Jensen D (2018) Response to experimental warming in northern eelgrass populations: comparison across a range of temperature adaptations. Marine Ecology Progress Series 589:59-72

Beer S (1989) Photosynthesis and photorespiration of marine angiosperms. Aquatic Botany 34:153-166

Bergmann N, Winters G, Rauch G, Eizaguirre C, Gu J, Nelle P, Fricke B, Reusch TBH (2010) Population-specificity of heat stress gene induction in northern and southern eelgrass *Zostera marina* populations under simulated global warming. Molecular Ecology 19:2870-2883

Björk M, Weil A, Semesi S, Beer S (1997) Photosynthetic utilisation of inorganic carbon by seagrasses from Zanzibar, East Africa. Marine Biology 129:363-366

Bonawitz ND, Chapple C (2010) The genetics of lignin biosynthesis: connecting genotype to phenotype. Annual Review of Genetics 44:337-363

Bouché N, Fait A, Bouchez D, Møller SG, Fromm H (2003) Mitochondrial succinic-semialdehyde dehydrogenase of the γ-aminobutyrate shunt is required to restrict levels of reactive oxygen intermediates in plants. Proceedings of the National Academy of Sciences 100:6843-6848

Bourguignon J, Rebéillé F, Douce R (1998) Serine and glycine metabolism in higher plants. In: BK S (ed) Plant amino acids: Biochemistry & biotechnology. Marcell Dekker, Inc, New York

Bruggemann W, Van Der Kooij T, van Hasselt PR (1992) Long-term chilling of young tomato plants under low light and subsequent recovery. II. Chlorophyll fluorescence, carbon metabolism and activity of ribulose-1, 5-bisphosphate carboxylase/oxygenase. Planta (USA)

Bulthuis D (1983) Effects of temperature on the photosynthesis-irradiance curve of the Australian seagrass, *Heterozostera tasmanica*. Marine Biology Letters

Bulthuis DA (1987) Effects of temperature on photosynthesis and growth of seagrasses. Aquatic Botany 27:27-40

Bundy JG, Davey MP, Viant MR (2008) Environmental metabolomics: a critical review and future perspectives. Metabolomics 5:3

Byrne M, Ho M, Wong E, Soars Natalie A, Selvakumaraswamy P, Shepard-Brennand H, Dworjanyn Symon A, Davis Andrew R (2011) Unshelled abalone and corrupted urchins: development of marine calcifiers in a changing ocean. Proceedings of the Royal Society B: Biological Sciences 278:2376-2383

Cambiaghi A, Ferrario M, Masseroli M (2016) Analysis of metabolomic data: tools, current strategies and future challenges for omics data integration. Briefings in Bioinformatics 18:498-510

Campbell JE, Fourqurean JW (2013) Effects of in situ CO2 enrichment on the structural and chemical characteristics of the seagrass *Thalassia testudinum*. Marine Biology 160:1465-1475

Campbell SJ, McKenzie LJ, Kerville SP (2006) Photosynthetic responses of seven tropical seagrasses to elevated seawater temperature. Journal of Experimental Marine Biology and Ecology 330:455-468

Casteel CL, O'neill BF, Zavala JA, Bilgin DD, Berenbaum MR, DeLucia EH (2008) Transcriptional profiling reveals elevated CO2 and elevated O3 alter resistance of soybean (Glycine max) to Japanese beetles (*Popillia japonica*). Plant, Cell & Environment 31:419-434

Ceccherelli G, Oliva S, Pinna S, Piazzi L, Procaccini G, Marin-Guirao L, Dattolo E, Gallia R, La Manna G, Gennaro P, Costa MM, Barrote I, Silva J, Bulleri F (2018) Seagrass collapse due to synergistic stressors is not anticipated by phenological changes. Oecologia

Celebi B (2016) Potential impacts of Climate Change on photochemistry in *Zostera marina* L. PhD Dissertation, Old Dominion University, Norfolk, VA

Celebi B, Zimmerman; R, Hill; V (2021) Impact of ocean carbonation on long term regulation of light harvesting in eelgrass, *Zostera marina* L. Marine Ecology Progress Series In Press

Cheng S-H, Moore Bd, Seemann JR (1998) Effects of Short- and Long-Term Elevated CO_2 on the Expression of Ribulose-1,5-Bisphosphate Carboxylase/Oxygenase Genes and Carbohydrate Accumulation in Leaves of *Arabidopsis thaliana* (L.) Heynh. Plant Physiology 116:715-723

Collier CJ, Langlois L, Ow Y, Johansson C, Giammusso M, Adams MP, O'Brien KR, Uthicke S (2018) Losing a winner: thermal stress and local pressures outweigh the positive effects of ocean acidification for tropical seagrasses. New Phytologist 219:1005-1017

Contento AL, Bassham DC (2010) Increase in catalase-3 activity as a response to use of alternative catabolic substrates during sucrose starvation. Plant Physiology and Biochemistry 48:232-238

Contento AL, Kim S-J, Bassham DC (2004) Transcriptome Profiling of the Response of Arabidopsis Suspension Culture Cells to Suc Starvation. Plant Physiology 135:2330-2347

Cottingham KL, Lennon JT, Brown BL (2005) Knowing when to draw the line: designing more informative ecological experiments. Frontiers in Ecology and the Environment 3:145-152

Dattolo E, Ruocco M, Brunet C, Lorenti M, Lauritano C, D'Esposito D, De Luca P, Sanges R, Mazzuca S, Procaccini G (2014) Response of the seagrass *Posidonia oceanica* to different light environments: Insights from a combined molecular and photo-physiological study. Marine Environmental Research 101:225-236

Davis MB, Shaw RG (2001) Range Shifts and Adaptive Responses to Quaternary Climate Change. Science 292:673-679

de Kok JB, Roelofs RW, Giesendorf BA, Pennings JL, Waas ET, Feuth T, Swinkels DW, Span PN (2005) Normalization of gene expression measurements in tumor tissues: comparison of 13 endogenous control genes. Laboratory Investigation 85:154-159

DeWitt TJ, Sih A, Wilson DS (1998) Costs and limits of phenotypic plasticity. Trends in Ecology & Evolution 13:77-81

Dillon C (1971) Comparative study of the primary productivity of estuarine phytoplankton and macrobenthic plants. P.h.D, University of North Carolina Chapel Hill, NC

Duarte CM (1991) Allometric scaling of seagrass form and productivity. Marine Ecology Progress Series Oldendorf 77:289-300

Durako MJ (1993) Photosynthetic utilization of CO2 (aq) and HCO-3 in *Thalassia testudinum* (Hydrocharitaceae). Marine Biology 115:373-380

Eberhard S, Finazzi G, Wollman F-A (2008) The dynamics of photosynthesis. Annual review of genetics 42:463-515

Ehlers A, Worm B, Reusch TB (2008) Importance of genetic diversity in eelgrass *Zostera marina* for its resilience to global warming. Marine Ecology Progress Series 355:1-7

Engle JM, Miller K Distribution and morphology of eelgrass (*Zostera marina* L.) at the California Channel Islands. Proc Proceedings of the sixth California Islands symposium (DK Garcelon and CA Schwemm, eds)

Evans AS, Webb KL, Penhale PA (1986) Photosynthetic temperature acclimation in two coexisting seagrasses, *Zostera marina* L. and *Ruppia maritima* L. Aquatic Botany 24:185-197

Evans TG, Hofmann GE (2012) Defining the limits of physiological plasticity: how gene expression can assess and predict the consequences of ocean change. Philosophical Transactions of the Royal Society B: Biological Sciences 367:1733-1745

Fiehn O (2002) Metabolomics – the link between genotypes and phenotypes. Plant Molecular Biology 48:155-171

Forde BG, Lea PJ (2007) Glutamate in plants: metabolism, regulation, and signalling. Journal of Experimental Botany 58:2339-2358

Franssen SU, Gu J, Bergmann N, Winters G, Klostermeier UC, Rosenstiel P, Bornberg-Bauer E, Reusch TBH (2011) Transcriptomic resilience to global warming in the seagrass *Zostera marina*, a marine foundation species. Proceedings of the National Academy of Sciences 108:19276-19281

Franssen SU, Gu J, Winters G, Huylmans A-K, Wienpahl I, Sparwel M, Coyer JA, Olsen JL, Reusch TBH, Bornberg-Bauer E (2014) Genome-wide transcriptomic responses of the seagrasses *Zostera marina* and *Nanozostera noltii* under a simulated heatwave confirm functional types. Marine Genomics 15:65-73

Gao Y, Jiang Z, Du M, Fang J, Jiang W, Fang J (2019) Photosynthetic and metabolic responses of eelgrass *Zostera marina* L. to short-term high-temperature exposure. Journal of Oceanology and Limnology 37:199-209

Gargallo-Garriga A, Preece C, Sardans J, Oravec M, Urban O, Peñuelas J (2018) Root exudate metabolomes change under drought and show limited capacity for recovery. Scientific Reports 8:12696

George R (2019) Seagrasses in warming oceans : physiological and biogeochemical responses. PhD, Stockholm University, Stockholm University

Govers LL, Suykerbuyk W, Hoppenreijs JH, Giesen K, Bouma TJ, van Katwijk MM (2015) Rhizome starch as indicator for temperate seagrass winter survival. Ecological Indicators 49:53-60

Gracey AY (2007) Interpreting physiological responses to environmental change through gene expression profiling. J Exp Biol 210:1584-1592

Green E, Short F (2003) World Atlas of Seagrasses. Prepared by the UNEP World Conservation Monitoring Centre. University of California, Press Berkeley, USA

Greiner JT, McGlathery KJ, Gunnell J, McKee BA (2013) Seagrass Restoration Enhances "Blue Carbon" Sequestration in Coastal Waters. PLOS ONE 8:e72469

Gu J, Weber K, Klemp E, Winters G, Franssen SU, Wienpahl I, Huylmans A-K, Zecher K, Reusch TB, Bornberg-Bauer E (2012) Identifying core features of adaptive metabolic mechanisms for chronic heat stress attenuation contributing to systems robustness. Integrative Biology 4:480-493

Hämmerli A, Reusch TBH (2002) Local adaptation and transplant dominance in genets of the marine clonal plant *Zostera marina*. Marine Ecology Progress Series 242:111-118

Hasler-Sheetal H, Fragner L, Holmer M, Weckwerth W (2015) Diurnal effects of anoxia on the metabolome of the seagrass *Zostera marina*. Metabolomics 11:1208-1218

Hayat S, Hayat Q, Alyemeni MN, Wani AS, Pichtel J, Ahmad A (2012) Role of proline under changing environments. Plant Signaling & Behavior 7:1456-1466

Ho C-L, Saito K (2001) Molecular biology of the plastidic phosphorylated serine biosynthetic pathway in *Arabidopsis thaliana*. Amino Acids 20:243-259

Hoffmann AA, Willi Y (2008) Detecting genetic responses to environmental change. Nature Reviews Genetics 9:421

Huber SC, Israel DW (1982) Biochemical basis for partitioning of photosynthetically fixed carbon between starch and sucrose in soybean (Glycine max Merr.) leaves. Plant Physiology 69:691-696

Hutchins D, Fu F-X, Zhang Y, Warner M, Feng Y, Portune K, Bernhardt P, Mulholland M (2007) CO2 control of Trichodesmium N2 fixation, photosynthesis, growth rates, and elemental ratios: Implications for past, present, and future ocean biogeochemistry. Limnology and Oceanography 52:1293-1304

Invers O, Zimmerman RC, Alberte RS, Pérez M, Romero J (2001) Inorganic carbon sources for seagrass photosynthesis: an experimental evaluation of bicarbonate use in species inhabiting temperate waters. Journal of Experimental Marine Biology and Ecology 265:203-217

IPCC (2014) Climate Change 2014: Synthesis Report. Contribution of Working Groups I, II and III to the Fifth Assessment Report of the Intergovernmental Panel on Climate Change

Jiang ZJ, Huang XP, Zhang JP (2010) Effects of CO2 Enrichment on Photosynthesis, Growth, and Biochemical Composition of Seagrass *Thalassia hemprichii* (Ehrenb.) Aschers. Journal of Integrative Plant Biology 52:904-913

Jones CG, Lawton JH, Shachak M (1994) Organisms as ecosystem engineers. Ecosystem Management. Springer

Jueterbock A, Franssen SU, Bergmann N, Gu J, Coyer JA, Reusch TB, Bornberg-Bauer E, Olsen JL (2016) Phylogeographic differentiation versus transcriptomic adaptation to warm temperatures in *Zostera marina*, a globally important seagrass. Molecular Ecology 25:5396-5411

Kaplan F, Zhao W, Richards JT, Wheeler RM, Guy CL, Levine LH (2012) Transcriptional and Metabolic Insights into the Differential Physiological Responses of *Arabidopsis* to Optimal and Supraoptimal Atmospheric CO2. PLOS ONE 7:e43583

Karrer EE, Rodriguez RL (1992) Metabolic regulation of rice α-amylase and sucrose synthase genes in planta. The Plant Journal 2:517-523

Kim Y-M, Nowack S, Olsen MT, Becraft ED, Wood JM, Thiel V, Klapper I, Kühl M, Fredrickson JK, Bryant DA (2015) Diel metabolomics analysis of a hot spring chlorophototrophic microbial mat leads to new hypotheses of community member metabolisms. Frontiers in Microbiology 6:209

Kind T, Wohlgemuth G, Lee DY, Lu Y, Palazoglu M, Shahbaz S, Fiehn O (2009) FiehnLib: mass spectral and retention index libraries for metabolomics based on quadrupole and time-of-flight gas chromatography/mass spectrometry. Analytical Chemistry 81:10038-10048

Kleypas JA, Feely RA, Fabry VJ, Langdon C, Sabine CL, Robbins LL Impacts of ocean acidification on coral reefs and other marine calcifiers: a guide for future research. Proc Report of a workshop held. Citeseer

Koch E, Beer S (1996) Tides, light and the distribution of *Zostera marina* in Long Island Sound, USA. Aquatic Botany 53:97-107

Koch KE, Nolte KD, Duke ER, McCarty DR, Avigne WT (1992) Sugar Levels Modulate Differential Expression of Maize Sucrose Synthase Genes. The Plant Cell 4:59-69

Kong F, Zhou Y, Sun P, Cao M, Li H, Mao Y (2016) Identification of light-harvesting chlorophyll *a/b*-binding protein genes of *Zostera marina* L. and their expression under different environmental conditions. Journal of Ocean University of China 15:152-162

Kraemer GP, Kohrs D, Alberte RS (1998) Developmental changes of sucrose synthase activity and abundance in root and leaf tissues of *Zostera marina*. Aquatic Botany 62:189-198

Kumari P, Reddy CRK, Jha B (2015) Methyl Jasmonate-Induced Lipidomic and Biochemical Alterations in the Intertidal Macroalga *Gracilaria dura* (Gracilariaceae, Rhodophyta). Plant and Cell Physiology 56:1877-1889

Lauritano C, Ruocco M, Dattolo E, Buia M, Silva J, Santos R, Olivé I, Costa M, Procaccini G (2015) Response of key stress-related genes of the seagrass *Posidonia oceanica* in the vicinity of submarine volcanic vents. Biogeosciences 12:4185-4194

Leakey AD, Ainsworth EA, Bernacchi CJ, Rogers A, Long SP, Ort DR (2009) Elevated CO2 effects on plant carbon, nitrogen, and water relations: six important lessons from FACE. Journal of Experimental Botany 60:2859-2876

Lewis E, Wallace D (1998) Program developed for CO2 system calculations. Carbon Dioxide Information Analysis Center. Oak Ridge National Laboratory, US Dept Energy, ORNL/CDIAC-105, Oak Ridge, TN, Oak Ridge National Laboratory, US Dept Energy, ORNL/CDIAC-105, Oak Ridge, TN

Macreadie P, Schliep M, Rasheed M, Chartrand K, Ralph P (2014) Molecular indicators of chronic seagrass stress: A new era in the management of seagrass ecosystems? Ecological Indicators 38:279-281

Marín-Guirao L, Bernardeau-Esteller J, García-Muñoz R, Ramos A, Ontoria Y, Romero J, Pérez M, Ruiz JM, Procaccini G (2018) Carbon economy of Mediterranean seagrasses in response to thermal stress. Marine Pollution Bulletin 135:617-629

Marsh JA, Dennison WC, Alberte RS (1986) Effects of temperature on photosynthesis and respiration in eelgrass (*Zostera marina* L.). Journal Experimental Marine Biology Ecology 101:10

Mazzella L, Alberte RS (1986) Light adaptation and the role of autotrophic epiphytes in primary production of the temperate seagrass, *Zostera marina* L. Journal of Experimental Marine Biology and Ecology 100:165-180

Mcleod E, Chmura GL, Bouillon S, Salm R, Björk M, Duarte CM, Lovelock CE, Schlesinger WH, Silliman BR (2011) A blueprint for blue carbon: toward an improved understanding of the role of vegetated coastal habitats in sequestering CO2. Frontiers in Ecology and the Environment 9:552-560

Mehrotra B, Mendes P (2006) Bioinformatics approaches to integrate metabolomics and other systems biology data. Plant Metabolomics. Springer

Minagawa J, Han K-C, Dohmae N, Takio K, Inoue Y (2001) Molecular characterization and gene expression of lhcb5 gene encoding CP26 in the light-harvesting complex II of *Chlamydomonas reinhardtii*. Plant Molecular Biology 46:277-287

Miro B, Ismail A (2013) Tolerance of anaerobic conditions caused by flooding during germination and early growth in rice (*Oryza sativa* L.). Frontiers in Plant Science 4

Moore B, Cheng SH, Rice J, Seemann J (1998) Sucrose cycling, Rubisco expression, and prediction of photosynthetic acclimation to elevated atmospheric CO2. Plant, Cell & Environment 21:905-915

Moore B, Cheng SH, Sims D, Seemann J (1999) The biochemical and molecular basis for photosynthetic acclimation to elevated atmospheric CO2. Plant, Cell & Environment 22:567-582

Moore KA, Jarvis JC (2008) Environmental Factors Affecting Recent Summertime Eelgrass Diebacks in the Lower Chesapeake Bay: Implications for Long-term Persistence. Journal of Coastal Research:135-147

Myers OD, Sumner SJ, Li S, Barnes S, Du X (2017) One Step Forward for Reducing False Positive and False Negative Compound Identifications from Mass Spectrometry Metabolomics Data: New Algorithms for Constructing Extracted Ion Chromatograms and Detecting Chromatographic Peaks. Analytical Chemistry 89:8696-8703

NOAA-ESRL (2018) Trends in Atmospheric Carbon Dioxide - Earth System Research Laboratory. Global Monitoring Division

Oliva S, Romero J, Pérez M, Manent P, Mascaró O, Serrão EA, Coelho N, Alberto F (2014) Reproductive strategies and isolation-by-demography in a marine clonal plant along an eutrophication gradient. Molecular Ecology 23:5698-5711

Olivé I, Silva J, Lauritano C, Costa MM, Ruocco M, Procaccini G, Santos R (2017) Linking gene expression to productivity to unravel long- and short-term responses of seagrasses exposed to CO2 in volcanic vents. Scientific Reports 7:42278

Olsen JL, Stam WT, Coyer JA, Reusch TBH, Billingham M, BostrÖM C, Calvert E, Christie H, Granger S, LumiÈRe RL, Milchakova N, Oudot-Le Secq M-P, Procaccini G, Sanjabi B, SerrÃO E, Veldsink JAN, Widdicombe S, Wyllie-Echeverria S (2004) North Atlantic phylogeography and large-scale population differentiation of the seagrass *Zostera marina* L. Molecular Ecology 13:1923-1941

Ort BS, Cohen CS, Boyer KE, Wyllie-Echeverria S (2012) Population Structure and Genetic Diversity among Eelgrass (*Zostera marina*) Beds and Depths in San Francisco Bay. Journal of Heredity 103:533-546

Orth RJ, Carruthers TJ, Dennison WC, Duarte CM, Fourqurean JW, Heck KL, Hughes AR, Kendrick GA, Kenworthy WJ, Olyarnik S (2006) A global crisis for seagrass ecosystems. Bioscience 56:987-996

Orth RJ, Williams MR, Marion SR, Wilcox DJ, Carruthers TJ, Moore KA, Kemp WM, Dennison WC, Rybicki N, Bergstrom P (2010) Long-term trends in submersed aquatic vegetation (SAV) in Chesapeake Bay, USA, related to water quality. Estuaries and Coasts 33:1144-1163

Palacios SL, Zimmerman RC (2007) Response of eelgrass *Zostera marina* to CO2 enrichment: possible impacts of climate change and potential for remediation of coastal habitats. Marine Ecology Progress Series 344:1

Paul M, de los Santos CB (2019) Variation in flexural, morphological, and biochemical leaf properties of eelgrass (*Zostera marina*) along the European Atlantic climate regions. Marine Biology 166:127

Pfannschmidt T, Yang C (2012) The hidden function of photosynthesis: a sensing system for environmental conditions that regulates plant acclimation responses. Protoplasma 249:125-136

Pigliucci M (1996) How organisms respond to environmental changes: from phenotypes to molecules (and vice versa). Trends in Ecology & Evolution 11:168-173

Piro A, Bernardo L, Serra IA, Barrote I, Olivé I, Costa MM, Lucini L, Santos R, Mazzuca S, Silva J (2020) Leaf proteome modulation and cytological features of seagrass *Cymodocea nodosa* in response to long-term high CO2 exposure in volcanic vents. Scientific Reports 10:22332

Pluskal T, Castillo S, Villar-Briones A, Orešič M (2010) MZmine 2: modular framework for processing, visualizing, and analyzing mass spectrometry-based molecular profile data. BMC bioinformatics 11:395

Procaccini G, Ruocco M, Marín-Guirao L, Dattolo E, Brunet C, D'Esposito D, Lauritano C, Mazzuca S, Serra IA, Bernardo L, Piro A, Beer S, Björk M, Gullström M, Buapet P, Rasmusson LM, Felisberto P, Gobert S, Runcie JW, Silva J, Olivé I, Costa MM, Barrote I, Santos R (2017) Depth-specific fluctuations of gene expression and protein abundance modulate the photophysiology in the seagrass *Posidonia oceanica*. Scientific Reports 7:42890

Ralph PJ (1998) Photosynthetic response of laboratory-cultured *Halophila ovalis* to thermal stress. Marine Ecology Progress Series 171:123-130

Ransbotyn V, Reusch TB (2006) Housekeeping gene selection for quantitative real-time PCR assays in the seagrass *Zostera marina* subjected to heat stress. Limnology and Oceanography: Methods 4:367-373

Raven JA, Geider RJ (2003) Adaptation, Acclimation and Regulation in Algal Photosynthesis. In: Larkum AWD, Douglas SE, Raven JA (eds) Photosynthesis in Algae Advances in Photosynthesis and Respiration, Book 14, Springer, Dordrecht

Repolho T, Duarte B, Dionísio G, Paula JR, Lopes AR, Rosa IC, Grilo TF, Caçador I, Calado R, Rosa R (2017) Seagrass ecophysiological performance under ocean warming and acidification. Scientific Reports 7:41443

Reusch TB, Veron AS, Preuss C, Weiner J, Wissler L, Beck A, Klages S, Kube M, Reinhardt R, Bornberg-Bauer E (2008) Comparative analysis of expressed sequence tag (EST)

libraries in the seagrass *Zostera marina* subjected to temperature stress. Marine Biotechnology 10:297-309

Reusch TBH, Stam WT, Olsen JL (1999) Size and estimated age of genets in eelgrass, *Zostera marina*, assessed with microsatellite markers. Marine Biology 133:519-525

Rhode JM, Duffy JE (2004) Relationships between bed age, bed size, and genetic structure in Chesapeake Bay (Virginia, USA) eelgrass (*Zostera marina* L.). Conservation Genetics 5:661-671

Rivas-Ubach A, Sardans J, Hódar JA, Garcia-Porta J, Guenther A, Oravec M, Urban O, Peñuelas J (2016) Similar local, but different systemic, metabolomic responses of closely related pine subspecies to folivory by caterpillars of the processionary moth. Plant Biology 18:484-494

Rivero-Calle S, Gnanadesikan A, Del Castillo CE, Balch WM, Guikema SD (2015) Multidecadal increase in North Atlantic coccolithophores and the potential role of rising CO2. Science 350:1533-1537

Roberts M, S. Albertson, A. Ahmed, and G. Pelletier (2014) South Puget Sound Dissolved Oxygen Study: South and Central Puget Sound Water Circulation Model Development and Calibration. Environmental Assessment Program Washington State Department of Ecology, Olympia, Washington

Roca G, Alcoverro T, de Torres M, Manzanera M, Martínez-Crego B, Bennett S, Farina S, Pérez M, Romero J (2015) Detecting water quality improvement along the Catalan coast (Spain) using stress-specific biochemical seagrass indicators. Ecological Indicators 54:161-170

Ruckelshaus MH (1998) Spatial Scale of Genetic Structure and an Indirect Estimate of Gene Flow in Eelgrass, *Zostera marina*. Evolution 52:330-343

Ruocco M, Marín-Guirao L, Procaccini G (2019) Within-and among-leaf variations in photo-physiological functions, gene expression and DNA methylation patterns in the large-sized seagrass *Posidonia oceanica*. Marine Biology 166

Ruocco M, Musacchia F, Olivé I, Costa MM, Barrote I, Santos R, Sanges R, Procaccini G, Silva J (2017) Genomewide transcriptional reprogramming in the seagrass *Cymodocea nodosa* under experimental ocean acidification. Molecular Ecology 26:4241-4259

Salo T, Reusch TB, Boström C (2015) Genotype-specific responses to light stress in eelgrass *Zostera marina*, a marine foundation plant. Marine Ecology Progress Series 519:129

Shelp BJ, Bown AW, McLean MD (1999) Metabolism and functions of gamma-aminobutyric acid. Trends in Plant Science 4:446-452

Sinclair EA, Krauss SL, Anthony J, Hovey R, Kendrick GA (2014) The interaction of environment and genetic diversity within meadows of the seagrass *Posidonia australis* (Posidoniaceae). Marine Ecology Progress Series 506:87-98

Singh SA, Christendat D (2006) Structure of Arabidopsis Dehydroquinate Dehydratase-Shikimate Dehydrogenase and Implications for Metabolic Channeling in the Shikimate Pathway. Biochemistry 45:7787-7796

Soerensen ST (2020) New Zealand seagrass (*Zostera muelleri*) response to acute sedimentation: Linking non-structural carbohydrate reserves to resilience. Doctor of Philosophy (PhD) Doctoral, The University of Waikato, Hamilton, New Zealand

Srivastava A, George J, Karuturi RKM (2019) Transcriptome Analysis. In: Ranganathan S, Gribskov M, Nakai K, Schönbach C (eds) Encyclopedia of Bioinformatics and Computational Biology. Academic Press, Oxford

Staehr PA, Borum J (2011) Seasonal acclimation in metabolism reduces light requirements of eelgrass (*Zostera marina*). Journal of Experimental Marine Biology and Ecology 407:139-146

Sumner LW, Amberg A, Barrett D, Beale MH, Beger R, Daykin CA, Fan TW-M, Fiehn O, Goodacre R, Griffin JL (2007) Proposed minimum reporting standards for chemical analysis. Metabolomics 3:211-221

Szabados L, Savouré A (2010) Proline: a multifunctional amino acid. Trends in Plant Science 15:89-97

Tabita FR, McFadden BA (1972) Regulation of ribulose-1,5-diphosphate carboxylase by 6-phospho-D-gluconate. Biochemical and Biophysical Research Communications 48:1153-1159

Thayer GW, Wolfe DA, Williams RB (1975) The Impact of Man on Seagrass Systems: Seagrasses must be considered in terms of their interaction with the other sources of primary production that support the estuarine trophic structure before their significance can be fully appreciated. American Scientist:288-296

Thomas E (2008) Descent into the Icehouse. Geology 36:191-192

Touchette BW, Burkholder JM (2000) Overview of the physiological ecology of carbon metabolism in seagrasses. Journal of Experimental Marine Biology and Ecology 250:169-205

van Lent F, Verschuure JM (1994) Intraspecific variability of *Zostera marina* L. (eelgrass) in the estuaries and lagoons of the southwestern Netherlands. I. Population dynamics. Aquatic Botany 48:31-58

Verbruggen N, Hermans C (2008) Proline accumulation in plants: a review. Amino Acids 35:753-759

Vergeer LHT, Aarts TL, de Groot JD (1995) The 'wasting disease' and the effect of abiotic factors (light intensity, temperature, salinity) and infection with *Labyrinthula zosterae* on the phenolic content of *Zostera marina* shoots. Aquatic Botany 52:35-44

Wang W, Vinocur B, Shoseyov O, Altman A (2004) Role of plant heat-shock proteins and molecular chaperones in the abiotic stress response. Trends in Plant Science 9:244-252

Weaver LM, Herrmann KM (1997) Dynamics of the shikimate pathway in plants. Trends in Plant Science 2:346-351

Whiteley AR, Fitzpatrick SW, Funk WC, Tallmon DA (2015) Genetic rescue to the rescue. Trends in Ecology & Evolution 30:42-49

Williams S, Orth R (1998) Genetic diversity and structure of natural and transplanted eelgrass populations in the Chesapeake and Chincoteague Bays. Estuaries 21:118-128

Winter H, Huber SC (2000) Regulation of Sucrose Metabolism in Higher Plants: Localization and regulation of Activity of Key Enzymes. Critical Reviews in Plant Sciences 19:31-67

Winters G, Nelle P, Fricke B, Rauch G, Reusch TB (2011) Effects of a simulated heat wave on photophysiology and gene expression of high- and low-latitude populations of *Zostera marina*. Marine Ecology Progress Series 435:83-95

Xu X, Yang Y, Liu C, Sun Y, Zhang T, Hou M, Huang S, Yuan H (2019) The evolutionary history of the sucrose synthase gene family in higher plants. BMC Plant Biology 19:566

Zang Y, Liu J, Tang XX, Zhou B (2018) Description of a *Zostera marina* catalase gene involved in responses to temperature stress. PeerJ 6:e4532

Zayas-Santiago CC, Rivas-Ubach A, Kuo L-J, Ward ND, Zimmerman RC (2020) Metabolic Profiling Reveals Biochemical Pathways Responsible for Eelgrass Response to Elevated CO2 and Temperature. Scientific Reports 10:4693

Zhang Y, Zhao P, Yue S, Liu M, Qiao Y, Xu S, Gu R, Zhang X, Zhou Y (2021) New insights into physiological effects of anoxia under darkness on the iconic seagrass *Zostera marina* based on a combined analysis of transcriptomics and metabolomics. Science of The Total Environment:144717

Zhang YG, Pagani M, Liu Z, Bohaty SM, DeConto R (2013) A 40-million-year history of atmospheric CO2. Philosophical Transactions of the Royal Society A: Mathematical, Physical and Engineering Sciences 371:20130096

Zimmerman RC (2021) Scaling up: Predicting the Impacts of Climate Change on Seagrass Ecosystems. Estuaries and Coasts 42:558-576

Zimmerman RC, Hill VJ, Gallegos CL (2015) Predicting effects of ocean warming, acidification, and water quality on Chesapeake region eelgrass. Limnology and Oceanography 60:1781-1804

Zimmerman RC, Hill VJ, Jinuntuya M, Celebi B, Ruble D, Smith M, Cedeño T, Swingle WM (2017) Experimental impacts of climate warming and ocean carbonation on eelgrass *Zostera marina*. Marine Ecology Progress Series 566:1-15

Zimmerman RC, Kohrs DG, Steller DL, Alberte RS (1995) Carbon partitioning in eelgrass (regulation by photosynthesis and the response to daily light-dark cycles). Plant Physiology 108:1665-1671

Zimmerman RC, Kohrs DG, Steller DL, Alberte RS (1997) Impacts of CO2 enrichment on productivity and light requirements of eelgrass. Plant Physiology 115:599-607

Zimmerman RC, Mobley CD Radiative transfer within seagrass canopies: impact on carbon budgets and light requirements. Proc Ocean Optics XIII. International Society for Optics and Photonics

Zimmerman RC, Smith RD, Alberte RS (1989) Thermal acclimation and whole-plant carbon balance in *Zostera marina* L. (eelgrass). Journal of Experimental Marine Biology and Ecology 130:93-109

Zinta G, AbdElgawad H, Domagalska MA, Vergauwen L, Knapen D, Nijs I, Janssens IA, Beemster GTS, Asard H (2014) Physiological, biochemical, and genome-wide transcriptional analysis reveals that elevated CO2 mitigates the impact of combined heat wave and drought stress in *Arabidopsis thaliana* at multiple organizational levels. Global Change Biology 20:3670-3685

Zou H-X, Pang Q-Y, Lin L-D, Zhang A-Q, Li N, Lin Y-Q, Li L-M, Wu Q-Q, Yan X-F (2014) Behavior of the Edible Seaweed *Sargassum fusiforme* to Copper Pollution: Short-Term Acclimation and Long-Term Adaptation. PLOS ONE 9:e101960

APPENDIX

% Survival

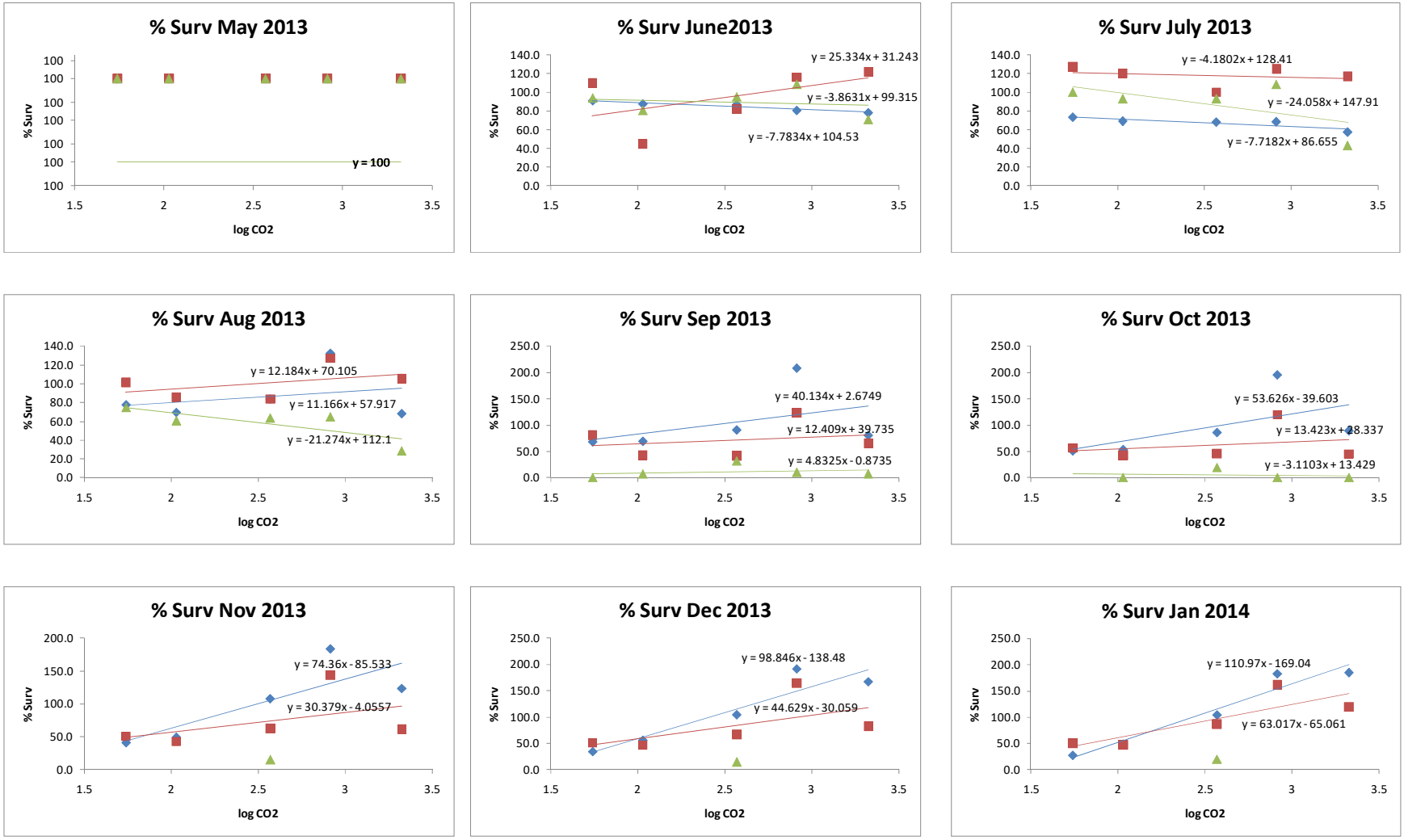

Figure 22. Monthly linear regressions of percent survival mean against log [CO_2] (♦) South Bay, VA (■) Dumas Bay, WA and (▲) Nisqually Bay, WA.

Figure 22 continued

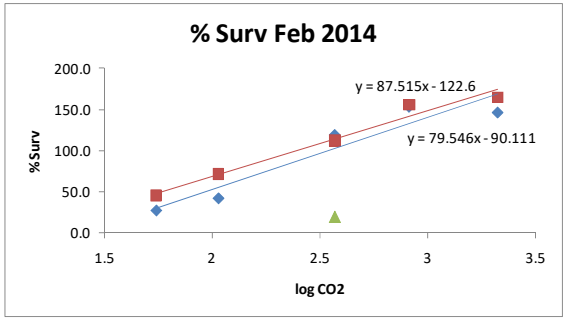

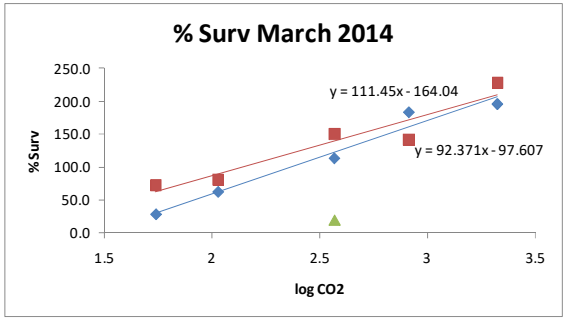

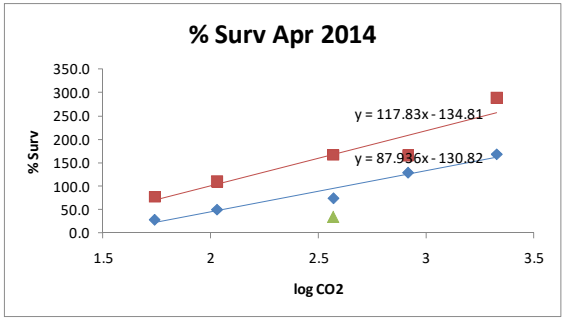

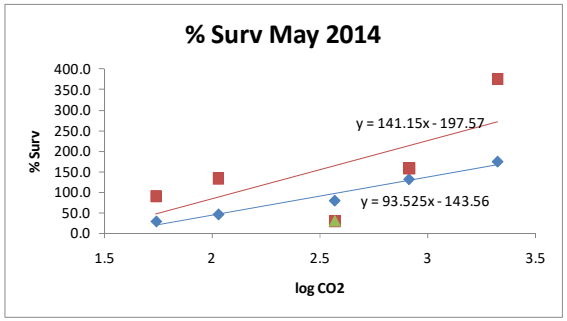

% Relative Growth

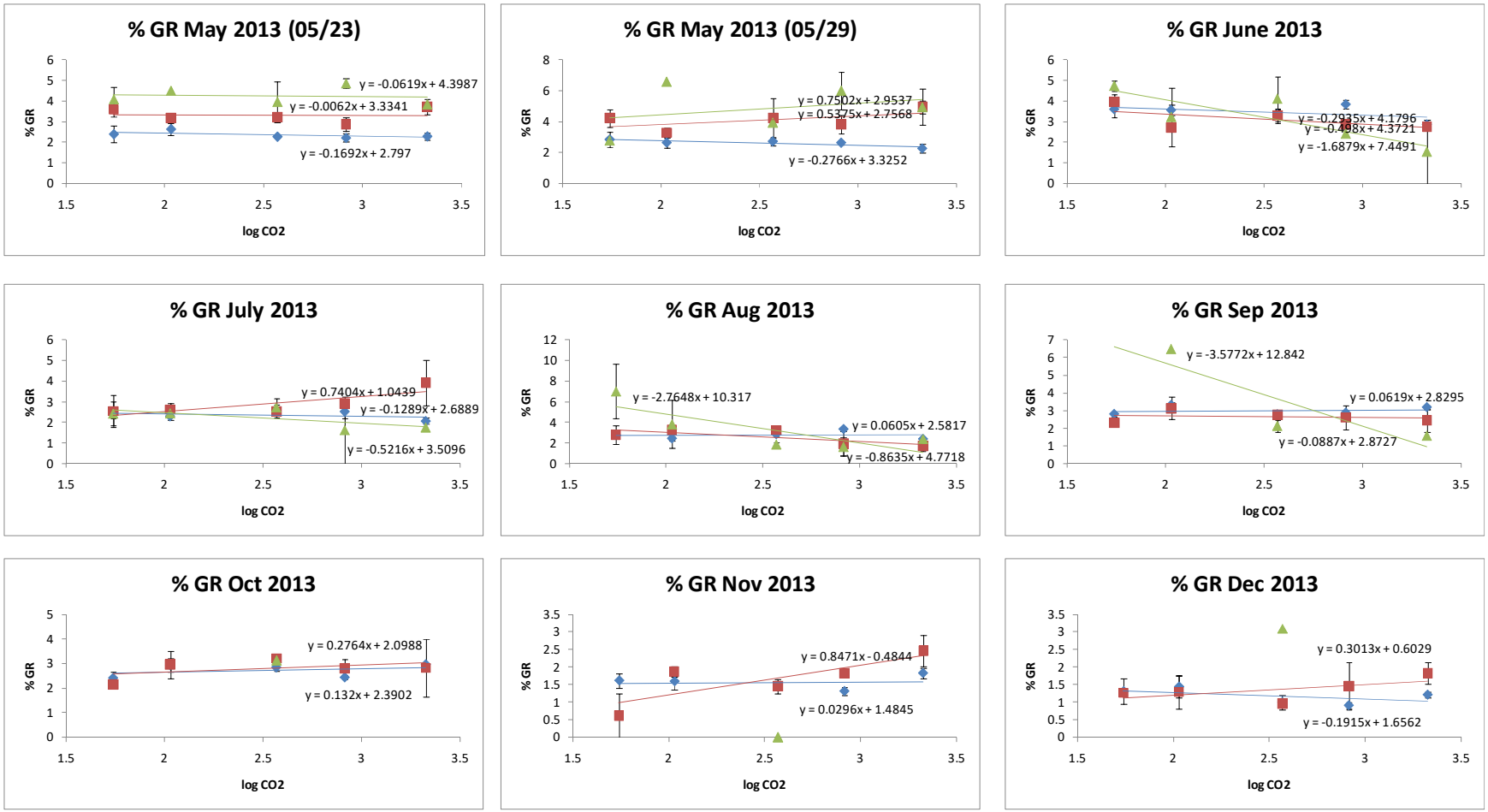

Figure 23. Monthly linear regressions of the mean of relative growth against log [CO_2] (♦) South Bay, VA (■) Dumas Bay, WA and (▲) Nisqually Bay, WA.

Figure 23 continued

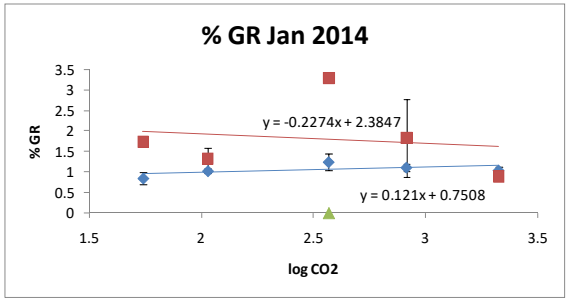

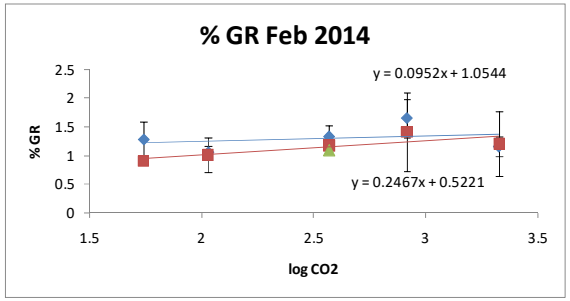

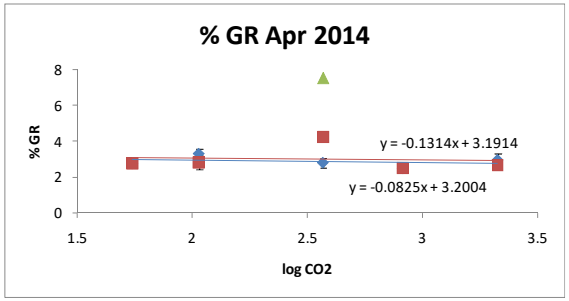

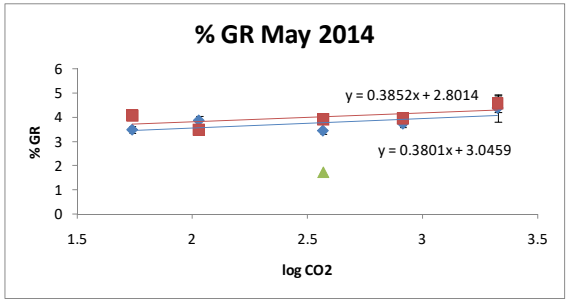

% Original Plant size

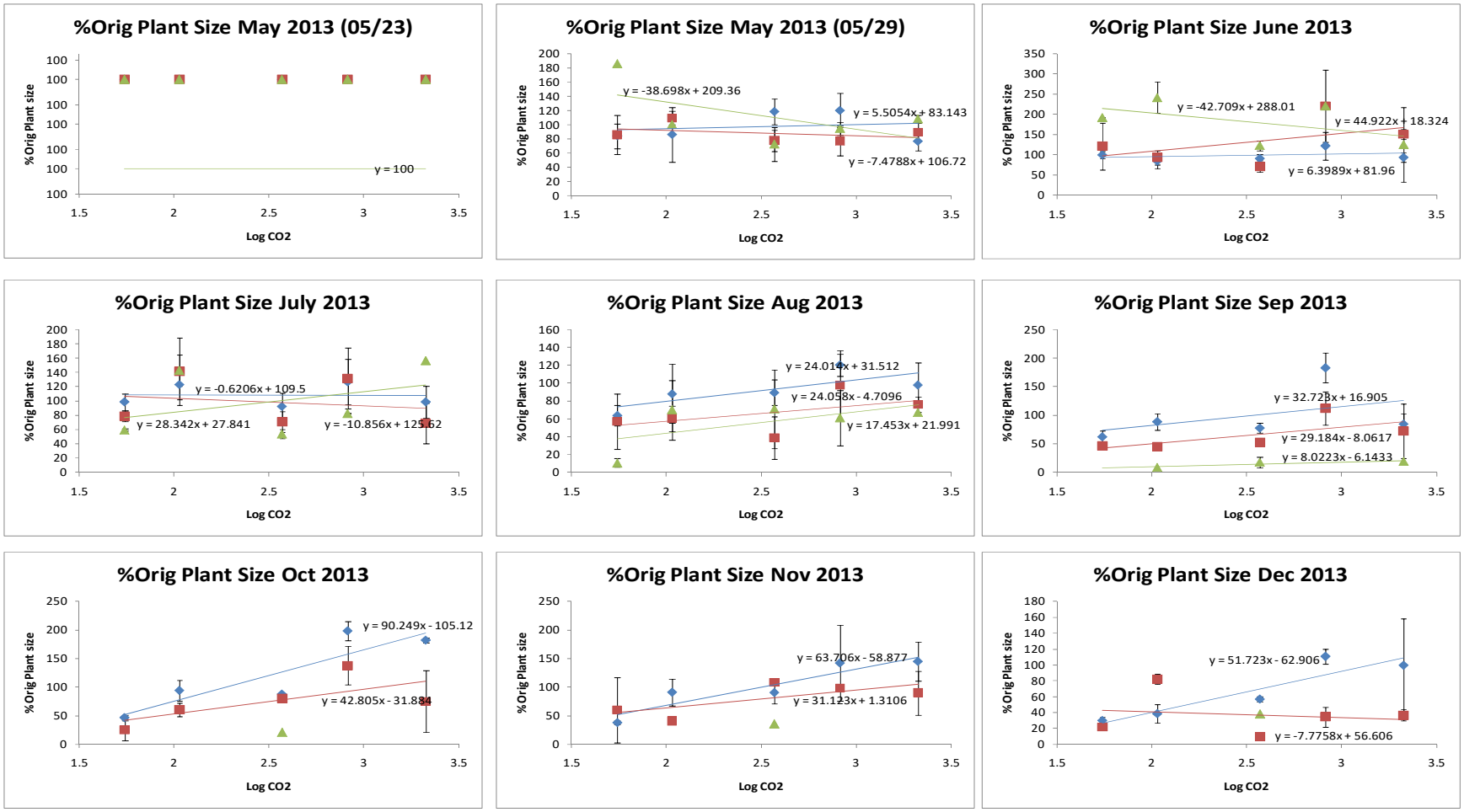

Figure 24. Monthly linear regressions of the mean of original plant size against log [CO_2] (♦) South Bay, VA (■) Dumas Bay, WA and (▲) Nisqually Bay, WA.

Figure 24 continued

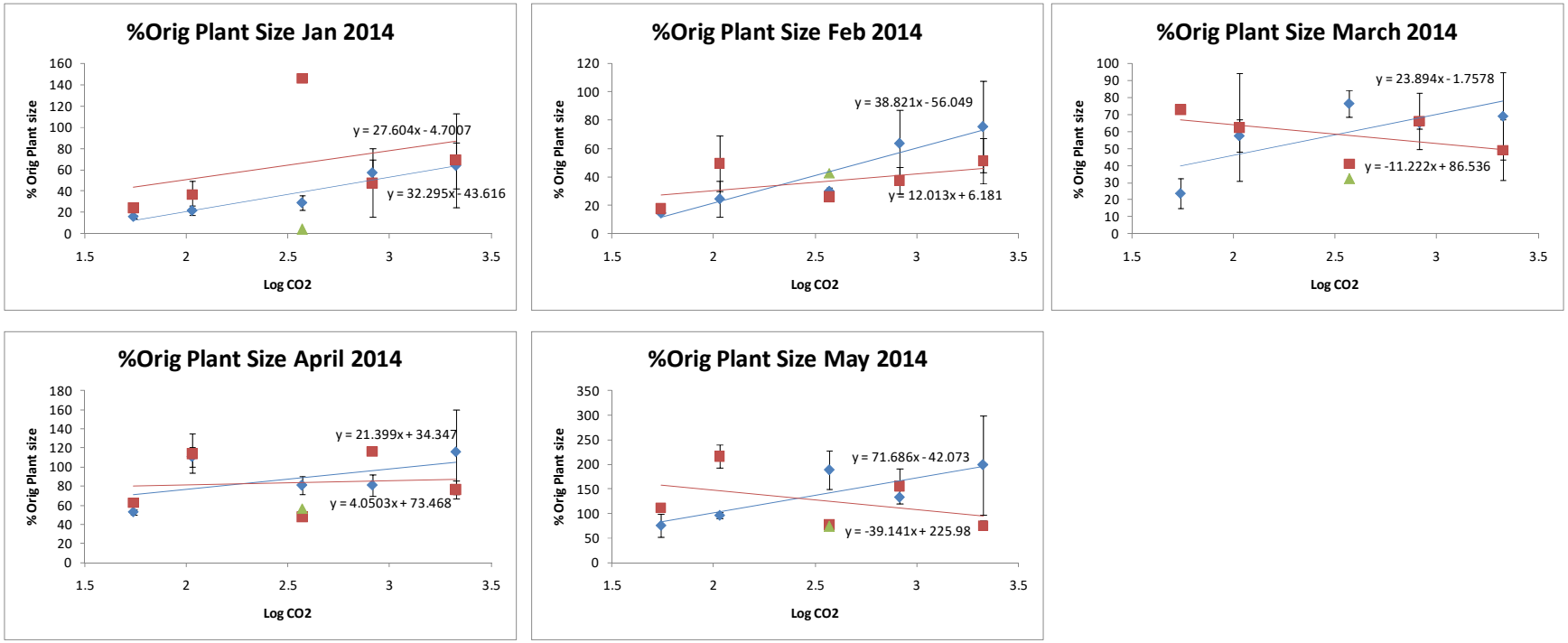

Sucrose concentration (µmol g^{-1} DW)

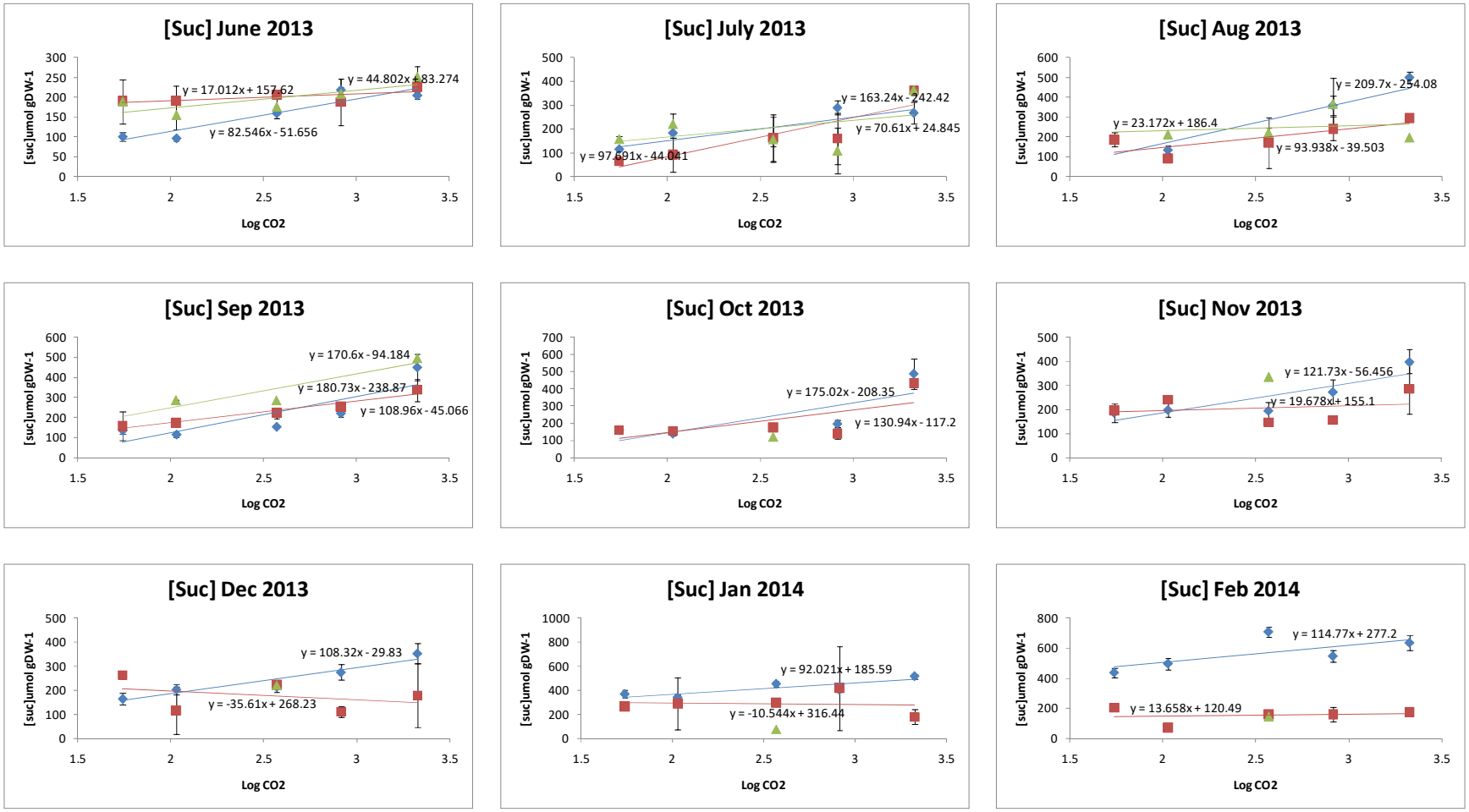

Figure 25. Monthly linear regressions of sucrose concentration mean against log [CO_2] (♦) South Bay, VA (■) Dumas Bay, WA and (▲) Nisqually Bay, WA.

Figure 25 continued

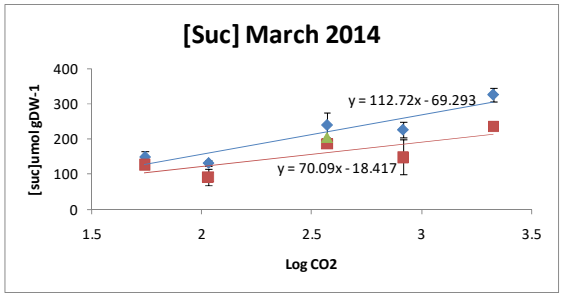

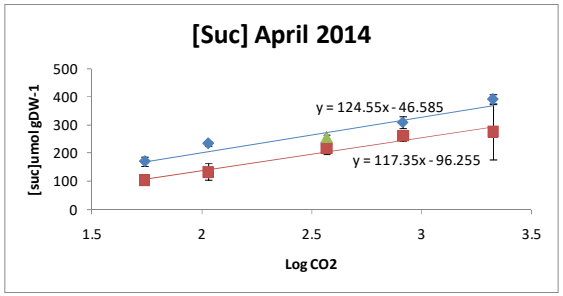

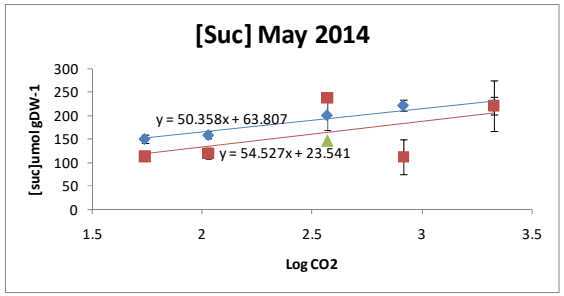

Total chlorophyll per LA (µg Chl/cm^2)

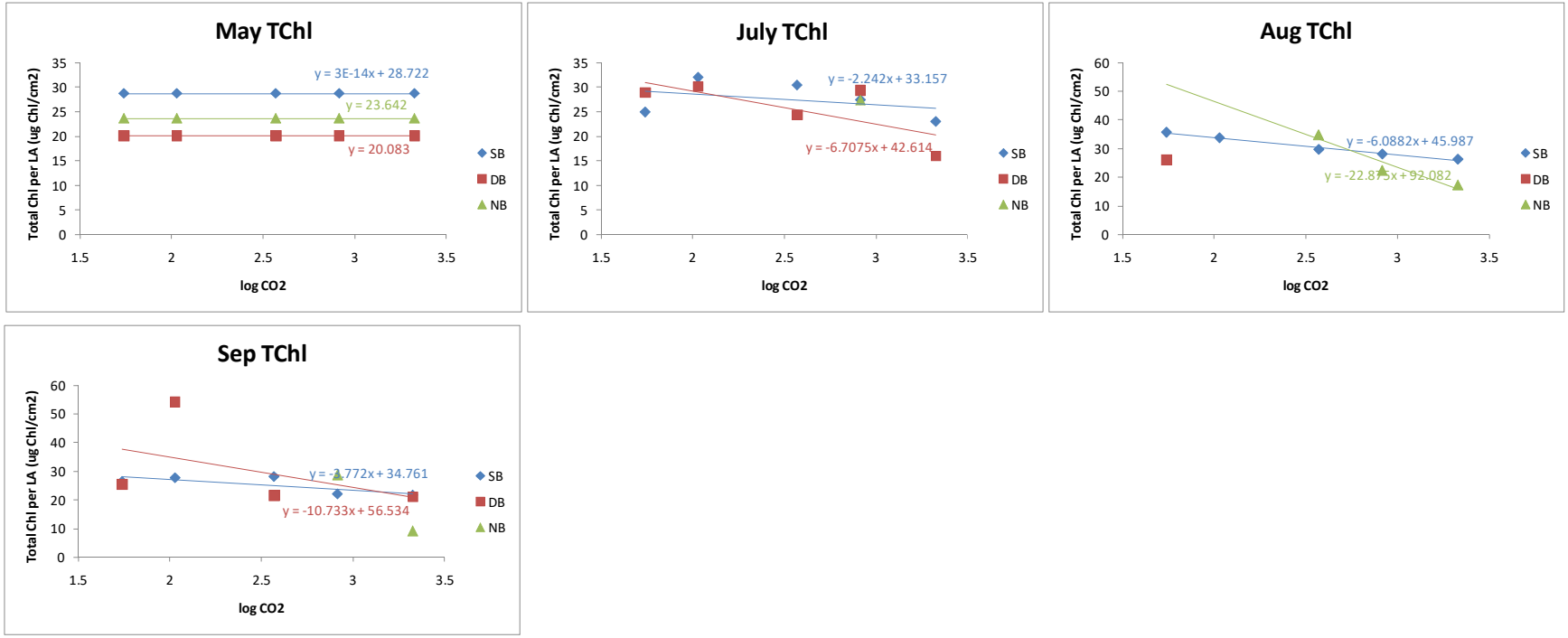

Figure 26. Monthly linear regressions of total chlorophyll mean against log [CO_2] (♦) South Bay, VA (■) Dumas Bay, WA and (▲) Nisqually Bay, WA.

Chlorophyll a:b

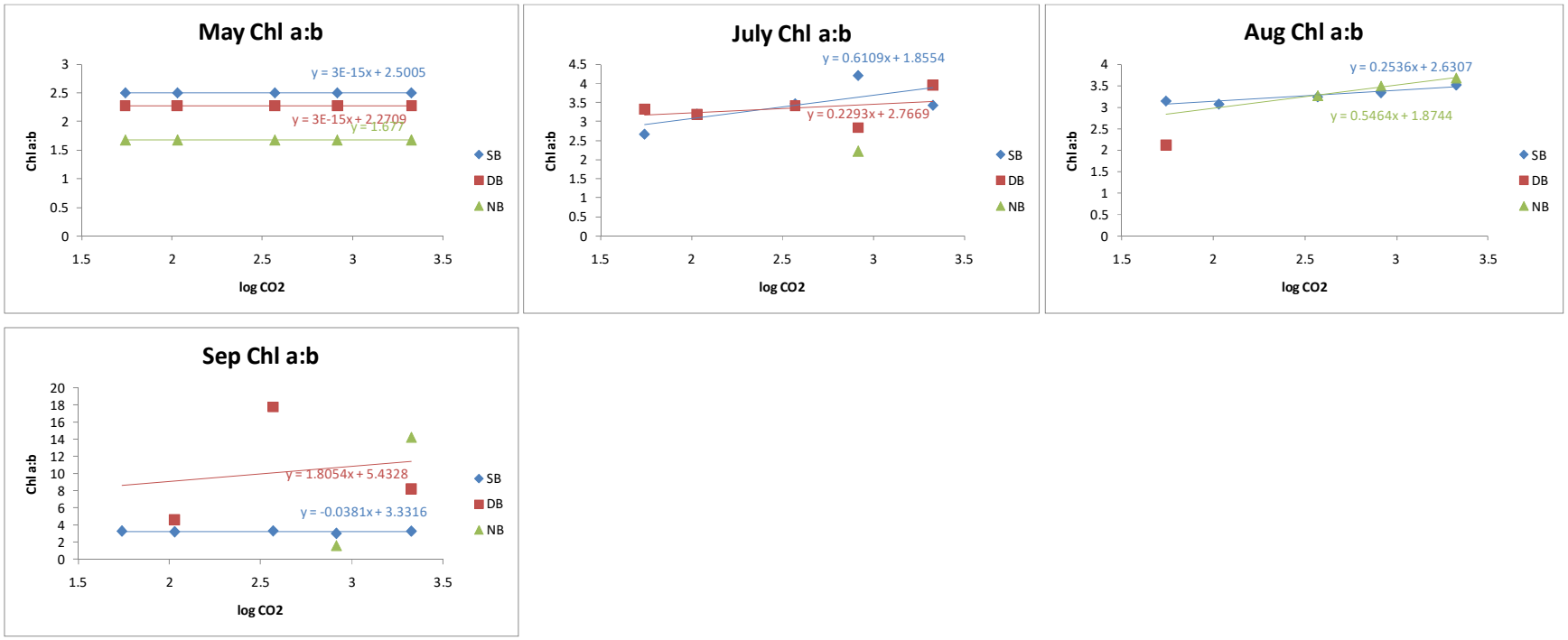

Figure 27. Monthly linear regressions of chlorophyll *a*:*b* ratio against log [CO_2] (♦) South Bay, VA (■) Dumas Bay, WA and (▲) Nisqually Bay, WA.

Table 29. Monthly slopes statistics of the percent original population vs. log [CO_2] derived from linear regression analysis.

% Survival

Month	Population	Slope	R^2	*F*	*p*
May	SBV	0	-	-	-
	DBW	0	-	-	-
	NBW	0	-	-	-
June	SBV	-7.78	0.92	33.82	0.01*
	DBW	25.33	0.26	1.07	0.38
	NBW	-3.86	0.03	0.09	0.78
July	SBV	-7.71	0.74	8.53	0.06
	DBW	-4.18	0.06	0.2	0.68
	NBW	-24.05	0.36	1.71	0.28
Aug	SBV	11.16	0.07	0.24	0.66
	DBW	12.18	0.2	0.75	0.45
	NBW	-21.27	0.6	4.58	0.12
Sep	SBV	40.13	0.19	0.71	0.46
	DBW	12.41	0.06	0.17	0.70
	NBW	4.83	0.06	0.21	0.68
Oct	SBV	53.62	0.35	1.59	0.30
	DBW	13.42	0.07	0.22	0.69
	NBW	-3.11	0.03	0.06	-
Nov	SBV	74.36	0.67	6.11	0.09
	DBW	30.38	0.23	0.9	0.41
Dec	SBV	98.84	0.87	19.81	0.02*
	DBW	44.62	0.35	1.66	0.29
Jan	SBV	110.97	0.94	49.39	0.005*
	DBW	63.02	0.70	6.93	0.078
Feb	SBV	87.51	0.90	27.49	0.013*
	DBW	79.54	0.97	106.6	0.001*
March	SBV	111.45	0.96	88.49	0.002*
	DBW	92.37	0.9	29.27	0.012*
April	SBV	87.93	0.96	72.82	0.003*
	DBW	117.83	0.88	23.84	0.016*
May	SBV	93.52	0.97	97.78	0.002*
	DBW	141.15	0.47	2.72	0.20

Table 30. Monthly slopes statistics of the relative growth rates vs. log [CO_2] derived from linear regression analysis.

% Growth rate

Month	Population	Slope	R^2	*F*	*p*
May	SBV	-0.22	0.69	6.76	0.08
	DBW	0.26	0.31	1.37	0.33
	NBW	0.24	0.1	0.33	0.60
June	SBV	-0.29	0.27	1.14	0.36
	DBW	-0.49	0.37	1.82	0.27
	NBW	-1.68	0.72	8.04	0.06
July	SBV	-0.13	0.2	0.73	0.45
	DBW	0.74	0.66	5.86	0.09
	NBW	-0.52	0.48	2.78	0.19
Aug	SBV	0.06	0.009	0.029	0.87
	DBW	-0.86	0.60	4.49	0.12
	NBW	-2.76	0.64	5.48	0.10
Sep	SBV	0.06	0.03	0.083	0.79
	DBW	-0.08	0.03	0.09	0.77
	NBW	-3.57	0.75	3.09	0.33
Oct	SBV	0.13	0.10	0.34	0.60
	DBW	0.27	0.20	0.78	0.44
Nov	SBV	0.03	0.01	0.03	0.87
	DBW	0.85	0.65	5.67	0.09
Dec	SBV	-0.19	0.32	1.42	0.32
	DBW	0.30	0.38	1.80	0.27
Jan	SBV	0.12	0.29	1.2	0.35
	DBW	-0.22	0.03	0.08	0.80
Feb	SBV	0.09	0.07	0.24	0.66
	DBW	0.25	0.66	5.88	0.09
March	SBV	-0.50	0.77	10.27	0.05
	DBW	-	-	-	-
April	SBV	-0.13	0.07	0.24	0.65
	DBW	-0.08	0.005	0.02	0.90
May	SBV	0.38	0.42	2.23	0.23
	DBW	0.38	0.40	1.96	0.25

Table 31. Monthly slopes statistics of the percent plant size vs. log [CO_2] derived from linear regression analysis.

		%Plant size			
Month	**Population**	**Slope**	**R^2**	***F***	***p***
May	SBV	5.51	0.03	0.09	0.78
	DBW	-7.48	0.13	0.47	0.54
	NBW	-38.69	0.33	1.48	0.31
June	SBV	6.40	0.82	0.20	0.64
	DBW	44.92	0.24	0.98	0.39
	NBW	-42.70	0.25	1.01	0.39
July	SBV	-0.62	0.00	0.002	0.97
	DBW	-10.85	0.04	0.12	0.75
	NBW	28.34	0.15	0.51	0.52
Aug	SBV	24.01	0.58	4.09	0.14
	DBW	17.45	0.26	1.05	0.38
	NBW	24.05	0.37	1.75	0.27
Sep	SBV	32.72	0.19	0.72	0.46
	DBW	29.18	0.45	2.43	0.22
	NBW	8.02	0.77	3.38	0.31
Oct	SBV	90.24	0.78	11.19	0.04*
	DBW	42.80	0.46	2.52	0.21
Nov	SBV	63.70	0.86	17.84	0.02*
	DBW	31.12	0.50	3.05	0.18
Dec	SBV	51.72	0.85	16.51	0.03*
	DBW	-7.77	0.03	0.10	0.77
Jan	SBV	32.29	0.91	30.97	0.01*
	DBW	27.60	0.13	0.47	0.54
Feb	SBV	38.82	0.90	30.29	0.01*
	DBW	12.01	0.28	1.18	0.35
March	SBV	23.89	0.56	3.80	0.14
	DBW	-11.22	0.31	1.35	0.33
April	SBV	21.39	0.29	1.23	0.35
	DBW	4.05	0.00	0.02	0.89
May	SBV	71.68	0.71	7.48	0.07
	DBW	-39.14	0.17	0.65	0.48

Table 32. Monthly slopes statistics of the sucrose concentration vs. log [CO_2] derived from linear regression analysis.

		[Sucrose]			
Month	**Population**	**Slope**	**R^2**	***F***	***p***
June	SBV	82.54	0.87	20.43	0.02*
	DBW	17.01	0.46	2.55	0.21
	NBW	44.80	0.62	4.89	0.11
July	SBV	97.69	0.71	7.35	0.07
	DBW	163.24	0.81	13.18	0.04*
	NBW	70.61	0.21	0.79	0.44
Aug	SBV	209.70	0.79	11.04	0.04*
	DBW	93.93	0.61	4.82	0.11
	NBW	23.17	0.02	0.05	0.83
Sep	SBV	180.73	0.71	7.66	0.07
	DBW	108.96	0.95	55.43	0.00*
	NBW	170.60	0.82	4.76	0.27
Oct	SBV	175.02	0.61	4.75	0.11
	DBW	130.94	0.45	2.54	0.21
Nov	SBV	121.73	0.75	9.22	0.06
	DBW	19.67	0.04	0.15	0.72
Dec	SBV	108.32	0.90	29.1	0.01*
	DBW	-35.61	0.11	0.40	0.57
Jan	SBV	92.02	0.72	7.56	0.07
	DBW	-10.54	0.006	0.02	0.90
Feb	SBV	114.77	0.46	2.59	0.21
	DBW	13.65	0.03	0.09	0.77
March	SBV	112.72	0.87	20.51	0.02*
	DBW	70.08	0.67	6.13	0.09
April	SBV	124.55	0.88	23.51	0.02*
	DBW	117.35	0.96	82.29	0.002*
May	SBV	50.35	0.92	34.87	0.009*
	DBW	54.52	0.31	1.35	0.33

Table 33. Monthly slopes statistics of photosynthetic pigments per leaf area vs. log [CO_2] derived from linear regression analysis.

T Chl

Month	Population	Slope	R^2	*F*	*p*
May	SBV	0	-	-	-
	DBW	0	-	-	-
	NBW	0	-	-	-
July	SBV	-2.42	0.15	0.52	0.52
	DBW	-6.70	0.53	3.48	0.16
Aug	SBV	-6.08	0.98	224.01	0.00*
	NBW	-22.88	0.92	11.47	0.18
Sep	SBV	-3.78	0.58	4.17	0.13
	DBW	-10.73	0.22	0.58	0.52

Table 34. Monthly slopes statistics of the of photosynthetic pigments chl *a:b* vs. log [CO_2] derived from linear regression analysis.

Chl *a:b*

Month	Population	Slope	R^2	*F*	*p*
May	SBV	0	-	-	-
	DBW	0	-	-	-
	NBW	0	-	-	-
July	SBV	0.61	0.50	3.03	0.80
	DBW	0.22	0.13	0.46	0.10
Aug	SBV	0.25	0.98	140.91	0.001*
	NBW	0.55	0.92	11.93	0.18
Sep	SBV	-0.04	0.58	4.23	0.13
	DBW	1.80	0.33	0.98	0.43

LC-MS and GC-MS Parameters

Table 35. Parameters applied to GC-MS chromatograms with Metabolite Detector 2.5 for the obtaining of the metabolomic profiles of Eelgrass.

Tool settings		
Centroid	Threshold begin	10
	Peak threshold end	-5
	Maximal baseline	30
	FWHM	0.1
Deconvolution	Peak threshold	10
	Minimum peak height	10
	Deconvolution width (scans)	8
Identification	Max RI difference	20
	Cutoff score	0.6
	Pure/Impure	0.6
	Scaled lib	Yes
	Combined score	Yes
Quantification	Minimal distance	0.5
	Minimal required quality index	1
	Exclude	72.5 to 73.5 146.5 to 147.5
Batch quantification Settings		
Compound matching	ARI	20
	Pure/Impure	0.6
	Req. Score	0.6
	RI+Spec	OK
Identification	ARI	20
	Pure/Impure	0.6
	RI+Spec	OK
Other settings	Compound reproducibility	0
	Max. Peak drisc. index	100
	S/N	15
	Number of ions	4
	Extended SIC Scan	Yes

Table 36. Score, retention index (RI), retention time (RT) and signal to noise ratio (S/N) of the matched metabolites in GC-MS chromatograms processed with Metabolite Detector 2.5.

	Score	RT Standard (min)	Measured Avg. RT (Min)	Avg. S/N	Considered for the study
α-Ketoglutaric Acid	0.86	13.85	13.91	14.43	YES
Arabitol	0.85	15.60	15.5	47.47	YES
Caffeic Acid	0.98	19.75	19.82	66.07	YES
Citric Acid	0.9	16.83	16.77	84.86	YES
D-Arabinose	0.89	15.19	15.28	22.82	YES
D-Lyxosylamine	0.91	14.73	14.74	89.01	YES
D-Malic Acid	0.92	12.79	12.85	143.04	YES
D-Mannose	0.96	17.66	17.72	77.96	YES
D-Trehalose	0.81	25.20	25.22	74.59	YES
Fructose	0.89	17.28	17.44	458.08	YES
Galactonic Acid	0.88	18.77	18.73	45	YES
Glyceric Acid	0.94	10.73	10.78	26.84	YES
Glycerol-3-Phosphate	0.93	16.05	16.17	58.68	YES
Glycine	0.99	10.45	10.44	26.99	YES
L-DOPA	0.76	19.08	19.24	107.04	YES
L-Glutamic Acid	0.86	13.33	13.34	22.99	YES
L-Glutamic Acid	0.93	13.23	13.27	147.83	YES
L-Proline	0.96	10.32	10.3	128.18	YES
L-Sorbose	0.72	17.23	17.55	364.34	YES
Linoleic Acid	0.84	20.39	20.4	11.92	YES
Myo-Inositol	0.93	19.70	19.62	604.44	YES
N-Acetyl-L-Glutamic Acid	0.62	13.06	12.94	66.37	YES
Palmitic Acid	0.93	18.84	18.86	104.36	YES
Shikimic Acid	0.84	16.43	16.6	23.86	YES
Sucrose	0.93	24.41	24.36	707.99	YES
Turanose	0.77	24.81	24.76	67.47	YES
2-Hydroxybutyric Acid	0.89	7.85	7.92	19.86	NO
4-Hydroxybenzoic Acid	0.81	14.50	14.49	32.52	NO
Arbutin	0.79	23.39	23.37	20.87	NO
Coniferyl alcohol	0.62	17.97	18	10.59	NO
D-Gluconic Acid	0.83	18.31	18.4	10.58	NO
D-Glucose	0.77	17.98	18.07	51.68	NO
D-Glucuronic Acid	0.65	18.15	18.13	16.73	NO
D-Sorbitol	0.8	17.89	17.91	23.75	NO
Dehydroascorbic Acid	0.81	18.01	18.28	4	NO
L-Glutamine	0.71	12.71	12.66	21.23	NO
Lactulose	0.78	23.86	23.88	82.46	NO
Lactulose	0.67	24.43	24.23	33.02	NO
Methyl-β-D-Galactopyranoside	0.64	16.93	16.87	31.65	NO
N-acetyl-L-cysteine	0.75	15.24	15.27	14.99	NO
Norvaline	0.92	9.46	9.15	12.02	NO
Ribitol	0.84	15.66	15.67	6.21	NO
Ribonic Acid, γ-Lactone	0.61	15.05	14.64	22.47	NO
Rosmarinic Acid	0.63	29.69	29.51	12.71	NO
Scyllo-inositol	0.82	19.10	18.99	9.02	NO
Sialic Acid	0.61	22.25	22.54	42.45	NO

Table 37. Parameters applied to LC-MS RAW files with MZMine 2.26 (Pluskal et al., 2010) to obtain the metabolomic fingerprintings of eelgrass samples from both positive and negative ionization modes.

		(+H) Chromatograms		(-H) Chromatograms
1	**Baseline correction – RollingBall baseline corrector**			
	Chromatogram type	TIC		TIC
	Use m/z bins	No		No
	wm	25		25
	ws	25		25
2	**Mass detection** (exact Mass)			
	Noise level	1×10^4		1×10^3
3	**Chromatogram builder (ADAP)**[58]			
	Min group size in num. of scans	3		3
	Group intensity threshold	1×10^4		1×10^3
	Min highest intensity	1×10^5		1×10^4
	m/z tolerance	0.0005 or 6ppm		0.0005 or 6ppm
4	**Smoothing**			
	Filter width	5		5
5	**Chromatogram deconvolution (local minimum search)**			
	Chromatographic threshold	40%		40%
	Search minimum in RT range (min)	0.25		0.25
	Minimum relative height	50%		50%
	Minimum absolute height	1×10^4		1×10^3
	Minimum ratio of peak top/edge	1.5		1.5
	Peak duration range	0-2 min		0-2 min
6	**Isotopic peak grouper**			
	m/z tolerance	0.0005 or 6ppm		0.0005 or 6ppm
	Retention Time tolerance	0.25 min		0.25 min
	Max charge	1		1
	Representative isotope	Most intense		Most intense
7	**Retention Time Normalizer**			
	m/z tolerance	0.0005 or 6ppm		0.0005 or 6ppm
	Retention Time tolerance	0.25 min		0.25 min
	Minimum Standard Intensity	1×10^5		1×10^4
8	**Chromatogram alignment (join alignment)**			
	m/z tolerance	0.0005 or 6ppm		0.0005 or 6ppm
	Weight for m/z	80		80
	RT tolerance	0.25		0.25
	Weight for RT	20		20

Table 37 continued

7	**Gap filling (Peak Finder)**			
	Intensity tolerance	60%		60%
	m/z tolerance	0.0005 or 6ppm		0.0005 or 6ppm
	Retention time tolerance	0.2		0.2
	RT correction	Yes		Yes
8	**Metabolite Assignation**			
	m/z tolerance	0.0005 or 6ppm		0.0005 or 6ppm
	RT tolerance	0.25		0.25

RT, retention time; m/z, mass to charge ratio

Table 38. Retention time (RT) and mass to charge ratio (m/z) of the deconvoluted ions in both negative and positive ionization modes assigned to metabolites with MZmine v.2.26 for LC-MS chromatograms. The assignment of the metabolites was based on the exact mass and RT of standards. RT and m/z of the standards are shown in the table. Error of m/z and RT of assigned ions to metabolites respect the m/z and RT of standards are shown. After applying the chromatogram builder and deconvolution algorithms from MZmine, several ions with the same exact mass may have been separated into two or more independent deconvoluted peaks presenting slightly different retention times. The following table show all the peaks assigned to a molecular compound based on the exact mass of their parent ion (in negative or positive mode). In the main manuscript, all identified metabolic features assigned to a same metabolite were summed to finally have a single variable per metabolite.

	m/z and RT of each ion assigned in MZmine v.2.26			Measured m/z and RT from Standards.		Error of m/z and RT (deconvoluted ions vs. Standard ions)		
Ionization mode	Name	m/z	RT	m/z	RT	m/z (absolute)	m/z (ppm)	RT
POS	1-2-Phenylenediamine	109.08	1.41	109.08	1.35	0.00	0.42	-0.06
POS	1-AMINOCYCLOPROPANE-1-CARBOXYLATE	102.05	1.42	102.06	1.29	0.00	1.33	-0.13
POS	1-METHYL-6,7-DIHYDROXY-1,2,3,4-TETRAHYDROISOQUINOLINE	180.10	1.42	180.10	1.39	0.00	0.84	-0.04
POS	1-Methyladenine-3-METHYLADENINE	150.08	1.40	150.08	1.30	0.00	1.24	-0.11
POS	1-PHENYLETHANOL	123.08	11.95	123.08	11.90	0.00	1.59	-0.05
POS	1-PHENYLETHANOL	123.08	12.01	123.08	11.90	0.00	1.67	-0.11
POS	2,6-DIHYDROXYPYRIDINE	112.04	1.41	112.04	1.41	0.00	0.77	0.00
POS	2-AMINOPHENOL	110.06	1.41	110.06	1.39	0.00	0.78	-0.03
POS	2-HYDROXYPYRIDINE	96.04	1.39	96.04	1.39	0.00	1.73	0.00
NEG	3,2-HYDROXYPHENYL PROPANOATE	165.06	11.12	165.06	10.74	0.00	1.78	-0.39
POS	AMINO -HYDROXYBENZOIC ACID	154.05	1.43	154.05	1.39	0.00	0.69	-0.05
POS	AMINO-HYDROXYBENZOIC ACID	154.05	1.73	154.05	1.76	0.00	1.08	0.03
NEG	3-AMINOISOBUTANOATE 2-AMINO-2-METHYLPROPANOATE	102.06	1.35	102.06	1.27	0.00	0.63	-0.08
NEG	3-DEHYDROSHIKIMATE	171.03	1.76	171.03	1.45	0.00	0.61	-0.31
POS	3-HYDROXYKYNURENINE	225.09	1.43	225.09	1.40	0.00	0.07	-0.04

Table 38 continued

	m/z and RT of each ion assigned in MZmine v.2.26			Measured m/z and RT from Standards.		Error of m/z and RT (deconvoluted ions vs. Standard ions)		
Ionization mode	Name	m/z	RT	m/z	RT	m/z	m/z	RT
POS	3-HYDROXYKYNURENINE	225.09	1.74	225.09	1.85	0.00	-0.28	0.11
NEG	3-METHOXY-4-HYDROXYMANDELATE	197.05	2.31	197.05	2.30	0.00	1.85	-0.01
POS	3-METHOXYTYRAMINE	168.10	1.42	168.10	1.35	0.00	0.60	-0.07
NEG	4-ACETAMIDOBUTANOATE	144.07	1.43	144.07	1.38	0.00	1.28	-0.06
POS	4-ACETAMIDOBUTANOATE	146.08	1.41	146.08	1.38	0.00	0.38	-0.04
POS	AMINOBUTANOATE	104.07	1.36	104.07	1.25	0.00	0.63	-0.11
POS	4.-UANIDINOBUTANOATE	146.09	1.40	146.09	1.32	0.00	0.18	-0.09
POS	4-HYDROXY-L-PHENYLGLYCINE PYRIDOXAL	168.07	1.41	168.07	1.35	0.00	0.51	-0.06
POS	4-HYDROXY-L-PROLINE	132.07	1.42	132.07	1.26	0.00	1.26	-0.16
POS	4-HYDROXYBENZALDEHYDE	123.04	7.70	123.04	7.71	0.00	1.51	0.01
POS	5-METHYLCYTOSINE	126.07	1.38	126.07	1.28	0.00	0.63	-0.10
POS	5-METHYLTHIOADENOSINE	298.10	2.74	298.10	2.86	0.00	0.39	0.12
POS	5-OXO-D-PROLINE	130.05	1.36	130.05	1.38	0.00	0.82	0.02
POS	5-OXO-D-PROLINE	130.05	1.72	130.05	1.78	0.00	1.20	0.06
NEG	5-OXO-L-PROLINE	128.04	1.36	128.04	1.37	0.00	0.89	0.01
NEG	5-OXO-L-PROLINE	128.04	1.75	128.04	1.37	0.00	-0.20	-0.38
POS	6-HYDROXYNICOTINATE	140.03	1.74	140.03	1.84	0.00	1.19	0.10
POS	6-Phosphogluconic Acid	277.03	1.42	277.03	1.55	0.00	-0.63	0.13
POS	ACETOACETATE	103.04	1.75	103.04	1.82	0.00	1.81	0.07
NEG	ADENINE	134.05	1.34	134.05	1.33	0.00	1.00	-0.01
POS	ADENINE	136.06	1.39	136.06	1.33	0.00	0.63	-0.06
POS	ADENOSINE	268.10	1.41	268.10	1.38	0.00	-0.16	-0.03

Table 38 continued

	m/z and RT of each ion assigned in MZmine v.2.26			Measured m/z and RT from Standards.		Error of m/z and RT (deconvoluted ions vs. Standard ions)		
Ionization mode	Name	m/z	RT	m/z	RT	m/z	m/z	RT
POS	ADENOSINE	268.10	1.73	268.10	1.85	0.00	-0.50	0.12
POS	ADENOSINE-5-MONOPHOSPHATE	348.07	1.42	348.07	1.49	0.00	-2.88	0.07
POS	ADENOSINE-5-MONOPHOSPHATE	348.07	1.42	348.07	1.49	0.00	-4.46	0.07
NEG	α-AMINOADIPATE	160.06	1.42	160.06	1.34	0.00	1.40	-0.08
POS	α-AMINOADIPATE	162.08	1.42	162.08	1.34	0.00	0.47	-0.08
POS	Sugars, Hexoses, Phosphate	261.04	1.43	261.04	1.54	0.00	-0.36	0.11
POS	AZELAIC ACID	189.11	11.07	189.11	11.30	0.00	0.82	0.23
NEG	CITRATE	191.02	1.73	191.02	1.48	0.00	1.38	-0.25
POS	CREATINE	132.08	1.37	132.08	1.32	0.00	1.03	-0.06
POS	CREATININE	114.07	1.40	114.07	1.27	0.00	0.14	-0.14
POS	CYTOSINE	112.05	1.35	112.05	1.26	0.00	0.68	-0.09
POS	D-3-PHOSPHOGLYCERIC ACID	187.00	1.46	187.00	1.62	0.00	0.49	0.16
POS	ASPARTATE	134.04	1.38	134.04	1.41	0.00	0.79	0.03
NEG	D-GLUCOSAMINE-6-SULFATE	259.01	1.37	259.01	1.34	0.00	2.94	-0.04
NEG	D-GLUCURONOLACTONE	193.04	1.37	193.04	1.36	0.00	2.02	-0.01
NEG	D-GLUCURONOLACTONE	193.04	1.40	193.04	1.36	0.00	1.96	-0.04
NEG	D-GULONIC ACID, γ-LACTONE	177.04	1.39	177.04	1.36	0.00	1.89	-0.04
POS	Amino-Sugars-C8	180.09	1.41	180.09	1.21	0.00	-5.10	-0.21
POS	D-PANTOTHENIC ACID	220.12	1.44	220.12	1.42	0.00	0.03	-0.03
NEG	D-SORBITOL GALACTITOL	181.07	1.33	181.07	1.31	0.00	2.07	-0.02
NEG	Sugars-Pentoses	149.05	1.39	149.05	1.32	0.00	1.44	-0.07
NEG	DEHYDROASCORBATE	173.01	1.41	173.01	1.39	0.00	2.16	-0.02

Table 38 continued

	m/z and RT of each ion assigned in MZmine v.2.26			Measured m/z and RT from Standards.		Error of m/z and RT (deconvoluted ions vs. Standard ions)		
Ionization mode	Name	m/z	RT	m/z	RT	m/z	m/z	RT
NEG	DEHYDROASCORBATE	173.01	1.63	173.01	1.39	0.00	1.41	-0.24
POS	DEHYDROASCORBATE	175.02	1.73	175.02	1.67	0.00	0.72	-0.07
POS	DIETHANOLAMINE	106.09	1.34	106.09	1.24	0.00	2.22	-0.10
POS	Eriodictyol	289.07	12.16	289.07	12.26	0.00	4.55	0.10
POS	Fisetin	287.05	10.10	287.06	10.13	0.00	0.93	0.03
NEG	Formononetin	267.07	14.35	267.07	14.28	0.00	3.12	-0.07
NEG	Formononetin	267.07	14.59	267.07	14.28	0.00	2.49	-0.31
NEG	FUMARATE	115.00	1.71	115.00	1.51	0.00	-0.14	-0.20
POS	GALACTITOL	183.09	1.43	183.09	1.35	0.00	2.98	-0.08
NEG	Gallic Acid	169.01	1.47	169.01	1.40	0.00	2.33	-0.07
NEG	Glutamic Acid	146.05	1.35	146.05	1.29	0.00	1.74	-0.06
POS	Glutamic Acid	148.06	1.36	148.06	1.29	0.00	1.32	-0.07
NEG	GLUTARATE	131.04	1.81	131.04	1.53	0.00	-0.50	-0.28
NEG	GLUTARATE	131.04	2.43	131.04	2.13	0.00	-0.89	-0.31
NEG	GLUTARATE	131.03	1.43	131.04	1.34	0.00	0.49	-0.10
NEG	GLYCERALDEHYDE	89.02	1.72	89.02	1.39	0.00	-0.74	-0.33
POS	GUANINE	152.06	1.40	152.06	1.33	0.00	0.76	-0.08
POS	GUANOSINE	284.10	1.43	284.10	1.36	0.00	-0.15	-0.08
POS	HISTAMINE	112.09	1.42	112.09	1.30	0.00	0.41	-0.12
POS	HYPOXANTHINE	137.05	1.42	137.05	1.37	0.00	0.85	-0.06
NEG	L-ALANINE	88.04	1.37	88.04	1.28	0.00	-0.07	-0.09
POS	L-ALANINE	90.05	1.35	90.05	1.28	0.00	2.40	-0.07

Table 38 continued

	m/z and RT of each ion assigned in MZmine v.2.26			Measured m/z and RT from Standards.		Error of m/z and RT (deconvoluted ions vs. Standard ions)		
Ionization mode	Name	m/z	RT	m/z	RT	m/z	m/z	RT
NEG	Sugars, Alcohol, Pentoses	151.06	1.35	151.06	1.31	0.00	1.42	-0.04
POS	L-ARGININE	175.12	1.34	175.12	1.25	0.00	0.83	-0.09
POS	L-ASPARAGINE	133.06	1.37	133.06	1.31	0.00	0.95	-0.06
NEG	L-ASPARAGINE	131.05	1.33	131.05	1.31	0.00	1.18	-0.02
NEG	L-GLUTAMINE	145.06	1.32	145.06	1.32	0.00	1.48	-0.01
POS	L-GLUTAMINE	147.08	1.36	147.08	1.32	0.00	0.65	-0.05
POS	L-ISOLEUCINE	132.10	1.75	132.10	1.82	0.00	1.33	0.07
POS	L-LEUCINE	132.10	1.44	132.10	1.37	0.00	1.33	-0.08
POS	L-PHENYLALANINE	166.09	1.43	166.09	1.36	0.00	0.58	-0.08
NEG	L-PHENYLALANINE	164.07	2.19	164.07	2.19	0.00	-0.04	-0.01
POS	L-PHENYLALANINE	166.09	2.18	166.09	2.19	0.00	0.64	0.01
POS	L-PIPECOLIC.ACID	130.09	1.41	130.09	1.35	0.00	0.97	-0.06
NEG	L-PROLINE	114.06	1.46	114.06	1.35	0.00	1.09	-0.12
POS	L-PROLINE	116.07	1.37	116.07	1.35	0.00	1.17	-0.03
POS	L-PROLINE	116.07	1.38	116.07	1.35	0.00	-5.89	-0.04
NEG	Deoxy-Sugars,-Hexoses	163.06	1.40	163.06	1.33	0.00	1.59	-0.07
NEG	L-SERINE	104.04	1.34	104.04	1.29	0.00	0.71	-0.05
POS	L-SERINE	106.05	1.35	106.05	1.29	0.00	1.85	-0.06
POS	L-SERINE	106.05	1.35	106.05	1.29	0.00	1.66	-0.06
POS	L-THREONINE	120.07	1.35	120.07	1.31	0.00	1.38	-0.04
POS	L-TYROSINE	182.08	1.42	182.08	1.37	0.00	0.36	-0.06
POS	L-TYROSINE	182.08	1.73	182.08	1.84	0.00	0.64	0.11

Table 38 continued

	m/z and RT of each ion assigned in MZmine v.2.26			Measured m/z and RT from Standards.		Error of m/z and RT (deconvoluted ions vs. Standard ions)		
Ionization mode	Name	m/z	RT	m/z	RT	m/z	m/z	RT
POS	L-VALINE	118.09	1.40	118.09	1.28	0.00	2.00	-0.12
POS	Luteolin	287.06	12.17	287.06	12.36	0.00	-0.08	0.19
POS	MALEAMATE	116.03	1.38	116.03	1.44	0.00	-0.81	0.06
NEG	MANDELIC ACID	151.04	5.35	151.04	5.35	0.00	-0.44	0.00
NEG	Sugars, Disaccharides	341.11	1.33	341.11	1.24	0.00	3.27	-0.09
NEG	Sugars, Hexoses	179.06	1.34	179.06	1.29	0.00	2.03	-0.05
POS	N-ACETYL-D-TRYPTOPHAN	247.11	10.27	247.11	10.29	0.00	0.31	0.02
NEG	N-ACETYL-D,L-GLUTAMIC.ACID	188.06	1.40	188.06	1.39	0.00	1.67	-0.02
POS	N-ACETYL-D,L-GLUTAMIC.ACID	190.07	1.44	190.07	1.39	0.00	0.45	-0.06
POS	N-ACETYL-L-ALANINE	132.07	1.73	132.07	1.82	0.00	0.88	0.09
POS	N-ACETYL-GLYCINE	118.05	1.44	118.05	1.55	0.00	1.66	0.11
POS	N-ACETYL-GLYCINE	118.05	1.74	118.05	1.55	0.00	1.49	-0.19
POS	N-α-ACETYL-L-LYSINE	189.12	1.40	189.12	1.28	0.00	0.40	-0.12
POS	Naringenin	273.08	13.23	273.08	13.31	0.00	0.39	0.08
POS	N-ε-N-ε-N-ε-TRIMETHYLLYSINE	189.16	1.31	189.16	1.30	0.00	0.51	-0.01
POS	NICOTINAMIDE	123.06	1.41	123.06	1.36	0.00	0.78	-0.05
POS	NICOTINAMIDE	123.06	1.73	123.06	1.71	0.00	1.02	-0.02
POS	NICOTINATE PICOLINIC ACID	124.04	1.71	124.04	1.70	0.00	1.18	-0.01
NEG	O-SUCCINYL-L-HOMOSERINE	218.07	1.37	218.07	1.36	0.00	3.55	-0.02
POS	O-SUCCINYL-L-HOMOSERINE	220.08	1.42	220.08	1.36	0.00	0.35	-0.07
POS	O-SUCCINYL-L-HOMOSERINE	220.08	1.42	220.08	1.36	0.00	0.25	-0.07
NEG	PHENYLACETIC ACID	135.05	4.00	135.05	3.82	0.00	-0.86	-0.18

Table 38 continued

	m/z and RT of each ion assigned in MZmine v.2.26			Measured m/z and RT from Standards.		Error of m/z and RT (deconvoluted ions vs. Standard ions)		
Ionization mode	Name	m/z	RT	m/z	RT	m/z	m/z	RT
NEG	Phloroglucinol	125.02	1.76	125.02	1.43	0.00	-0.53	-0.34
POS	Phloroglucinol	127.04	1.39	127.04	1.43	0.00	1.31	0.04
POS	Phloroglucinol	127.04	1.40	127.04	1.43	0.00	0.68	0.03
NEG	Phloroglucinol	125.02	2.33	125.02	1.88	0.00	-0.61	-0.46
POS	Phloroglucinol	127.04	1.72	127.04	1.88	0.00	1.07	0.16
POS	PYRIDOXAMINE	169.10	1.41	169.10	1.35	0.00	0.57	-0.07
POS	PYRIDOXINE	170.08	1.41	170.08	1.29	0.00	0.62	-0.13
NEG	PYRUVATE	87.01	1.70	87.01	1.67	0.00	-1.91	-0.03
NEG	PYRUVIC.ALDEHYDE	71.01	1.36	71.01	1.38	0.00	-1.35	0.02
NEG	PYRUVIC.ALDEHYDE	71.01	1.41	71.01	1.38	0.00	-1.63	-0.03
POS	QUINOLINE	130.07	2.18	130.07	2.23	0.00	1.12	0.05
NEG	RESORCINOL.MONOACETATE	151.04	11.00	151.04	10.87	0.00	1.88	-0.13
POS	ROSMARINIC.ACID	361.09	11.02	361.09	11.18	0.00	-0.29	0.16
NEG	Mevalonic Acid	147.07	1.91	147.07	1.78	0.00	0.10	-0.13
NEG	S-MALATE	133.01	1.42	133.01	1.45	0.00	1.23	0.03
POS	SALICYLATE	139.04	11.40	139.04	11.39	0.00	1.55	-0.01
NEG	SHIKIMATE	173.05	1.41	173.05	1.39	0.00	1.93	-0.02
NEG	SUCCINATE	117.02	1.76	117.02	1.41	0.00	0.12	-0.36
NEG	SUCCINATE SEMIALDEHYDE	101.02	2.00	101.02	1.79	0.00	-1.35	-0.21
POS	THYMINE	127.05	1.74	127.05	1.85	0.00	1.23	0.11
POS	TRIGONELLINE	138.05	1.40	138.06	1.36	0.00	0.84	-0.05
POS	TYRAMINE	138.09	1.41	138.09	1.34	0.00	1.42	-0.07

Table 38 continued

	m/z and RT of each ion assigned in MZmine v.2.26			Measured m/z and RT from Standards.		Error of m/z and RT (deconvoluted ions vs. Standard ions)		
Ionization mode	Name	m/z	RT	m/z	RT	m/z	m/z	RT
POS	URACIL	113.03	1.42	113.03	1.37	0.00	0.58	-0.05
NEG	URIDINE	243.06	1.78	243.06	1.37	0.00	1.95	-0.42
POS	URIDINE	245.08	1.42	245.08	1.37	0.00	-0.10	-0.06
POS	UROCANATE	139.05	1.41	139.05	1.33	0.00	0.98	-0.09

RT, retention time m/z, mass to charge ratio ppm, parts per million

VITA

Carmen C. Zayas-Santiago
Department of Ocean, Earth and Atmospheric Sciences
Old Dominion University 4600 Elkhorn Ave, Norfolk, VA 23259
Email: ccastula@gmail.com

EDUCATION

2021 PhD in Biological Oceanography, *Old Dominion University Norfolk, VA*
2011 Master of Science in Biological Oceanography, *University of Puerto Rico at Mayagüez*
2004 Bachelor of Science in Coastal Marine Biology, *University of Puerto Rico at Humacao*

PROFESSIONAL EXPERIENCE

2013 – 2016 Teaching Assistant, Old Dominion University Norfolk, VA
2013 – 2014 Research Assistant, Old Dominion University Norfolk, VA
2012 – 2012 Sea Grant Marine Educator, Sea Grant Puerto Rico UPR Mayagüez
2011 – 2012 Research Assistant, Mississippi State University at Vivero Peces Maricao, PR
2010 – 2011 Research Assistant, University of Puerto Rico Mayagüez NOAA NCAS
2008 – 2010 Investigator, University of Puerto Rico, Mayagüez PR NASA Space Grant

PUBLICATIONS AND PRESENTATIONS

Zayas-Santiago, C.C., Rivas-Ubach, A., Kuo, L., Ward N D., Zimmerman R C. Metabolic Profiling Reveals Biochemical Pathways Responsible for Eelgrass Response to Elevated CO_2 and Temperature. *Sci Rep* 10, 4693 (2020). https://doi.org/10.1038/s41598-020-61684-x

Puerto Rico Climate Change Council (PRCCC) Working Group 2. 2021. Ecology and Biodiversity WG2, 85 – 250. In Puerto Rico's State of the Climate 2010-2013: Assessing Puerto Rico's Social-Ecological Vulnerabilities in a Changing Climate. Eds. Jacobs, K.R., L. Carrubba, E. Diaz. Puerto Rico Coastal Zone Management Program, Department of Natural and Environmental Resources, NOAA Office of Ocean and Coastal Resource Management. San Juan, PR (*In Progress*).

Zayas-Santiago C., Zimmerman R., Hill V., Gaeckle J., Short F. Differential response of *Zostera marina* L. (eelgrass) populations to CO_2 and temperature Coastal and Estuarine Research Federation; November 2015 Portland, Oregon, USA (Oral Presentation). Ocean Sciences Meeting; February 2015 Honolulu, Hawaii, USA

Alicea D., Casillas J., Bejarano I.(2014) Las praderas de hierbas marinas: Guía educativa para maestros. Mayagüez, Puerto Rico. Sea Grant Puerto Rico. ISBN: 978-881719-58-8. Collaborator: Zayas-Santiago,C.

GRANTS/ AWARDS

Zayas-Santiago, CC. 2019. ASLO Multicultural Program. Full support for ASLO meeting.
Zayas-Santiago, CC. 2018. Kirk Student Research Award. $3,250.
Zayas-Santiago, CC. 2015. ODU Dorothy Brown Smith Scholarship. $1,859.
Zayas-Santiago, CC. 2012.Hall-Bonner Program for Minority Doctoral Scholars. $19,600.